



ENGR9700: Thesis Project

***The Design and Development of a Wearable
Device to Assess Lower-limb Impact Dose
during Competitive Netball Play***

Anika Talukder

2152571

21st October 2019

Supervisors: Dr David Hobbs, Dr Kym Williams and Professor Mark Taylor


***Submitted to the College of Science and Engineering in partial fulfilment of the requirements
for the degree of Bachelor of Engineering (Biomedical) (Honours)/Master of Engineering
(Biomedical) at Flinders University, Adelaide, Australia.***

Declaration of Originality

I certify that this work does not incorporate without acknowledgment any material previously submitted for a degree or diploma in any university and that to the best of my knowledge and belief it does not contain any material previously published or written by another person except where due reference is made in the text.

Name: Anika Talukder

Date: 21/10/2019

Signed:  _____

Statement of Ethical Conduct

I hereby certify that all methodology involving humans was approved by the Social and Behavioural Research Ethics Committee (SBREC), under project number 8017. The research methodology was conducted as submitted and approved with SBREC, unless where modification requests were submitted and approved. Documentation certifying the approval or modification of research methodology used throughout this thesis is found in APPENDIX A.

Name: Anika Talukder

Date: 21/10/2019

Signed:  _____

Acknowledgment

Firstly, I would like to express my appreciation for my supervisors, Dr Kym Williams, Dr David Hobbs and Professor Mark Taylor for their guidance, knowledge, enthusiasm and support throughout the project. I am grateful to have worked with such dedicated and passionate academics, who ensured I felt well supported throughout the year.

I would also like to acknowledge Michael Russo, who supported me through troubleshooting and navigation of the Flinders University Motion Analysis and Rehabilitation Laboratory, despite high PhD workloads.

I would like to express my deepest gratitude towards Lucas Kleiss, for his integral role in the software development of my prototype. Lucas provided his software interfacing expertise, critical to the functionality and user-display of the final design.

Thank you to the Flinders University Engineering Services team and IDS team for assistance throughout the project regarding technical queries and specification clarifications.

I would like to acknowledge Lyndon Huf and Leanne Eichler, both of whom assisted in the identification of my project objectives through their personal experiences, insights and expectations of the wearable device.

A special mention to Thomas Beltrame, for his constant support throughout the project. Thomas provided advice, assistance with data collection and feedback from both an engineering and athletic perspective.

Finally, I would like to thank all the participants who volunteered their time, my family and my friends for their continued support and encouragement throughout this year.

Abstract

Netball is a prominent team sport, predominantly played by females worldwide ranging from leisure play to elite-level participation. Due to the high degree of speed, strength and repeated explosive loading to the lower limb placed during gameplay, high occurrence of lower limb injuries has been documented throughout the decades. The frequency of lower limb injuries can lead to a reduction in the level of sports activity, the need for medical treatment, and adverse social and economic effects for athletes. The current active injury countermeasures are either subjective training practices, that fail to quantify the loading of lower limbs, or wearable devices for impact monitoring which are laboratory-based, expensive and generally inaccessible to sub-elite players. Due to the lack of active monitoring of the lower limb impact forces in training and games, preventative measures unique to each player cannot be taken, contributing to the onset of chronic injuries. An initial review of the literature identified the growth of Inertial Measure Units (IMU) with the potential application for accelerometers to measure general energy expenditure and lower-limb shock attenuation. Therefore, the primary objective of this project was to contribute to the design and development of an inexpensive accelerometer-based wearable device that could quantify lower limb related impact dose, cumulative counts of low, moderate and high impact activities experienced during netball play.

When an accelerometer-based device was placed on the shank of the participant, with the acceleration amplitude in the inferior/superior axis (A_{IS} amplitude) to the shank was considered for the measurement of impact dose. Laboratory-based force plates (AMTI OR6-7) and accelerometers (Delsys Trigno Avanti™ Research+) were used to validate a commercially available IMU manufactured by Texas Instruments (SensorTag CC2650), to provide a measure of impact dose. When assessed against the requirements of range, sampling frequency and connectivity, significant data loss and connection issues were observed due to line of sight interruptions and data streaming restrictions of Bluetooth. Through in situ and laboratory-based studies, it was concluded that the SensorTag did not meet the required specifications of a practical and reliable wearable device to be used during netball gameplay and hence was deemed not viable. An alternative solution was then to create a working prototype using a Wi-Fi enabled device with a user interface, such that chosen accelerometer variable data could be displayed to the user. The working prototype was equipped with onboard processing capabilities, such that the maximum sampling frequency could be achieved, reducing data loss.

Finally, a pilot correlation and feasibility study was conducted with the prototype to ensure the A_{IS} amplitude could be correlated with Vertical Ground Reaction Force (VGRF) data obtained from AMTI OR6-7 plates. Subsequent testing with three participants enabled the correlation of A_{IS} amplitude with the VGRF and activities performed by participants could be classified into low, moderate and high impact zones, providing a visual representation of movements to users.

Table of Contents

Declaration of Originality	i
Statement of Ethical Conduct	i
Acknowledgment	ii
Abstract	iii
Table of Contents	v
List of Tables	ix
List of Figures	x
<i>Introduction</i>	<i>1</i>
<i>Chapter 1:.....</i>	<i>5</i>
<i>Literature Review</i>	<i>5</i>
1.1 Netball.....	6
1.1.1 Popularity of Netball	6
1.1.2 Origin of Netball.....	6
1.1.3 Objective and Rules.....	7
1.1.4 Activity Profile	9
1.2 Epidemiology and Incidence of Netball Injuries.....	12
1.2.1 Incidence of Injuries	12
1.2.2 Location and Classification of Injuries.....	15
1.2.3 Cause of Injuries.....	18
1.2.4 Similar Injuries in Other Sports	22
1.3 Current Injury Countermeasures for Netball	25
1.3.1 Training Techniques	25
1.3.2 Educational Programs	26
1.3.3 Footwear	27
1.3.4 Taping and Bracing.....	28
1.3.5 Codes of Conduct	29
1.3.6 Netball Surface.....	29
1.3.7 Landing Techniques.....	30
1.4 Athlete Workload Monitoring Practices	32

1.4.1	Internal Workload	32
1.4.2	External Workload	34
1.5	Conclusion	45
Chapter 2:	47
Project Overview	47
2.1	Problem Statement.....	48
2.2	Project Objectives	48
2.3	Methodology Overview	49
Chapter 3:	50
Testing and Validation of SensorTag.....	50
3.1	Introduction	51
3.2	Aim.....	51
3.3	Methods	52
3.3.1	Laboratory Testing	52
3.3.2	In-Situ Testing.....	59
3.4	Results.....	61
3.5	Discussion.....	65
Chapter 4:	69
Development of a Wearable Prototype.....	69
4.1	Introduction	70
4.2	Aim	70
4.3	Methods.....	71
4.3.1	Hardware Development.....	71
4.3.2	Software Development	78
4.4	Results	82
4.5	Discussion	84
Chapter 5:	87

<i>Correlation and Feasibility Study Using Wearable Prototype</i>	87
5.1 Introduction	88
5.2 Aim	88
5.3 Methods	89
5.3.1 Participant Selection	89
5.3.2 Data Collection	90
5.3.3 Data Export and File Processing	91
5.3.4 Data Analysis	91
5.4 Results	94
5.5 Discussion	98
5.5.1 Individual Participant Analysis	98
5.5.2 Combined Analysis: Impact Zone and Feather Feasibility	101
5.5.3 Limitations.....	102
<i>Chapter 6:</i>	104
<i>Conclusion</i>	104
6.1 Summary of Findings	105
6.2 Future Recommendations	108
<i>References</i>	110
Reference List	111
<i>Appendices</i>	123
Appendix A: SBREC Application Modification Request	124
MODIFICATION (No.3) APPROVAL NOTICE	124
MODIFICATION (No.4) APPROVAL NOTICE	126
Appendix B: Vicon AMTI OR6-7 Force Plate Specifications	130
Appendix C: Texas Instruments SensorTag Specifications	131
Appendix D: Delsys Trigno Research+ Specifications	132
Appendix E: Vicon Protocols	133
SYSTEM CALIBRATION	133
DATA ACQUISITION CONFIGURATION	133

SUBJECT MARK-UP	134
DATA COLLECTION	135
REVIEWING DATA.....	135
Appendix F: SensorTag Data Acquisition Setup.....	136
Appendix G: ESP8266 Specifications	137
Appendix H: ADXL345 Specifications	138
Appendix I: Adafruit Feather Huzzah ESP8266 Pinout.....	139
Appendix J: Data Acquisition Arduino Code.....	140
Header Function:.....	140
Main Function:	142
Appendix K: Participant Consent Forms.....	155
Appendix L: Individual Participant Analysis MATLAB Script	156
main.m:	156
mass.m:	157
extractFeature.m:	158
correlate.m:.....	160
plotFeatures.m:.....	161
vector.m:	164
tabulate.m:.....	165
Appendix M: Combined Analysis MATLAB Script: Scatter	166
main.m:	166
createfigure.m:.....	169
Appendix N: Combined Analysis MATLAB Script: Bar.....	182
barp.m:.....	182
createBarPlot.m:	184
Appendix O: Impact Zones: 4 Participants	185

List of Tables

<i>Table 1: Mean percentage of active time spent performing activities by each court position</i>	10
<i>Table 2: Incidence of netball injuries in the literature</i>	14
<i>Table 3: Location of injuries</i>	16
<i>Table 4: Classification of injuries</i>	16
<i>Table 5: Perceived reasoning for injuries in the literature</i>	18
<i>Table 6: Summary of VGRF and BF in the literature</i>	21
<i>Table 7: Basketball and netball injury comparisons</i>	24
<i>Table 8: Number of papers reporting the use of IMUs to assess workload</i>	38
<i>Table 9: Impact zones in Rugby using GPS</i>	43
<i>Table 10: Game-based and simulated netball movements performed by each participant</i>	57
<i>Table 11: Specification comparison of SensorTag against the requirement</i>	67
<i>Table 12: Hardware specification for working prototype</i>	72
<i>Table 13: Component cost</i>	82
<i>Table 14: Feather prototype comparison with specifications</i>	85
<i>Table 15: Pilot study participant details</i>	89

List of Figures

Figure 1: Netball court positions (Sports Ball Blog, 2018)	8
Figure 2: Netball court position movements ((Singapore Sports Council, 2017)	8
Figure 3: Relative time spent in different intensity zone during matches (Young et al., 2016)	11
Figure 4: Vertical Ground Reaction Force (VGRF) and Braking Force (BF) in netball	19
Figure 5: The overall injury distribution	23
Figure 6: Landing technique suggestion for bilateral and unilateral landings (Mothersole et al., 2013)	31
Figure 7: Methodology overview	49
Figure 8: Delsys Trigno Research+ Avanti™ (Tracklab, 2018)	52
Figure 9: Texas Instruments SensorTag CC2650	53
Figure 10: SensorTag BLE Data Acquisition application	54
Figure 11: Participant lower body mark-up	55
Figure 12: SensorTag axis orientation (A _{IS} --Inferior/Superior axis; AML--Medical/Lateral axis)	55
Figure 13: Trigno axis orientation (A _{IS} --Inferior/Superior axis; AML--Medical/Lateral axis)	55
Figure 14: Two SensorTags (red) and 6 Delsys sensors (blue)	56
Figure 15: Force plate positioning	56
Figure 16: Indoor court positioning layout	59
Figure 17: Participant running trial of 7 second duration	61
Figure 18: Loss of data and Bluetooth dropout (circled red)	62
Figure 19: Participant jumping on the spot and landing (right leg) acceleration data	62
Figure 20: 5.6 minutes of continuous movement data	63
Figure 21: 5.6-minute trial of continuous activities	64
Figure 22: Adafruit Feather Huzzah with ESP8266	74
Figure 23: Sparkfun ADXL345	74
Figure 24: Arrangement of components and wiring	75
Figure 25: Positioning of the accelerometer	76
Figure 26: 3D printed base case	76
Figure 27: Feather and battery secured inside casing (without cover)	77
Figure 28: Final prototype (with cover and taping)	77
Figure 29: Acceleration amplitude calculation (x axis) 1 second epoch	79
Figure 30: Web Interface	80
Figure 31: Activity impact zones during multiple activities	81
Figure 32: Example of activity log	81
Figure 33: Activity: Slow walk (green), followed by jogging (amber)	82
Figure 34: Activity: Sprint and rapid change in direction (red)	83
Figure 35: Participant 2 with the Feather prototype sensor (Right shank) and four Trigno sensors	90
Figure 36: Example walk data (Participant 3) demonstrating peak force (BW), heel strike and Toe off	92

Figure 37: Example 440 step data (Participant 3)	92
Figure 38: MATLAB dataflow for individual analysis	93
Figure 39: A _{IS} amplitude (shank) vs Fz (VGRF) correlation: Participant 1	94
Figure 40: A _{IS} amplitude (shank) vs Fz (VGRF) correlation: Participant 2	94
Figure 41: A _{IS} amplitude(shank) vs Fz (VGRF) correlation: Participant 3	95
Figure 42: Average Fz peak VGRF (BW) based on movements for participant 1, 2 and 3	95
Figure 43: Average A _{IS} amplitude at the shank for movements for of each participant	96
Figure 44: Continuous data collection of participants 3 undertaking laboratory movement protocols	96
Figure 45: A _{IS} amplitude (g) vs Fz peak VGRF (BW) correlation with three impact zones	97
Figure 46: Jump trial comparison: Participant 1 Vertical Ground Reaction Force (VGRF) vs Time	99
Figure 47: Jump trial comparison: Participant 2 Vertical Ground Reaction Force (VGRF) vs Time	99
Figure 48: Jump trial comparison: Participant 3 Vertical Ground Reaction Force (VGRF) vs Time	100
Figure 49: Vicon AMTI OR6-7 Force Platforms Specifications	130
Figure 50: Texas Instruments SensorTag CC2650 Specifications	131
Figure 51: Delsys Trigno Avanti Research+ Specification	132
Figure 52: Delsys Trigno Research+ Axis'	132
Figure 53 - Plugingait Full Body Marker Positions	135
Figure 54: Esp8266 Specification	137
Figure 55: ADXL345 Specifications	138
Figure 56: Adafruit Feather Huzzah ESP8266 pinout diagram	139
Figure 57: A _{IS} amplitude (g) vs Fz peaks (BW) correlation with impact zones	185

INTRODUCTION

Netball is one of the top ten team sports for females in Australia, commonly played in school, community, state, national and international competitions, ranging from leisure play to elite-level participation (IFNA, 2011). The physically demanding sport involves multiple short dynamic sprints, landings, pivots, and rapid changes of directions. The restriction of contact and footwork rules of the game also introduces swift deceleration, typically after performing a landing from a jump or sprint, with over 60 high-intensity movements in 60-minute gameplay (Kearney, 2019). With the high number of participants, together with the physical demands placed on players during gameplay, a significant incidence of injuries has been observed in netball throughout the decade (Hopper, 1986; Hopper *et al.*, 1995; Hume and Steele, 2000; Otago and Peake, 2007; Saunders and Otago, 2009). The incidence of injuries per 1000 hours of gameplay has been recorded to range from 9.08 up to 500.7, the ankle and knee as the most commonly injured site (Best, 2016; Langeveld *et al.*, 2012). The majority of the injury occurrences were soft tissue-related such as ligamentous, sprains and strains, followed by bruising and fractures (Best, 2016; Langeveld *et al.*, 2012).

Research has indicated that excessive, repeated ground reaction forces place the lower extremities at high risk for articular degeneration, ligament damage, cartilage degeneration, osteoarthritis or chronic musculoskeletal disorders (Steele, 1990a). For the lower limbs, the most common mechanism of injury was identified to be incorrect landing techniques, with 52.17% of the total number of injuries (Ferreira and Spamer, 2011). Incorrect landing technique, rapid deceleration, surface conditions, footwear and many other factors could affect the rate and magnitude ground reaction forces player experiences throughout a game, resulting in knee stiffness, decreased flexion angle, ankle instability and trunk stabilisation (Mcgrath and Ozanne-Smith, 1998). These biomechanical instabilities and stiffness can significantly increase the impact dose, cumulative counts of low, moderate and high impact activities experienced, hence resulting in a much higher incidence of lower extremity injuries (Elvin *et al.*, 2007).

Considering the prevalence of lower limb injuries in netball, effective countermeasures are vital. Current countermeasures include educational programs, training regimes, appropriate footwear for shock attenuation, taping and bracing. The overall workload can be classified in terms of internal or external workloads, with work completed by an athlete is defined as external workload, and the relative psychological or physiological stress is defined as internal workload (Halson, 2014). The combination of internal and external load monitoring during training and gameplay provide information regarding the physiological response to training,

changes in athlete performance and risk of overloading and fatigue-related injuries and illnesses (Halson, 2014). Through assessment of workload data, the load-performance relationship can be examined, while also allowing the coach to make informed decisions during competition training schedule planning. However, current internal workload monitoring practices are subjective training practices, that provide an overall fitness and workload assessment of the athlete and fail to quantify the loading of at-risk lower limbs (Halson, 2014). External workload monitoring devices include wearable sensors for impact monitoring which are laboratory-based, expensive or generally inaccessible to sub-elite players (Camomilla *et al.*, 2018; Cummins *et al.*, 2013; Hausler *et al.*, 2016). Due to the lack of active monitoring of the lower limb impact forces in training and games, preventative measures unique/specific to each player cannot be taken, contributing to the onset of chronic injuries. Thus, the overall objective of this project was to contribute to the design and development of an inexpensive and compact wearable device that could quantify lower limb related impact dose experienced during training and competitive netball play. The prototype device would be used by the netball coaches to assess the impact loading of each player during training and matches. This would help coaches identify “at-risk” players and can assist in the development of appropriate training regime, hence allowing proactive injury prevention. The review of the literature identified the growth of wearable devices, such as low cost, portable and widely used Inertial Measurement Unit (IMU), in particular, accelerometer-based units to measure general energy expenditure and lower-limb shock attenuation (Adesida *et al.*, 2019; Camomilla *et al.*, 2018).

This project was initially undertaken as an Honours project in 2018, with a focused objective to determine an accelerometer-based variable which could then be used to deduce impact dose (Corbo, 2018). Findings from the unpublished study using laboratory-based Delsys Trigno Avanti™ Research+ sensors, AMTI OR6-7 force plates and four participants demonstrated that accelerometer variable could be used to represent peak vertical ground reaction force experienced by the lower limb during movement protocols (Corbo, 2018). The best placement of an accelerometer was found to be the shank of a participant, and the acceleration amplitude in the inferior/superior (A_{IS}) axis in a 1-second time window or epoch was correlated to the peak vertical ground reaction force when netball-simulated movements were performed (Appendix O). Impact dose of the lower limb was then deduced based on the accumulative count of low, moderate and high impact activities classified by the impact zones (Corbo, 2018). However, the accelerometer used in the study (Delsys Trigno Avanti™ Research+ sensors) were laboratory-based, with no onboard processing capabilities and 16 sensors exceeded to a

cost of approximately AUD\$20k (cost estimation provided by Flinders University Motion and Rehabilitation Laboratory Supervisor); hence were not a viable solution for sub-elite netball participants. The study further recommended an implementation plan with the potential use of commercially available IMU SensorTag CC2650, manufactured by Texas Instruments to develop a low-cost wearable prototype (Texas Instruments, 2015).

Therefore, the specific aim of the current study was to contribute to the development of an inexpensive accelerometer-based wearable device that could reliably categorise netball simulated movements into impact zones, validating the findings of previous research (Corbo, 2018). Firstly, the SensorTag was assessed to ensure the capabilities of the device were suitable for wearable device development. Laboratory and in situ testing were conducted to validate data streaming, accelerometer sensitivity, range and onboard processing. A subsequent objective was then to create a working prototype sensor and incorporate a user interface, such that A_{IS} amplitude measured at the shank in a 1-second epoch could be displayed to the user. Finally, a correlation and feasibility study was repeated with the prototype sensor to ensure the A_{IS} amplitude was correlated with ground reaction force data obtained from laboratory force plates.

This thesis provides a review of current literature in Chapter 1, providing background information regarding activity profiles amongst netball participants, factors influencing the incidence of netball related injuries, followed by the current injury countermeasures and athlete monitoring technologies. Chapter 2 outlines the project objectives and a general methodology of the three phases of the project. The first phase of the project, as explored in Chapter 3, considers the recommendation of the previous study and conducts laboratory and in situ testing of the SensorTag. The next phase describes the hardware and software development of a working prototype sensor in Chapter 4, and Chapter 5 details a correlation and feasibility study to ensure impact dose could be inferred from the A_{IS} amplitude calculated by the prototype. Finally, the findings from all three studies were summarised and future recommendations were highlighted in Chapter 6.

CHAPTER 1:
LITERATURE REVIEW

1.1 Netball

1.1.1 Popularity of Netball

According to the International Federation of Netball Association (IFNA), netball is played worldwide in over 70 countries (IFNA, 2011). IFNA is the internationally recognised and sole governing body for netball, currently affiliated with over 67 National Netball Associations grouped into 5 regions: Africa, Asia, Europe, America and Oceania. The regions incorporate approximately 20 million people participating in Netball around the world (IFNA, 2011).

In recent years, netball is commonly associated with the top team sport for women and girls in Australia. Netball is played in school, community, state, national and international competitions, ranging from leisure play to elite-level participation. According to the Australian Sports Commission's (ASC) *AusPlay* participation data from 2018, it was recorded that 570,871 players aged above 15 years (approximately 5% of the female population) were participating in netball over the course of the year, with females accounting for 89% of the total participation (ASC, 2019a).

ASC also estimated that 331,031 children between the age 0-14 years participated in Netball at a social club with 97% female participants (ASC, 2018). In particular, netball is the most popular after school sport amongst girls aged between 12-14 years, with approximately a third of the population participating in the sport (ASC, 2018).

1.1.2 Origin of Netball

Netball originated from early adaptations of basketball and was introduced by physical education teachers in 1892 to maintain fitness during bad weather between football and baseball seasons (Taylor, 2001). While it was not specifically designed for female participation, more women began participating in the game in American Colleges, giving rise to *women's basketball* (McLachlan, 2016). The game went through many modifications, such as no dribbling, no contact, and rules that ensured the posture of participants remained graceful (McLachlan, 2016).

Chapter 1: Literature Review

The game was introduced to England by travelling American teachers between 1895 to 1897 and soon gained popularity as the game could be played in a manner that retained femininity and decorum (Taylor, 2001). The rules were further modified over the years, such as moving the game outdoors and replacing baskets by rings with nets. The rules were formalized in 1901 by the Ling Association (The Physical Education Association of Great Britain and Northern Ireland), and hence, the game was named *netball* (McLachlan, 2016).

Soon after gaining popularity in England, netball began spreading to other countries through travelling English physical education teachers, with variations of rules and names. Between 1897 and 1906, a version of netball known as *women's (outdoor) basketball* arrived in Australia and was played in primary and secondary schools (Jobling and Barham, 1991) (Taylor, 2001). Jobling and Barham reported that by 1927, All Australian Women's Basketball Association (*AAWBA*) was formed, and the version of netball known as *women's basketball* was played across the states as part of tournaments (Jobling and Barham, 1991).

By 1960, the rules of netball were standardized across the globe by the establishment of the International Federation of Women's Basket and Netball (IFWBN), which was also known as INFA and currently INF. In 1970, *women's basketball* was officially termed *netball* in Australia (Taylor and Darcy, 2001). INFA also established the Netball World Cup in 1963, held quadrennially, for its 67 member countries, with the most recent tournament occurring 2019 (Taylor and Darcy, 2001). The annual netball season is usually between April to September in Australia, traditionally a winter sport. At elite levels, national championships are held each year, in mainly five competition groups: 17 and under, 19 and under, 21 and under, open age and finally, National Disabled Championship group (Taylor and Darcy, 2001).

1.1.3 Objective and Rules

A game of netball is played between two teams comprised of seven players each on a rectangular court divided into thirds, and the objective is to score as many goals as possible by shooting the ball through the ring. Each of the seven players in a team are assigned a role (Figure 1), including goal shooter (GS), goal attack (GA), wing attack (WA), centre (C), wing defence (WD), goal defence (GD), and finally goalkeeper (GP) (INF, 2018).

***Image removed due to
copyright restriction***

Figure 1: Netball court positions (Sports Ball Blog, 2018)

The length of the netball court is 30.5 meters, and the width is 15.25 meters (INF, 2018). A standard netball game comprises of four 15 minutes quarters, and the team that scores the most goals by the end of fourth-quarter wins. Each player is required to adhere to strict uniform, shoes and wearable policies as listed by International Netball Federation (INF), which also includes wearing a “bib” showing the abbreviation of position. The movements of the players are limited to their specific areas of the court according to their position (Figure 2).

***Image removed due to
copyright restriction***

Figure 2: Netball court position movements ((Singapore Sports Council, 2017)

As the movement within the semi-circle is only allowed by the GS and GA, they are the only two players that can shoot for goal (INF, 2018). WA is defended by the opposing WD and works to move the ball from the centre of the court to an attacking position (INF, 2018). Similarly, WD works to block offensive plays from the opposing team, and guard against GA and GS by preventing their entry into the semi-circle (INF, 2018). GD defends against the GA and assists in defending the goal against opposing team. GK is a very specialised defence, as the last person to prevent the opposing shooter from scoring. Finally, C is the most physically demanding position, as they are involved in offensive and defensive plays and can enter anywhere in the court except the goal circles (INF, 2018).

According to INF, netball has a rigorous set of rules, which includes the players being able to land on either one or both feet when they are in possession of the ball. However, the players are then permitted to take 1.5 steps in any direction while in possession of the ball without counting pivoting as a step (INF, 2018). If the landing foot is lifted, players are to balance on the other foot, and a breach of this rule is known as ‘stepping’ (INF, 2018). Netball has a strict rule of non-contact play and ‘no stepping’, and in addition, defending players are not allowed within 3 feet of the player in possession of the ball. Due to the nature of the footwork rules, the distance in which the players can move is greatly restricted. Hence a player is required to accelerate and decelerate rapidly and maintain a position which provides stability without infringing the footwork rules (Steele, 1990a).

1.1.4 Activity Profile

Netball is a physically demanding sport that requires a high degree of speed, strength, power, endurance and flexibility to deliver consistent performance throughout the 60-minute gameplay, while also effectively recovering between efforts. The nature of the game demands rapid acceleration, deceleration, sudden and explosive changes in direction in a combination of high jumps to receive a pass, intercept a ball or rebound the ball after attempted goals (Steele, 1990a). Throughout the years, many studies have quantified the activity pattern of different position players both in elite and non-elite levels (Bailey *et al.*, 2017; Fox *et al.*, 2013a; Otago, 1983; Thomas *et al.*, 2019; Young *et al.*, 2016).

1.1.4.1 Activity pattern

In a 2013 study conducted by Fox *et al.*, video footage of netball players was captured and analysed for each individual player throughout the match, and the activities were classified into eight game-based activities and five-movement activities. The movement activities included walking, jogging, shuffling, running, and sprinting whereas the game based activities were classified as a goal, pass, catch, jump, rebound, guard, off-ball guard and defend (Fox *et al.*, 2013b). The resultant mean percentage of activities performed by each court positions was summarised (Table 1).

Table 1: Mean percentage of active time spent performing activities by each court position (adapted from (Fox et al., 2013b))

	GK	GD	WD	C	WA	GA	GS
Walking	35.2	40.4	45.4	38.9	46.6	46.3	51.7
Jogging	5.2	16.2	10.8	20.5	15.6	15.9	5.0
Shuffling	51.7	20.8	31.2	26.1	21.9	20.7	23.6
Running	1.7	6.7	5.0	5.5	6.4	6.7	5.4
Sprinting	0.2	3.1	3.7	3.0	4.8	3.0	3.4
Goal	-	-	-	-	-	3.7	7.5
Pass	1.7	2.4	3.3	6.2	5.1	3.8	3.7
Guard	1.8	2.4	4.2	2.9	1.4	1.7	0.9
Off-Ball Guard	34.3	19.7	15.7	10.0	4.9	2.1	0.7
Defend	5.3	3.3	-	-	-	-	-

Fox *et al.* concluded that the active period did vary based on court position, with Centre performing the highest frequency of activities conducted throughout the game (Table 1).

The most significant influence on the active time was the court space restrictions, where positions with lower restrictions exhibited a higher percentage of activity. The explosive nature of the game also resulted in average Work: Rest (W:R) ratio performed by all positions to be 1:5 or higher (Fox *et al.*, 2013b). A similar study was undertaken by Otago in 1983, which displays some differences and similarities in the game demands when compared to the study conducted by Fox *et al.* in 2013. In the 30-year period, there has been an increase in the percentage of active time in a game, with a greater number of game movements and increased “work” period. Both studies, therefore, confirm that positional differences exist regarding the amount and type of activities.

1.1.4.2 Player Workload

Due to the varying levels of activities, positional differences between the players also exhibit a difference in player workload, which has been confirmed by several studies (Bailey *et al.*, 2017; Cormack *et al.*, 2014; Hopper *et al.*, 1992; Young *et al.*, 2016). In a recent study by Young *et al.*, accelerometry was used to measure player load amongst different court positions, and activities were categorised into sections of low, low-moderate, moderate and high-intensity zones (Figure 3).



***Image removed due to
copyright restriction***

Figure 3: Relative time spent in different intensity zone during matches (Young et al., 2016)

It must also be noted that in these studies, “load” is defined as workload according to the intensity and type of activities performed, not the calculated force by taking mass and acceleration into consideration.

As indicated in Figure 3, C, WD, WA and GA positions exhibited the highest playing intensity and the least amount of time spent in the low-intensity zone, however GS, GK and GD positions displayed opposing characteristics (Young *et al.*, 2016). This is consistent with the findings of another study conducted by Bailey *et al.*, who concluded that players in defending positions exhibit more substantial non-locomotor activities to the total match load for different positions, compared to players in attacking positions (Bailey *et al.*, 2017). These findings can be applied to elite netball to aid in the design and implementation of training programs according to the specific need to the physical requirement of each position.

1.2 Epidemiology and Incidence of Netball Injuries

1.2.1 Incidence of Injuries

In a 2016 study conducted by ASC with standardised data from October 2015 to September 2016, it was found that netball was within the top 20 most popular activities for adult Australian players, with 630,638 participants accounting for the 3.2% population (ASC, 2016). The participation data from 2019 showed that the total number of adults participating in netball was 570,871, accounting for 2.8% of the population (ASC, 2019a). Therefore, a noticeable decline of 60 thousand adult participants was observed in the 2-year window. ASC also reported that about 22% of the dropout occurred, with poor health or injury acquired during netball gameplay being one of the top two reasons (ASC, 2019a).

Netball is a physically demanding sport that requires a high degree of speed, strength, endurance and flexibility. With the high number of participants, together with the demands placed on players during participation, there is a risk that injury will occur. Throughout literature, incidence of netball injuries has been highly publicised due to the high frequency of occurrence.

In a 1995 study, Finch reported that, of all injuries leading to emergency hospitalisations amongst adults above 15 years of age, 6.6.% of the injuries were sporting related, with netball ranked as the seventh greatest cause of sport-related emergency hospitalisation (Finch, 1995). In 1986, Hopper investigated 3108 netball players of varying age and skill level in Western Australia over a fourteen-week season (Hopper, 1986). In total, 158 injuries were recorded, accounting for a 5.2% injury rate (Hopper, 1986). The insurance claims made in a 12 months period made in Victoria during 1999 was studied by Otago and Peake in 2007, and it was found that there were 9.49 injuries per 1000 players, with 829 total claims for netball related injuries (Otago and Peake, 2007). This finding was consistent with another study undertaken in 1996 by McKay *et al.*, comparing the injuries sustained by female basketball and netball players, and found 17.30 injuries occurring per 1000 netball players in elite level (McKay *et al.*, 1996).

Several studies also quantified the number of injuries in terms of hours of gameplay for both elite and community levels. During the 1995 New South Wales Netball Championships, 131 injuries occurred amongst 940 elite participants, which results in 139.4 injuries per 1000

players or 23.8 injuries per 1000 playing hours (Hume and Steele, 2000). In 2002 Finch *et al.* found that in a cohort of 379 community level netball players in Western Australia, about 11.3 injuries occurred per 1000 hour of gameplay (Finch *et al.*, 2002). An overall increase in injury occurrence is observed at the elite level compared to the community level, which was also verified by Hopper *et al.* For example, in a single match, internationally competing netballers can perform up to 81 high intensity sprints with an average duration of 1.4–1.6s and elite netballers also complete up to 63 manoeuvres (split step, side step shuffle, spin and stop and back), and 83 jumps, hence completing activities above 85% maximal heart rate for majority of the match time (Fox *et al.*, 2014, 2013b; Kennedy *et al.*, 2011). Upon review of a range of player levels and age in Australia, Simpson *et al.* concluded that elite players express greater lower limb powers and higher number of sprints compared to community players, and the increase in repeated high-intensity activity can act as a catalyst for observed higher incidence of injuries in elite players (Simpson *et al.*, 2019).

Internationally, in a more recent injury audit of Netball Super League season in England, Best reported 9.08 injuries occurred per 1000 hours of gameplay in elite levels (Best, 2016). Another study was conducted of a mixed cohort of South African netball players in 2009, with Langeveld *et al.* reporting the incidence of 500.7 injuries per 1000 playing hours (Langeveld *et al.*, 2012). Best studied the cohort size of 103 participants with 59 recorded injuries, whereas Langeveld *et al.* studied 1280 participants with 205 recorded injuries. The injury rate collected through the South African study is higher than both England and Australia based studies, potentially due to differences in data collection methods or environmental constraints. Hume and Steele, Hopper *et al.* and Best used insurance claims made by injured participants to calculate injury data, whereas Langeveld *et al.* collected data based on how many participants received medical attention during netball gameplay (Best, 2016; Hume and Steele, 2000; Langeveld *et al.*, 2012). Overall, the epidemiological studies provide overwhelming evidence of the risk of injuries associated with both elite and non-elite netball gameplays. In comparison, at the elite level. sprint and middle distance runners had an injury rate of 5.6 to 5.8 per 1000 hours of training, and basketball players had 9.8 injuries per 1000 hours of gameplay (Cumps *et al.*, 2007; Lysholm and Wiklander, 1987). The incidence of injuries in netball found in literature from 1986 to 2018 is summarised in Table 2.

Chapter 1: Literature Review

Table 2: Incidence of netball injuries in the literature (adapted from (Mcgrath and Ozanne-Smith, 1998))

Author	(Hopper, 1986)	(Steele, 1990a)	(Hopper and Elliott, 1993)	(Hopper <i>et al.</i> , 1995)	(McKay <i>et al.</i> , 1996)	(Hume and Steele, 2000)	(McManus <i>et al.</i> , 2006)	(Otago and Peake, 2007)	(Langeveld <i>et al.</i> , 2012)	(Best, 2016)	(Hides <i>et al.</i> , 2018)
Data Source	Winter competition in Western Australia	Elastoplast-Nivea Netball Classic	All Australian Netball Championships	Winter competition in Western Australia	Victoria competition	New South Wales Championship	Data from 1997-1998	Insurance claims made during 1999, Victoria	2009 USSA championship, South Africa	Super league netball team, England	9 division with different skills
Subjects	3,108 female (158 injuries)	1053 (47 injuries)	52	11,228 females (608 injuries)	9910	940 females (131 injuries)	336 (252 injuries)	829 injuries	1280 (205 injuries)	103 (59 injuries)	269 (169 injuries)
Age range	Mixed	Above 30 years	-	Mixed	-	14 – 22.2 years	16-30 years	Mixed	Under 19, under 21, senior	-	Mixed
Skill level	Elite and recreational	Veteran	-	Elite and recreational	Elite and recreational	Premier League	Non-elite	All skill	Elite	Elite	Community
Period	14-week winter season	Tournament	Tournament	5 years of 14 week season	2 seasons	Three-day tournament	2 years of 14-week winter season	One year	Three netball tournaments (447 games)	One season	3324 games and 8918 training hours
Injury rates (per 1000 hours)	-	-	-	-	-	23.8	14	9.49	500.7	9.08	Game: 32.2 Training: 4.7

Note: - (dash) refers to data not reported in the respective study

1.2.2 Location and Classification of Injuries

Hospital data collected by Australian Institute of Health and Welfare (AIHW) in 2013 show netball to be the principal cause of knee injury leading to hospitalisation (29%) amongst females, followed by ice and snow sports at 11.1% (AIHW, 2013). In the same AIHW report, netball was also identified to be in the top 3 sports for highest hospitalisation due to anterior cruciate ligament injury, acetabular fracture, wrist dislocation and meniscal tears (AIHW, 2013). It has been revealed that players in Premier League divisions and in higher age groups (with a higher level of skills) are more susceptible to injuries (Langeveld *et al.*, 2012).

Epidemiological literature from 1986 to 2018 (Table 3), regarding netball injuries revealed the most commonly injured location to be lower limb of participants (Best, 2016; Hopper, 1986; Hume and Steele, 2000; Langeveld *et al.*, 2012; McKay *et al.*, 1996; Otago and Peake, 2007; Steele, 1990b). Due to rapid change of direction and speed, ankles and knees are most injured, and other potential injury sites were summarised (Table 4).

Table 3: Location of injuries (adapted from (Mcgrath and Ozanne-Smith, 1998))

Author	(Hopper, 1986)	(Steele, 1990a)	(Hopper and Elliott, 1993)	(Hopper <i>et al.</i> , 1995)	(McKay <i>et al.</i> , 1996)	(Hume and Steele, 2000)	(McManus <i>et al.</i> , 2006)	(Otago and Peake, 2007)	(Langeveld <i>et al.</i> , 2012)	(Best, 2016)	(Hides <i>et al.</i> , 2018)
Location of injuries (%)											
Upper limb	13.3	22.8	-	2.8	25.7	4	15	8.7	16.1	-	-
Lower limb	86.7	70.4	-	92.6	65.9	-	66	85.3	-	-	60
Calf/ Shin	-	13.6	19.2	-	10.1	-	5.5	-	-	-	-
Foot	-	13.6	11.5	-	0.8	-	-	-	-	-	-
Knee	15.2	9.1	17.3	8.3	17.8	14	17	44.4	18.5	-	-
Ankle	58.2	29.6	36.6	84.3	30.2	14	32	31	36.1	35.6	Most common
Other	26.6	34.1	15.4	7.4	41.1	72	45.5	24.6	45.4	64.4	-

Table 4: Classification of injuries

Author	(Hopper, 1986)	(Steele, 1990a)	(Hopper and Elliott, 1993)	(Hopper <i>et al.</i> , 1995)	(McKay <i>et al.</i> , 1996)	(Hume and Steele, 2000)	(McManus <i>et al.</i> , 2006)	(Langeveld <i>et al.</i> , 2012)
Classification of injuries (%)								
Soft tissue injuries/ Sprain	-	52.3	-	8	62.9	Ligament: 37 Muscle: 17	22	12.3
Fracture	-	9.1	-	-	-	-	-	-
Bruising	-	15.9	-	-	17.6	18	15	14.8
Other	-	22.7	-	92	19.5	28	63	72.9
New	71.3	-	63.5	65	-	-	-	-
Chronic	28.7	-	36.5	35	-	-	-	8.8

Chapter 1: Literature Review

The difference in the method of data collection, method of the data treatment, sample size and the classification of an “injury”, contributed to the big range is present in the data. It must also be noted that more injuries were observed in gameplays in elite tournaments compared to training and gameplays during a season, due to the higher intensity efforts causing substantial increases in lower limb stress in elite players.

Table 3 illustrates that across literature from 1986 to 2016, lower extremities account for 65.9% to 92.2% injuries, with the ankle being the most frequent site of injury. Injuries in upper extremities are considerably smaller, been reported between 2.8% to 25.7%. Across the literature, the most common site of injury was ankle with 14% to 84.3% injuries, followed by knee injuries with 9.1% to 44.4% injuries (Table 3). Other common sites of lower limb injuries included calf/shin accounting for 5.5% to 13.6% injuries and foot accounting for 0.8% to 13.6% injuries.

Although most literature throughout the 30 year analysis recognised ankle being the most common site of injury, Otago and Peake assessed insurance claims made during 1999 in Victoria, and reported higher cases of knee-related injuries: such as ligament sprain, knee reconstruction, Anterior Cruciate Ligament (ACL) rupture and knee arthroscopy, combining up to 44.4% of all injuries (Otago and Peake, 2007).

In an earlier study, Finch reported that injuries concerning the ankle most commonly involved sprains or tears of the anterior talofibular ligament (56%), while ACL was the leading site of injury in the knee (22%) (Finch, 1995). In a recent 2012 South African study, Langeveld *et al.* reported that 89% of the ankle injuries were associated with the ligaments, with 4.9% to the deltoid ligament and 28% sustained to the lateral ligament complex (Langeveld *et al.*, 2012). Menisci sustained the majority of the injuries for the knee (36.1%), including bruising (19.4%) and lacerations (11.1%) at the knee (Langeveld *et al.*, 2012). In most studies, the majority of the injuries were considered minor as the player was available in a few days for the next game. However, Langeveld *et al.* reported that 12.4% of the players could not return to play for more than 7 days, and required extensive medical attention such as reconstructive surgery (Langeveld *et al.*, 2012).

Due to the large proportion of female participants in netball, throughout literature females were the dominant group injured representing 85% of cases, in particular, those aged 20-24 years

(33%) (Hopper, 1986). The majority of the injury occurrence were soft tissue related such as ligamentous, sprains and strains, accounting for 8% to 62.9% of cases followed by bruising with 14.8% to 15.9% of the cases (Table 4). Fractures were less common but have been reported in studies to account for 9.1% of injuries. Chronic injuries were also less prevalent when compared to new injuries, which ranged from 63.5% to 71.3% of the cases.

1.2.3 Cause of Injuries

Netball consists of running to meet a pass, to catch a ball, and coming to a sudden stop on either one of two feet, and the speed at which these movements occur influences the muscle activity, range of motion and Ground Reaction Forces (GRF). The overall explosive nature of play of netball and the rapid change in direction and acceleration and repeated lower limb loading in combination has led to a significant rate of injuries. Consequently, this culminated in high injury rates as demonstrated through literature (Table 5):

Table 5: Perceived reasoning for injuries in the literature (adapted from (Mcgrath and Ozanne-Smith, 1998))

Author	(Hopper, 1986)	(Hopper and Elliott, 1993)	(Hopper <i>et al.</i> , 1995)	(McKay <i>et al.</i> , 1996)	(Hume and Steele, 2000)	(Langeveld <i>et al.</i> , 2012)	(Hides <i>et al.</i> , 2018)
Perceived reason for injuries (%)							
Collision	16.7	28.8	22.6	20.2	15	60.8	28
Overuse		9.6	-	-	5	-	-
Slip/fall	28.6	9.7	23.2	13.4	8	-	-
Landing	33.3	28.8	38.7	15.1	13	-	27
Sudden stop	-	11.5	-	1.8	-	-	-
Other	7.1	11.4	15.5	9.5	16	-	-

When considering the cause of the injuries, 15% to 60.8% of the injuries were caused by collisions with other players, contact from the ball, followed by incorrect landing leading to 13% to 38.7% of the injuries (Table 5). Other perceived reasons for injuries also included slipping or falling (8% to 28.6%), sudden stop (1.8% to 11.5%), overuse of muscles or overextension (5% to 9.6%) and finally other causes (i.e. surface, footwear, fatigue) accounting for 7.1% to 15.5% of injuries.

Research has indicated that excessive, repeated GRFs, which has a vertical component expressed as VGRF and a horizontal component (HGRF), or braking force (BF) (Figure 4) place the lower extremities at a high risk for articular degeneration, ligament damage, cartilage degeneration, osteoarthritis or chronic musculoskeletal disorders (Steele, 1990a). For the lower limbs, the most common mechanism of injury was identified to be incorrect landing techniques, with 52.17% of the total number of injuries (Ferreira and Spamer, 2011). Incorrect landing technique, rapid deceleration, surface conditions, footwear and many other factors could affect the rate and magnitude of VGRF, and BF a player experiences throughout a game, resulting in knee stiffness, decreased flexion angle, ankle instability and trunk stabilisation (Elvin *et al.*, 2007; McGrath and Ozanne-Smith, 1998). These biomechanical instabilities and stiffnesses can significantly increase the impact dose, hence resulting in a much higher incidence of lower extremity injuries (Elvin *et al.*, 2007).

***Image
removed
due to
copyright
restriction***

Figure 4: Vertical Ground Reaction Force (VGRF) and Braking Force (BF) in netball

Although many sports such as football, basketball and rugby require landing, how the body reacts in different sporting conditions significantly differ due to match-play movement demands, rules and surface conditions. It is therefore important to understand netball GRF and how various factors can affect it by analysing literature.

In 1987, Steele and Milburn tested four different types of footwear and how VGRF and BF would change after landing on one foot (Steele, JR, Milburn, 1987). Amongst the 15 elite athletes, VGRF ranged between 3.9-4.3 times their body weight (BW) and 4.2-4.6 times their BW for BF. It must also be noted that Steele and Milburn only used centre position players and concluded that by altering the landing mechanics, GRF could be reduced more significantly than any specific footwear (Steele, JR, Milburn, 1987).

Chapter 1: Literature Review

In a follow-up study in 1988 by Steele and Milburn, the influence of 12 types of synthetic sports surface of GRF was examined by using 10 skilled netball players (position of players were not specified) (Steele and Milburn, 1988). These players performed an attacking movement on these surfaces, and the mean VGRF for dominant foot landings were 3.8 BW, and for BF, the mean was 3.4 BW (Steele and Milburn, 1988).

In another study in 1989, Steele and Lafortune compared the GRF produced by either a heel or forefoot dominated landing while using match specific maneuverers amongst 10 skilled netball players (Steele and Lafortune, 1989a). The whole movement involved running forwards, evading a defender, jumping into the air to receive a pass and then landing on the dominant leg. The mean VGRF for the heel and forefoot was 5.3 and 5.7 BW respectively, while the mean BF for the heel and forefoot was 3.3 and 2 BW (Steele and Lafortune, 1989a). These are considered high in comparison to other impact sports such as basketball, which has shown a median VGRF of 4.3 BW during vertical jump landings (McClay *et al.*, 2016)

In other similar studies, the mean VGRF was found to be 5.3 BW, and while testing different landing techniques, the VGRF ranged from 3.4 to 4.25 BW, and BF ranged from 0.83 to 1.75 BW (Table 6) (Hopper *et al.*, 1999)

Table 6: Summary of VGRF and BF in the literature (adapted from (Steele, 1990) and (Mothersole et al., 2013))

Study	Subjects	Movement researched	Number of trials per subject	Activity for each subject	Average VGRF (BW)	Average BF (BW)
(Steele, JR, Milburn, 1987)	15 Elite netball players, the centre position	Typical netball landing manoeuvre while barefoot or wearing shoes	3 trials per subject per foot condition	Change of shoes (barefoot or wearing shoes)	Barefoot: 4.3	Barefoot: 4.6
					Shoe:3.9	Shoe: 4.2
(Steele and Milburn, 1988)	10 on elite (skilled) netball players	An attacking movement which involves accelerating from a standing position, sudden stop onto a force platform, receiving a pass, and off-loading the ball to another player	3 trials per subject	Change of surface condition	3.8	3.4
(Otago, 2004)	14 under 21 netball players	Range of landing movements while performing a task	Unspecified	Subjects were asked to perform landing on a force plate while performing a task	Pivot landing: 4.25	Pivot landing:1.36
					Two-foot landing: 5.74	Two-foot landing: 1.75
					Run-on landing: 3.53	Run-on landing: 0.83
(Hopper <i>et al.</i> , 1999)	15 Elite netball players	Single leg forward jumps while 125 times their length	3 trials per subject	Each subject performed the jump	3.4	Not available
(Steele and Lafortune, 1989a)	10 on elite (skilled) netball players	A movement involving running forward, evading a defended, leaping to receive a pass and landing on the dominant leg	unspecified	Subjects were instructed to land on either their forefoot or heel	Forefoot: 5.7 Heel: 5.3	Forefoot: 2.0 Heel: 3.3

In summary, the literature shows the average VGRF and BF to range from 3.51 – 5.74 BW and 0.83 – 4.56 BW, respectively. This can pose significant stress on the lower limb when performing repetitive landing in netball, hence contributing to the overwhelming lower limb injuries as landing dose increases. Some of the landing factors to consider may be drop height: which directly impacts the landing velocity, jump distance: which determines the angular momentum, and finally, landing strategy: as landing with 1 or 2 feet required different muscular recruitment process and balance (Mothersole *et al.*, 2013). Secondary factors such as knee angle during initial ground contact, knee flexion, trunk stabilisation, foot placement and ankle stability during landing have also contributed to higher GRFs (Mothersole *et al.*, 2013).

Research throughout the decades has demonstrated how these injuries lead to a reduction of the level of sports activity, need for medical treatment, and adverse social and economic effects for that athlete. Recent data from ASC shows that poor health or injury was the catalyst for a 22% adult drop out of netball in 2018, with fear of injury adding another 5% drop out rate (ASC, 2019a). As previously discussed, in just two years, netball in Australia has seen approximately 60 thousand adult participants drop out, further demanding the need for proper consideration of countermeasures to be placed for netball injury prevention.

1.2.4 Similar Injuries in Other Sports

There is an abundance of literature available surveying the incidence of injuries amongst a range of contact and non-contact sports. As netball originated from basketball, the prevalence of injuries in basketball throughout the literature was analysed. According to ASC participation data, in Australia, there are 699,007 adult basketball participants, with the male majority (ASC, 2019b). With such high participation, ASC found poor health/injury was the reason for a 15% drop out along with fear of injury being the following reason for drop out of up to 10% (ASC, 2019b). The injury dropout rate is 7% less than Netball as previously reported by ASC.

In 1985, Smithers and Myers reported the survey of injury rates from several Brisbane hospitals alongside the relevant sporting injuries (Smithers and Myers, 1985). In this study, netball was identified to be the sports with the highest incidence of ankle sprains (Smithers and Myers, 1985). The type of injury within basketball was not specified; however, joint sprain and fracture were deemed as the leading cause of injuries (Smithers and Myers, 1985). In a 1996 study by McKay *et al.*, it was found that netball players sustained more severe injuries at a 3.3 times

higher rate than female basketball players, as on average netball had one severe injury per 250 games in contrast to one per 625 games in basketball (McKay *et al.*, 1996). A study was conducted with 6,972 female basketball players and 9,190 netball players, with an injury rate of 18.2 and 17.3 per 1000 hours of participation, respectively (McKay *et al.*, 1996). Although head and neck injuries were prevalent in basketball, knee, ankle and calf/shin were the most commonly injured body parts in terms of both minor and severe injuries (McKay *et al.*, 1996).

A further study specifically exploring the ankle injury surveillance in basketball from McKay *et al.* identified ankle as the most common injury site, with 3.83 ankle injuries per 1000 participants (McKay *et al.*, 2001). In 2009, Flood and Harrison conducted a population-based retrospective descriptive epidemiological study about netball and basketball relating injuries using the data from the National Hospital Morbidity Databases from July 2000 to June 2004 (Flood and Harrison, 2009). It was found that netball displayed a higher rate of injuries amongst females compared to basketball (Figure 5) (Flood and Harrison, 2009). More importantly, netball displayed a significant increase in Achilles tendon injury and dislocation, sprain or strains of joints of the knee compared to basketball (Flood and Harrison, 2009). The incidence of forearm fracture was, however, more evident in basketball, possibly due to more frequent collisions with other players on the field, which is prevented in netball due to the “no contact” rule. Literature comparing injury surveillance in netball and basketball was summarised (Table 7).

***Image removed
due to
copyright
restriction***

Figure 5: The overall injury distribution amongst the 5090 basketball related and 4596 netball related hospital admission (Flood and Harrison, 2009)

Chapter 1: Literature Review

Table 7: Basketball and netball injury comparisons

Studies	Study type	Sport	Participants	Injury	Top 3 frequent injury sites and relative injuries	Injury severity
(Smithers and Myers, 1985)	Survey of casualty at several Brisbane hospitals	Basketball	Over 12 months, 1652 cases of injuries were assessed	45 (2.8%)	Lower limb (47%), upper limb (40%), head/neck (8%)	Joint sprain (37%), fracture (34%)
		Netball		68 (4.3%)	Lower limb (75%), upper limb (20%), head/neck (3%)	Highest incidence of ankle sprain (48%)
(McKay <i>et al.</i> , 1996)	A comparative study (basketball and netball)	Basketball	6,972	18.22 per 1000 players	Ankle, hand, knee	1 severe injury per 625 games
		Netball	9,190	17.30 per 1000 players	Ankle, knee, hand	1 severe injury per 250 games (3.3 times higher)
(McKay <i>et al.</i> , 2001)	Ankle injury surveillance in basketball	Basketball	10,393 (77.9% recreational and 22.1% elite)	40 ankle injuries	Ankle: 3.85 injuries per 1000 participants	45.9% of injured players missed one week or more competition
(Flood and Harrison, 2009)	Epidemiology of basketball and netball injuries resulting in hospitalisation (2000-2004)	Basketball	National Hospital Morbidity Database data (1 July 2000 to 30 June 2004)	5090 (71.5% male)	Knee or leg (1,248), elbow/forearm (962) and wrist/hand (813)	ACL rupture (7% hospital admissions), Achilles tendon injury (7%)
		Netball		4596 (88.9% female)	Knee or leg (1700), ankle/foot (954), and elbow/forearm (735)	ACL rupture (16.5%), Achilles tendon rupture (15.9%)

Despite the similarities between netball and basketball due to the shared origin, epidemiological studies conducted from 1985 to 2009 show more lower limb injuries, such as Achilles tendon sprain, ACL rupture, strains and soft tissue injuries are observed in netball than basketball. These injuries are increasing the hospital admissions, and the long-term consequences will impact the social and personal wellbeing of the individual, as well as the community.

1.3 Current Injury Countermeasures for Netball

Currently, there are a number of countermeasures that were categorised by Watt and Finch, into primary, secondary and tertiary interventions (Watt and Finch, 1996). Primary interventions were acts prior to an event to prevent injury, while secondary interventions were acts during the event to prevent injury and reduce the severity, and finally, tertiary interventions were acts after the event to minimise the consequences of injuries (Watt and Finch, 1996). The primary and secondary intervention methods are discussed in this review as methods of injury countermeasures.

1.3.1 Training Techniques

One of the primary intervention methods to prevent injuries is ensuring a proper training regime based on the physiological demands placed on the individual players during a game. Warming up before a game can raise body temperature, increase blood flow to the muscles, increase muscle elasticity and improve the range of motion of the joints (Mcgrath and Ozanne-Smith, 1998). Warming up may be carried out for 10-20 minutes prior play, and stretching exercises, with limited time window in between play and warm-up activities (Mcgrath and Ozanne-Smith, 1998). Continuous movement is encouraged during gameplay if the player is not actively engaged for the duration of gameplay, to prevent the body from cooling down and staying alert. Cooldown is also very critical to ensure excess fluid and waste products are removed from muscles, which can reduce muscle stiffness and soreness, and gradually return the body to resting state (Mcgrath and Ozanne-Smith, 1998).

To reduce the risk of musculoskeletal injuries, warm-up, stretching and cool down are implemented in Netball gameplay according to the guidelines of Netball Australia (Mcgrath and Ozanne-Smith, 1998). Laboratory studies conducted by Woo *et al.* demonstrated that joint range of motion is dependent on the mechanical properties of connective tissues, which is altered in response to load and variations in temperature (WOO and L-Y., 1990). In New Zealand, implementation of warm-up programs such as NetballSmart Dynamic Warm-up demonstrated significant improvement on a cohort of 81 youth high school netball players in terms of vertical jump and prone hold (McKenzie *et al.*, 2019).

In addition, it is critical to ensure periodisation is applied during training implementations. Periodisation considers that training is designed according to the physiological need of each individual players, such as ensuring sufficient time for recovery, and the intensity and volume of training are increased gradually with enough rest in between training sessions. Incorrect training regime can lead to chronic and overuse injuries due to muscle fatigue and exhaustion. It is important to ensure that training programs enable athletes to peak when required and maintain an enhanced fitness standard during competition season. Therefore, training programs are developed with well-equipped coaches with advanced planning and knowledge of the sports requirement and the individual fitness of players.

1.3.2 Educational Programs

In direct response to the overwhelming incidence of injuries in lower limb amongst netball players, several netball officials have established educational programs to raise awareness regarding injury prevalence in netball.

In 1993, the Accident Compensation and Rehabilitation Corporation (ACC) and New Zealand netball officials established a formal program targeted towards secondary school students titled “Your Body-Your Choice” (Mcgrath and Ozanne-Smith, 1998). The program kits were distributed amongst 10 Dunedin based secondary schools, and each kit consisted of an 11-minute instructional video, wobble board and printed educational resources highlighting the cause of injuries, training guidelines, techniques, strengthening exercises, injury treatment and sources of further information (Mcgrath and Ozanne-Smith, 1998). The primary objectives of the program were to reduce the number and severity of injuries in netball while raising awareness for the correct techniques and training programs and increasing proper first aid and rehabilitation procedures. The program was deemed successful as the number of injuries was reported to reduce by 14% from the year 1991. Due to the success of this pilot program, the kit was further introduced to all New Zealand secondary schools, with expected long term reduction in injuries overall by 5% (Mcgrath and Ozanne-Smith, 1998). No further study has reported on the injury reduction since the pilot of the program.

In 2015, Netball Australia and Australian Institute of Sport (AIS) followed on the footsteps of New Zealand, by introducing “Knee injury prevention for Netballers and Enhance performance and Extend play” (KNEE) program, an on-court warm-up program designated to prevent injury

and increase movement efficiency (Netball Australia, 2019). The KNEE program is digitally available for free, includes a wide range of warm-up, strength, balance/landing, and agility training. The program targets junior, recreational and elite level athletes, with tailored exercises to match the capabilities of each group. The program is reported to reduce the incidence of lower limb injuries, in particular, ACL injuries, by educating coaches, players and staff involved through appropriate landing techniques, safe changes of direction and efficient movement around the court (Netball Australia, 2019). For best result, the program requires minimum completion of twice a week and continuous maintenance throughout the season (Netball Australia, 2019).

“Down to Earth” (D2E) is another educational program devised by researchers at the University of Ballarat, focused on safe landing techniques during netball to prevent lower limb injuries such as ACL rupture (Saunders *et al.*, 2018). D2E is a home-based 6 weeks long program that can be incorporated into their normal training, with suggested warm-up activities and safe landing techniques (Saunders *et al.*, 2018). In 2019, a pilot study was conducted by Zulkarnain *et al.*, where a group 42 varsity netball players were split into two groups and half were provided with the D2E program in their training regime for the entire duration of 6 weeks (Zulkarnain and Khairullina, 2019). It was found that the number of injuries during training in the control group and 0.01 (injuries) higher rate of lower limb injury than those participating in the D2E program, hence the study concluded the D2E program was beneficial in reducing risk in lower limb injuries (Zulkarnain and Khairullina, 2019). However, for a more statistically reliable result, the study should be re-recorded with a higher number of participants from different skill levels.

1.3.3 Footwear

Footwear is an essential countermeasure to netball injuries, as it has the role of providing support, comfort, stability and shock absorption for the participant. In the design of netball footwear, the following considerations must be accounted for, such as conditions experienced by players during movements, activities performed, surface, comfort, shock attenuation, lateral stability and optimal friction characteristics between tread patterns and playing surface (Hopper, 1986). In a 1987 study, Steele and Milburn undertook a kinematic analysis of netball landing techniques on 21 centre position players, with four types of footwear (running shoe, netball shoe, ankle support with netball shoe and barefoot). It was found that when landing

barefoot, subjects altered the landing limb alignment, with greater knee flexion, the angular velocity of the leg, reduced horizontal velocity of the lateral malleolus when compared to when wearing shoes (Steele, JR, Milburn, 1987).

The authors also concluded the design of the shoe does not necessarily allow transmission of reduced force to the player's body, but rather the effectiveness of the footwear is directly influenced by the landing techniques (Steele, JR, Milburn, 1987). In more recent studies, it has been reported that if the repetitive impact GRF during netball gameplay exceed the shock absorption system of the footwear, it may be subjected to a displacement limit or bottom out (Jaiyesimi, 2018).

1.3.4 Taping and Bracing

Taping and bracing has been used consistently throughout the years, and aid in the reduction of movement in a joint, which in turn is reported to reduce the severity of an injury (Mcgrath and Ozanne-Smith, 1998). Taping and bracing can be prophylactic (lessen the severity of an injury), rehabilitative (protect injured joints) or functional (stability for unstable joints) (Mcgrath and Ozanne-Smith, 1998). Numerous studies have been conducted to evaluate the effectiveness of taping and bracing, on ankles and knees, with very conflicting results. a 1994 study was conducted by Sitler *et al.* on semi-rigid ankle stabilisers to reduce ankle injuries in basketball with 13,430 participants, with no prior evidence of ankle instability (Sitler *et al.*, 1994). The study by Sitler *et al.* found that the ankle stabilisers significantly reduced the incidence of ankle injuries, in particular, contact injuries, whereas, in the same year, Grana *et al.* found no significant improvement while wearing ankle stabilisers (Grana, 1994; Sitler *et al.*, 1994). Hopper *et al.* also concluded in a 1999 study that although using ankle braces can lead to some changes in muscle activity, the magnitude of the changes was not enough to influence the time to peak VGRF or position of the foot (Hopper *et al.*, 1999). Therefore no evidence was found to conclusively state whether ankle bracing had a positive or negative effect on the injury incidence (Hopper *et al.*, 1999). Warden *et al.* performed a meta-analysis of various studies from 7 electronic databases (up to November 2006) to evaluate the effectiveness of patellar taping and bracing in the management of chronic knee pain, and found insufficient evidence to draw conclusions regarding the efficiency of patellar bracing due to high heterogeneity between study outcomes and significant publication bias (Warden *et al.*,

2008). Due to the conflicting literature findings and insufficient results, the use of taping and bracing during netball should remain as a personal choice for the athletes.

1.3.5 Codes of Conduct

Several rules have been established throughout the years by officials to reduce injury occurrences, such as the penalty given for obstructions and contact with the player while in possession of the ball. This reduces the number of collisions and subsequent falls, resulting in the prevention of severe injuries. In addition, jewellery, hair clips, long nails and protruding wearables such as activity watches are not allowed in netball. If a player sustains an injury, the play can be stopped for up to two minutes or as indicated by the umpire. In case of severe injuries and subsequent removal of the player, substitution can be made (Mcgrath and Ozanne-Smith, 1998).

1.3.6 Netball Surface

Netball is played on a wide range of surfaces, such as timber, natural turfs, concrete, bitumen, synthetic grass and variations of synthetic rubber, both indoors and outdoors. It was theorised in early literature, that the shock absorption and frictional properties of these surfaces can affect the distribution of VGRF, and BF experienced by joints and tendons of lower limbs, and harder surfaces are said to increase mechanical shock, resulting in overloaded lower limb joints (Mcgrath and Ozanne-Smith, 1998).

In a 1987 study conducted by Steele and Milburn, attenuation of VGRF and BF were assessed across different surfaces during landing manoeuvres (Steele, JR, Milburn, 1987). Results from the 10 skilled netball players showed that the highest braking force (N) and shortest time to peak VGRF (s) was observed when landing on concrete and bitumen (Steele, JR, Milburn, 1987), while, the time to peak VGRF was significantly longer (s), and time to peak braking was significantly shorter when landing on synthetic grass (s) (Steele, JR, Milburn, 1987). The study concluded that bitumen and concrete display a greater potential of injury in comparison to other synthetic surfaces (Steele, JR, Milburn, 1987). In a follow-up study, Steele assessed a total of 45 players, with fewer injuries occurring in synthetic surfaces than natural grass or

bitumen (Steele, 1990b). Despite this finding, no significant difference was observed when the frequencies of injuries were adjusted by the number of gameplays.

In a 1986 study by Hopper, a significant association was found between surface type and injury site (Hopper, 1986). Results from the study showed that bitumen resulted in increased knee injuries, and hand injuries were more prominent on natural grass. In a review conducted by Nigg and Yeadon in 1987, it was concluded that material testing should not be used for the prediction of injury occurrence caused by the surface, but should instead be used to understand the kinematics of individual players (Nigg and Yeadon, 1987). The netball surface is critical to ensure sufficient friction is provided to enable the player to perform the explosive netball movements without sliding or slipping and further studies must be completed to draw a conclusive result on the frictional and stability profile of various netball surfaces.

1.3.7 Landing Techniques

Landing techniques can be complex, as they are influenced by intrinsic and extrinsic factors, and incorrect landing technique being cited as the primary cause of lower limb injuries in netball (Hopper, 1986; Hopper and Elliott, 1993; Steele, 1990a). As previously highlighted in Table 6, during landing, VGRF is greater than BF with mean peak values of 5.7 BW and 4.6 BW, respectively. The incorrect landing was identified to cause 13% to 38.7% of the netball related injuries amongst analysed literature (Table 5).

As previously discussed, landing is heavily influenced by a number of factors, including drop height which determines the landing velocity, jump distance which impacts angular momentum, and finally landing strategy, as landing with one or both feet require different balance strategies and muscular recruitment (Mothersole *et al.*, 2013). Hence, proper landing technique has been defined, which must display reasonable flexion of the knee, ankles and hips, hence dissipate the majority of the energy (Steele and Lafortune, 1989b). The immediate effect of landing can be reduced by increasing the amount of time allowed for the absorption of impact force. The suggested landing technique for bilateral and unilateral landing is given in Figure 6:

***Image removed due to
copyright restriction***

Figure 6: Landing technique suggestion for bilateral and unilateral landings (Mothersole et al., 2013)

Hewett *et al.* also indicated that during landing, excessive adduction or abduction of the knees should be avoided, as the impact stress can be reduced by ensuring equal distribution of impact forces across both the lateral and medial compartments of the knee (Hewett *et al.*, 1996). Several studies have also considered foot placement, but as a general consensus, to spread the forces evenly throughout the foot, the forefoot to heel ground contact pattern is recommended (Kovács *et al.*, 1999).

1.4 Athlete Workload Monitoring Practices

Workload monitoring of an athlete provides information regarding the physiological response to training, indicates changes in the athletes' performance and provides valuable insights such that precautions can be taken to reduce the risk of overloading fatigue-related injuries and illness (Halsen, 2014). By assessing workload data, the load-performance relationship can be examined, while also allowing the coach to make an informed decision when planning training for a competition. The workload can be measured in various ways, classified in terms of internal or external workloads. The work completed by an athlete is defined as external workload, and the relative psychological or physiological stress is defined as internal workload (Halsen, 2014). The combination of internal and external load monitoring can provide information regarding fatigue and enable better monitoring of training. In the following sections, internal and external workload practices are explored:

1.4.1 Internal Workload

Some of the key internal workload monitoring practices are explored in this section:

Rating of Perceived Exertion (RPE): RPE is a commonly used method for assessing workload, which utilises the notion that athletes can subjectively monitor their physiological effort and provide details following competition or training. RPE has a strong correlation with heart rate (HR) during high-intensity interval cycling training but a weak correlation during the short duration of high-intensity soccer drills (Borresen and Lambert, 2009). In 1998, Forster multiplied the RPE of the athlete with the length of the session, to produce the session RPE (Foster, 1998). This very simple yet effective method has consistently shown more validity and reliability (Halsen, 2014). However, there are still many unexplained variances in this method as the measure is highly subjective and cannot be standardised across all athletes (Halsen, 2014). This training measure also identifies the average intensity per game and does not represent chronic or acute training dose.

Heart Rate (HR): One of the most common, and frequently used the methods of internal workload monitoring in both sports and leisure activities is the HR monitor. HR monitors are most commonly used to indicate the intensity of effort and physiological adaptations, either while strapped to the chest (electrical activity using electrodes) or worn at the wrist (detect peripheral pulse using optical sensing technology). The price of a commercial HR monitor can

range anywhere from AUD\$30 AUD\$470 and are incorporated into most smartwatches such as Apple Watch or Fitbit (American Heart Association, 2019). The cheaper HR monitors provide minimal information, whereas the more expensive HR monitors, such as Polar, has additional data storage, and directional information (Polar, 2018). The ratio of HR-RPE combined can aid in the identification of fatigue. Portable heart rate monitors in conjunction with kinematic analysis have become the most common method of estimating the intensity of various activities, and metabolic demand during team sports such as rugby and basketball (Li *et al.*, 2016). However, HR is a physiological indicator only, and cannot provide any information regarding the impact dose and biomechanical forces that contribute to chronic and acute injuries in netball.

Training Impulse (TRIMP): TRIMP is a unit of physical effort based on information such as resting, average HR during an activity and training duration (Halsen, 2014). Multiple studies have defined their own TRIMP methods and are chosen by the coaches according to their subjective judgment (Haddad *et al.*, 2017; Halsen, 2014). For example, during a netball training session, an individual player with an average heart rate of 150 bpm can be recorded for a 120 minutes session, resulting in 18,000 TRIMP (time x HR). Although this method allows coaches with different activities a measure of training workload, there are various limitations present. For example, netball incorporates types of activities with various intensities (Figure 3), hence the TRIMP score does not accurately depict the variety of movements undertaken by the individual player. To counter this issue, coaches have modified the TRIMP method, for example, different HR zones according to the intensity of training. However, the measures are not consistent across the board as coaches often implement their own subjective measures and variations of TRIMP, while TRIMP does not apply to strength, speed, agility or power of training sessions (Haddad *et al.*, 2017; Halsen, 2014).

Currently, in netball, internal workload monitoring practices are not capable of capturing or representing GRFs and are mostly subjective measures. As there is no standardised method of representing different activity intensity zones, coaches may also disagree with opinions on the measured parameters according to their personal expertise, introducing further subjectivity bias in captured data sets. A netball training session includes a variety of movements, with short periods of highly intense activities. Average measurements for internal workload such as TRIMP, RPE or HR only provide a brief measure of physiological endurance, but do not depict the continuous workload or repeated lower limb loading of the athlete throughout the session.

1.4.2 External Workload

External workload monitoring systems are commonly reported through systematic reviews of wearable and non-wearable technologies (Camomilla *et al.*, 2018; Cummins *et al.*, 2013; Hausler *et al.*, 2016). A few key external workload monitoring practices are discussed in this section:

1.4.2.1 Stationary systems for measuring GRF

Several studies have reported various stationary systems, such as the use of instrumented treadmill devices and force plates and in the measurement of GRF, with the limitation that only one stride can be recorded per stationary force plate. For laboratory testing, often sensors are placed along the floor in a room equipped with cameras to track markers and force plates on the floor to record GRF. From the movement of the athletes on the force plates, the GRF will be produced to calculate the VGRF and resultant BF accurately. When the floor sensors are used in a Gait lab, motion capture systems are used to produce a 3D kinematic model of the participants, hence the exact GRF exerted during various movements can be simulated and assessed. The Vicon motion capture system (Oxford Metrics, Oxford, UK) is used as a gold-standard reference for external workload measurement systems used in rugby, football, baseball, netball and athletics (Adesida *et al.*, 2019). Some examples of commercial force calculating floor sensors are (Muro-De-La-Herran *et al.*, 2014):

- Force platform AMTI series OR6-7 of Biometrics France
- Kistler force plates of different types
- MatScan System made by Tekscan (43.6 × 36.9 cm)
- Walking mat made by RM. Lab (150 × 50 cm)
- FootScan Plates made by RSScan.Lab (up to 200 × 40 cm)
- Dynamometric mat ADAL of Tecmachine
- FDM-T System for stance and gaits analysis made by Zebris (150 × 50 cm)

The limitation of stationary force plates can be overcome by employing an instrumented treadmill, with two force plates under treadmill to allow for continuous stride of the athlete. However, this method is not suitable for the explosive movement required by netball, such as jump landing techniques. In this circumstance, multiple stationary force plates are required to

record most netball specific movements. In addition, 10 Vicon cameras and 4 AMTI force plates can cost upwards of AUD\$110k, in total, without considering the cost of markers, the laboratory fitting or any other consumables required for such testing (cost estimation provided by Flinders University Motion and Rehabilitation Laboratory Supervisor). The players will also be taken outside of the netball court to partake in activities in the laboratory; thus, the original condition of play will not be accurately represented. Therefore, although gait analysis with force plates will provide a gold standard of GRF data, athletes cannot use such an approach during training or gameplay, and thus cannot capture game-related GRFs.

1.4.2.2 Inertial Measurement Unit (IMU)

Technological development in the last decade has led to the production of inexpensive, portable, non-invasive sensors, that can measure activity during training or competition and provide a brief overview of the performance of individual athletes. In total, 286 studies and 23 reviews have been published regarding the use of IMUs in sport to assess the workload of athletes (Camomilla *et al.*, 2018). The development of Micro-Electro-Mechanical-Systems (MEMS) technology allowed manufacturing of three very efficient and low-cost sensors: accelerometer, gyroscope and magnetometer (Camomilla *et al.*, 2018).

An accelerometer is a type of inertial sensor that can provide movement data (acceleration) in three different axes. An accelerometer comprises a mechanical suspension system, with a proof mass attached to it with respect to a reference frame (Tao *et al.*, 2012). According to Newton's second law, where $F=ma$, (Force= mass x acceleration), when the sensor is moved from its position in any direction, gravity will force the mass to deflect by the inertial force, and this physical displacement of the mass is measured as an electrical signal which is read as acceleration. When accelerometers are attached to the lower limb, the velocity of the limb can be measured and estimate the force if the mass of the limb is known (Tao *et al.*, 2012).

A gyroscope is a type of angular velocity sensor that can measure the apparent force proportional to the angular rate of rotation (Coriolis force) in a rotating reference frame (Tao *et al.*, 2012), which can be used to calculate the angular rate. Gyroscopes can also be electronic, microchip-packages MEMS gyroscope, fibre optic gyroscopes, and even quantum gyroscopes. From the angular velocity and angle of the leg during gait, various gait phases can be recognised by attaching a gyroscope to the lower limb. Magnetometers are based on the

magneto-resistive effect that can estimate changes in the orientation of a segment in reference to magnetic north (Tao *et al.*, 2012).

The quantities measured by all three of the sensors can be used to assess angular velocity, the sum of inertial and gravitational acceleration, and local magnetic field components can be combined to learn about the orientation of a body and force estimation can be calculated if the mass is known. Previously, IMU had been used broadly in aircraft satellites, underwater submarines, and many other military usage, but the development of MEMS allowed IMU to be integrated into human movement kinematics due to the compact size and low cost (Camomilla *et al.*, 2018).

IMU Parameters

IMUs can also be used to measure a wide range of sensor-derived parameters such as temporal, kinematic and dynamic, which can then be used for athlete monitoring. Brief information regarding each of the parameters are given below:

Temporal Parameters:

Detection features such as minimum, maximum and slope changes can be detected in the acceleration signals or measured angular velocity cost (Camomilla *et al.*, 2018). Studies have used these measurements for the following purposes:

- Time intervals of different activities such as stride, stance, step during locomotion, landing during netball or stroke during swimming
- Segmentation of sports tasks using time instants
- Frequency of cyclic movements
- Time instance identifying the beginning and end of a movement, such as time to leap into the air and then foot contact when landing, allowing isolation of the area of interest

Kinematic Parameters:

Kinematic parameters are used to estimate the orientation of a body segment or desired object and their centre of mass using linear and angular position, velocity and acceleration. Studies have identified the usefulness of the various kinematic parameters (Camomilla *et al.*, 2018):

- As the IMU can be orientated in 3D using the angular velocity provided by gyroscope and positional data by an accelerometer, joints kinematics can be estimated using the relative orientation between adjacent body segments
- In theory, the acceleration data can be used to predict linear velocity and displacement. However, this calculation in practical application is prone to errors due to the low-frequency gyroscope drift. The gyroscope component cannot be avoided either as it is critical for the orientation of the IMU. Therefore, studies employ model-based approaches when estimating linear position using IMU data, which has proven to be a time-consuming task (Sabatini, 2011).
- In a study conducted by Myklebust *et al.*, centre of mass (CoM) parameters were extracted using the acceleration of a single sensor on the near position of CoM in the static upright posture (lower trunk) (Myklebust *et al.*, 2015). Although the accuracy of the method is in question due to not considering the dynamic movement of the lower and upper limbs, this method can be useful in fast and easy performance evaluation in-game without requiring a complicated setup.

Dynamic Parameters:

Dynamic parameters also consider both linear and angular variables, velocity and acceleration. Few studies have identified the dynamic parameters using IMUs due to the complexity associated with the measurements cost (Camomilla *et al.*, 2018).

IMU in Literature

Camomilla *et al.* in a 2017 systematic analysis study found a total of 286 studies using IMU sensors to assess the workloads of different individuals. Some of the key team sports and the number of papers published are highlighted (Table 8).

Table 8: Number of papers reporting the use of IMUs to assess workload (team sports) (adapted from (Camomilla et al., 2018))

Team Sport	Number of studies reporting the use of IMU
Rugby	20
Australian Football	12
Soccer	10
Baseball	5
Cricket	4
Volleyball	4
Field Hockey	4
Netball	3
Ice Hockey	3
Basketball	2

For an example of a netball related study, a triaxial accelerometer (x8m-3mini, Gulf Data Concepts, Waveland, MS, USA) sampling at 100 Hz was attached to individual elite players (Bailey *et al.*, 2017). The method of data collection and workload calculation was based on a study by Boyd and colleagues (Boyd *et al.*, 2011) in which an accelerometer was sewn into a pouch to the waistband of the uniform of each player, and the raw accelerometer data were collected and converted to an arbitrary measurement unit for workload using Boyd’s vector-magnitude modification formula (Boyd *et al.*, 2011). Through this study, it was concluded that Centre positions produced the greatest workload, and the categorised data were previously explored in Section 1.1.4.

In a 2012 study, Anna *et al.* used IMUs to develop a system that was used to quantify gait symmetry and gait normality. This was then compared in the lab with 3D kinematic measurements and examined in situ against clinical assessments of a hip-replacement patient.

Chapter 1: Literature Review

A reasonable correlation was obtained between different methods (Sant'Anna *et al.*, 2012). In another study, Ferrari *et al.* created an algorithm with IMUs to estimate gait features. These features were then compared with the gold standard camera-based system, and a difference in step length below 5% was shown when considering median values (Ferrari *et al.*, 2013). In another clinical study conducted by Tay *et al.*, IMUs were used to create a system, which was located at the ankle of the patient with Parkinson's Disease (Tay *et al.*, 2013). The IMUs could then be used to track gait movements, and body posture was also monitored by placing another sensor near the cervical vertebra (Tay *et al.*, 2013). The system successfully measured vital parameters such as the maximum acceleration of patient during standing up and time needed to stand up from a seated position.

IMUs can also be integrated into the insoles of shoes for gait analysis, such as the development of Veristride insoles (Bamberg *et al.*, 2008). The design of the insoles also included pressure sensors for the plantar force distribution sensing, inductive charging system and Bluetooth communication module (Bamberg *et al.*, 2008).

There are a vast range of commercially available IMUs in the market that can be used for gait analysis or activity monitoring in sports. For example, Xsens Motion Technologies (Enschede, The Netherlands) produced a wearable monitoring device, inclusive of force and moment sensors and compact IMUs to estimate joint moments and workload of the lower limb. The measurements of the sensor were used to calculate the 3D displacements of the centre of mass (Schepers *et al.*, 2009). Another system called M3D was commercialized by TEC GIHAN Co. (Kyoto, Japan) which was a more compact system including all the 3D force and motion sensors in shoes. This was beneficial for clinical gait analysis and the embedded control systems. In addition, Mills *et al.* produced a commercialised Motion Capture System named Polhemus Liberty ETS system (Polhemus Incorporated, Colchester, VT, USA) to obtain 3D gait kinematics (Mills *et al.*, 2007). Some other sensors that are commercially available include SensorTag by Texas Instruments, MinimaxX by Catapult, Myotestm by SPI-PRO, and Physiology by GaitUp. The cost of these sensors can range anywhere from AUD\$30 to up to AUD\$5000, depending on the available features and compatibility. Finally, EMG sensors were also modified for gait analysis by incorporating IMU sensors; some commercialized products include the Surface EMG Sensors of Delsys Incorporated (Boston, MA, USA) and the SX230 EMG Sensor of Biometrics Ltd. (Newport, UK) (Tao *et al.*, 2012).

Limitations of IMU

There are multitude factors that must be maintained and kept in consideration for IMU sensors, which could be considered as limitations. For example, the sensors must be chosen appropriately depending on the sporting application. Some of the factors of IMU sensors include sampling frequency, portability, integration with other software and communication methods such as Bluetooth, full range sensitivity and power consumption (Camomilla *et al.*, 2018). Some IMU devices may have shown promising results in laboratory testing, but were not found to be practical when tested in-game due to connection failure or disruption in data transfer (Camomilla *et al.*, 2018).

Another major disadvantage is that IMUs cannot currently be used to calculate biomechanical loading observed by the lower limb directly. Currently, devices such as ImeasureU can monitor lower limb impacts by measuring tibial shocks and calculating Daily Load Stimulus (DLS). DLS is a metric of cumulative load describing the relationship between mechanical load stimuli, and skeletal tissue remodelling as a function stimuli (Besier, 2019). Therefore, DLS is the product of load frequency and magnitude, and integrated with the IMeasureU sensor, provides a quantitative measure of mechanical workload. However, these sensors can cost up to \$6,000 dollars a year for 3-year subscription (Auckland, New Zealand). Due to the higher data processing capabilities (1000 Hz), onboard processing, portability and additional capabilities, the cost of IMeasureU sensors are significantly elevated, further reducing the accessibility of the product to non-elite athletes with limited funding.

Finally, another significant limitation of IMUs that must always be taken into consideration is the drifting error, which becomes more significant with data acquisition. In addition, if the sensor is not rigid with the body with an effective method of fixation, the motion artefact can further increase the error by increasing noise data, and hence must be regularly assessed and calibrated accordingly.

1.4.2.3 Global Positioning Systems (GPS)

GPS is a satellite-based system that is used for time-motion analysis in various sports to provide information regarding the position, movements and velocity of an object. The recent development of portable GPS units has expanded the usability, as the units can be used in sports training and competition to provide an additional means of quantifying physical activities. GPS can determine players movement patterns, speed, number of accelerations and decelerations and distance travelled (Cummins *et al.*, 2013). Quantification of such parameters allows coaches to identify the period of intense gameplay, identifying the level of activity per player to detect fatigue, examine the performance of individual players throughout a game to gather tactical information, and define activity profiles based on unique positions (Cummins *et al.*, 2013).

GPS in Literature

Cummins *et al.* and Hauslet *et al.* each produced a systematic review of the scope of GPS measures in team sports, concluding the extensive use of GPS in rugby league, Australian Football League (AFL), cricket, rugby union, soccer and even netball. Literature has shown that by measuring player movements pattern, GPS can quantify levels of physical stress and exertion in the athletes (Cummins *et al.*, 2013; Hausler *et al.*, 2016)

Literature has also shown that integration between GPS and IMUs can provide further information regarding the physical load and work rate patterns experienced by the athlete on the field. Body load is the collation of the forces imposed on the athlete, which may include a change in direction, acceleration/ deceleration, GRF caused by landing and contact with the floor and collision between players (Cummins *et al.*, 2013). These body forces and other associated impact measures quantify the intensity and number of collisions between athletes. Although GPS cannot directly compute these body loads, the speed and impact of the players can be classified using GPS and IMU sensors into activity zones known as speed zones and impact zones, with zone one and six corresponding to lowest and highest activity, respectively. Currently, impact data is extracted manually through cross-referencing video footage with the GPS data, which is a time-consuming process and these zones have been used to compare player performances and intensity of sessions both in training and gameplay.

Chapter 1: Literature Review

Several studies were conducted in rugby league and rugby union that categorised the impact intensity into six impact zones (Table 9) (Cunniffe *et al.*, 2009). The studies show that forward (F) positions experienced higher loading than back (B) positions such as centres and wingers. Cunniffe reported the F experienced up to 3.8 times more frequent impacts than the B during a single competition game, however it must be noted that the data size was extremely small with a single participant in each F and B category (Cunniffe *et al.*, 2009). Other studies with a higher sample size also reported that F sustained up to 63 more impacts than B (McLellan *et al.*, 2011). No further report was found regarding the body loading during gameplay.

The two major GPS systems that can be used to monitor an entire team of athletes have been developed by Catapult Sports (Catapult Sports, Melbourne, VIC, Australia; MinimaxXTM S4 device) and GPSports (GPSports, Canberra, ACT, Australia; SPI-Pro IITM and SPI HPUTM devices) (Hausler *et al.*, 2016). MinimaxXTM has integrated IMU sensors into the GPS device, enabling the device to provide an assessment of player loads and work-rate patterns using measures of metabolic load, collisions and impact, and accumulative mechanical stress derived from the magnitude vector of acceleration (Hausler *et al.*, 2016). In addition, prior to the change in unit orientation, there must be a spike in instantaneous player load (Hausler *et al.*, 2016). Catapult, in comparison, cannot assess the impact as it does not have an integrated IMU component. Instead, it enables collision detection and automated tackle. GPS units are used to collect both match training time-motion data in a team sport setting to correlate on-field performances, fitness tests and energy requirements for specific player positions.

Table 9: Impact zones in Rugby using GPS (adapted from (Cummins et al., 2013))

		Mean Impact zones (per participants) (G)													
Study	Sample size	Zone 1 (Light 5-6 G)		Zone 2 (light-moderate) (6-6.5 G)		Zone 3 (moderate – heavy) (6.5-7 G)		Zone 4 (heavy) (7-8 G)		Zone 5 (very heavy) (8-10 G)		Zone 6 (severe) (>10 G)		Total	
		B	F	B	F	B	F	B	F	B	F	B	F	B	F
(Cunniffe <i>et al.</i> , 2009)	2	349	563	328	398	55	143	38	101	24	56	4	13	798	1,274
(Suárez-Arrones <i>et al.</i> , 2012)	9	382	501.6	326	341.3	54.3	161.6	29.8	143.1	35.2	66.6	6.3	10.4	883	1,225
(Venter <i>et al.</i> , 2011)	17	-	-	-	-	-	-	-	-	-	-	8	12.16	683.4	474.33
(McLellan <i>et al.</i> , 2011)	17	214	215	154	146	334	392	50	47	26	39	20	21	795	858

*B = outside backs (centres and wingers), F = forwards

- (dash) = Not reported

Limitations of GPS

Despite the increased and continued application of GPS in sports worldwide, significant limitations of GPS can be uncovered from literature. The reliability of GPS parameters are influenced by the velocity and duration of movements being analysed, and the sampling frequency of the system (Cummins *et al.*, 2013; Halson, 2014). With increasing velocity or shorter duration of movements or decreased sampling rate of the GPS, the reliability significantly decreases (Halson, 2014). GPS is acceptable for assessing low-speed movement patterns such as jogging, walking and striding rather than a sudden explosive change of movements and rapid bursts of movements to decelerate or accelerate (Cummins *et al.*, 2013). GPS devices normally range from a 1 to 15 Hz sampling frequency, significantly less than the capability of most accelerometers, hence small changes in movement may be missed and inaccurately represented (Li *et al.*, 2016). The reliability and application of GPS in indoor court-based sports that require small travel distances but greater intensities such as netball are still unproven (Li *et al.*, 2016).

In addition, Cummins *et al.* further reported the absence of normalised “speed zones” between multiple sports and within individual sports. This prevents comparison of different physiological demands between sports and players without the use of other sensors and post-analysis.

According to a 2015 estimate, GPS system for a team can cost on average AUD\$100k per year, therefore, inaccessible to most elite and sub-elite teams (Langsdon, 2015). Furthermore, as GPS units are satellite-based, only limited sampling frequency range, they are not effective for indoor contact sports such as netball which incorporates short bursts of high-intensity movements (Cummins *et al.*, 2013).

Finally, GPS devices strapped onto the back, torso, or shoulder of the body is not equipped to produce any kind of mechanical loading data in the lower limbs of players (Halson, 2014). GPS calculates position-based data in outdoor-based sports and does not take into consideration VGRF or BF, the main area of interest in explosive team sports with a high rate of lower limb injuries such as netball.

1.5 Conclusion

Netball is classed as one of the top team sports for women and girls, and literature throughout the years has shown the progression of the game to what it is today, and the epidemiology of associated injuries. The explosive nature netball gameplay and the rapid change in direction and acceleration due to the “no stepping” rule once the player has the ball causes a significant increase in the peak VGRF and the maximum BF. Incorrect landing technique, rapid deceleration, surface conditions, footwear and many other factors could affect the rate and magnitude of GRFs player experiences throughout a game, resulting in knee stiffness, decreased flexion angle, ankle instability and trunk stabilisation (Mcgrath and Ozanne-Smith, 1998). Excessive, repeated VGRF that has been reported to exceed 5 times the body weight in netball, place the lower extremities at high risk for articular degeneration, ligament damage, cartilage degeneration, osteoarthritis or chronic musculoskeletal disorders (Steele, 1990a). As the top team sport for girls between 14-16-year-old, the frequency of such injuries can lead to a reduction of the level of sports activity, need for medical treatment, and adverse social and economic effects for young athletes

More recent studies are required to assess the activity profiles and GRFs associated with netball specific movements, as the most recent study found to provide such information was held in 2004. Considering the high incidence of injuries and participation dropout rate compared to similar sports (i.e. basketball), primary and secondary countermeasures are extremely important to ensure more participants are kept safe.

However, current internal workload monitoring practices are subjective training practices that provide an overall fitness and workload assessment of the athlete but fail to quantify the loading of at-risk lower limbs (Halsn, 2014). External workload monitoring devices include wearable sensors for impact monitoring which are laboratory-based, expensive, complex in terms of data capture and analysis or generally inaccessible to sub-elite players (Camomilla *et al.*, 2018; Cummins *et al.*, 2013; Hausler *et al.*, 2016). Without active monitoring of the lower limb impact forces in training and games, preventative measures unique/specific to each player cannot be taken, hence generating chronic injuries.

Chapter 1: Literature Review

The review of the literature identified the growth of wearable devices, such as low cost, portable and widely used IMU, in particular, accelerometer-based units to measure general energy expenditure and lower-limb shock attenuation (Adesida *et al.*, 2019; Camomilla *et al.*, 2018). Very few studies have been conducted investigating the ability of IMUs to measure mechanical loading or impact dose through the lower-limbs, proving a gap in the literature for the potential development of a wearable solution that can effectively calculate lower limb mechanical loading during netball training and gameplay.

Other wearable technologies, such as the GPS are effective in using player position and velocity to assess overall workload based on “speed” zones. However, the technology cannot quantify mechanical loading or explosive movement through the lower limbs. As netball indicated high GRF, quantification of the mechanical loading would provide critical information.

Recent research has shown more promising results by extracting impact data from the combination of IMU and GPS with a video recording of athletes (Cummins *et al.*, 2013). In this case, an “impact zone” could be determined depending on the intensity and level of activity of the player, providing a realistic load data for individual athletes. However, the process of data extraction is time-consuming and must be done in post analysis, as no other reports were found detailing streamlining the process and collecting impact load data from wearable devices during gameplay in real-time.

Based on the findings of this literature review, a gap in the market was identified as a thorough investigation was required regarding the development of an inexpensive wearable device to measure lower-limb impact dose during competitive netball play. Findings from the literature survey also confirmed that application of IMUs was promising for this investigation due to the cost, portability and wide availability.

CHAPTER 2:
PROJECT OVERVIEW

2.1 Problem Statement

Netball is a physically demanding sport that requires a high degree of speed, strength, fitness, flexibility. This results in repeated-explosive loading to the lower limb, hence accumulating a high number of ankle and knee injuries (Hopper, 1986; Hopper *et al.*, 1995; Hume and Steele, 2000; Otago and Peake, 2007; Saunders and Otago, 2009). The current active injury countermeasures are either subjective training practices, that fail to quantify the loading of lower limbs, or wearable devices for impact monitoring which are laboratory-based, expensive and generally inaccessible to sub-elite players. Due to the lack of active monitoring of the lower limb impact forces in training and games, preventative measures cannot be taken, hence generating chronic injuries.

2.2 Project Objectives

The overall objective of this project was to contribute to the design and development of an inexpensive and compact accelerometer-based wearable device that can quantify the lower limb related impact dose experienced during training and competitive netball play. The prototype device will be used by the netball coaches to assess the impact loading of each player throughout the week of training and matches. This will help coaches identify “at-risk” players and can assist in the development of the appropriate training regime, hence allowing proactive injury prevention.

The main objective of the project was to develop an accelerometer-based device that could be used to measure the activity impact zones during laboratory-based netball simulated movements. To meet the objective, firstly, a commercially available sensor manufactured by Texas Instruments, SensorTag CC2650, recommended by the previous project was explored to ensure the capabilities of the device were suitable for wearable device development (Corbo, 2018; Texas Instruments, 2015). Laboratory and in situ testing were conducted to validate data streaming, accelerometer sensitivity, range and onboard processing. A subsequent objective was then to create an accelerometer-based working prototype and incorporate a user interface, such that chosen A_{IS} amplitude data could be displayed to the user. Finally, a pilot validation study was conducted with the prototype to ensure the acceleration variable can be correlated with VGRF data obtained from laboratory force plate data.

2.3 Methodology Overview

The objectives of the study were addressed gradually by performing various testing and building analytics tools. The project methodology was separated into three phases (Figure 7). Phase 1 of the study involved testing and validation of SensorTag (Chapter 3). Phase 2 then involved the development of a functioning prototype and user interface (Chapter 4) and finally, phase 3 involved collecting and analysing pilot testing data using the developed prototype (Chapter 5).

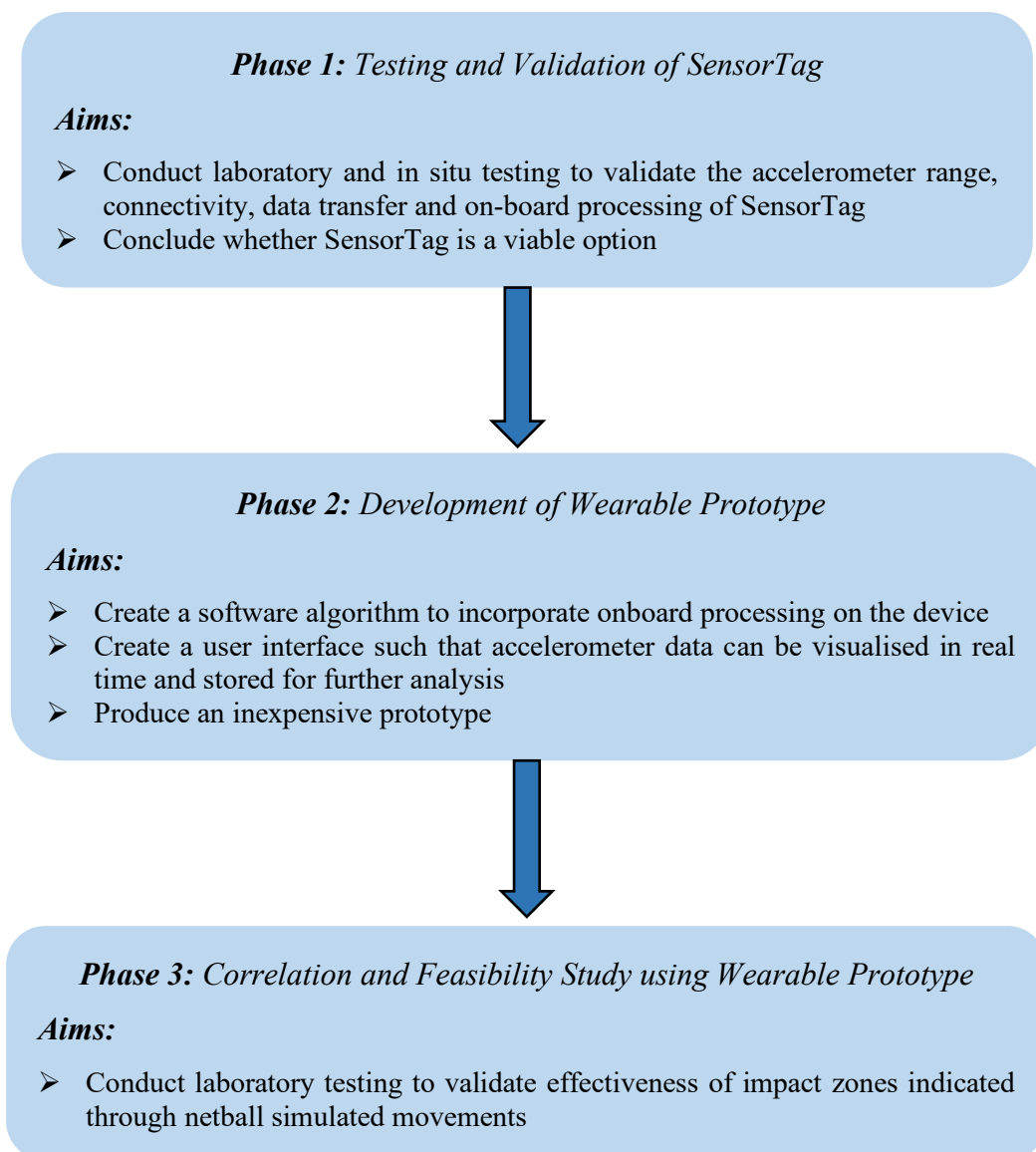


Figure 7: Methodology overview

CHAPTER 3:
TESTING AND VALIDATION
OF SENSORTAG

3.1 Introduction

In the previous study, it was concluded that by fixing an accelerometer to the shank and collecting A_{IS} amplitude could be used to deduce an impact dose measurement over a time period (Corbo, 2018). The suggested implementation plans involved using the commercially available Texas Instruments Simplelink Bluetooth Low Energy (BLE) SensorTag as it met the initial requirements to the project. This section includes the methodology and results from the study, to subsequently conclude whether SensorTag is a viable solution.

3.2 Aim

The primary aim of this phase was to conduct laboratory and in situ testing to validate the accelerometer range, connectivity, maximum sampling frequency, and onboard data processing for easy data transfer. The findings from the laboratory and in situ testing were considered to determine the viability of the SensorTag as a wearable impact dose monitoring device. According to the SensorTag specifications (Appendix C), a sampling frequency of 400 Hz was expected, with a transmission range of 50 meters. The laboratory and in situ testing informed the following requirements to meet the aims of the study:

- A reliable streaming sampling frequency of 100 Hz was required in the laboratory and in situ with less than 2% data loss such that no peak data is missed (laboratory and in situ testing)
- BLE connection was required to be maintained in situ even if other players were obstructing the line of vision between the sensor and the BLE receiver dongle (In situ testing)
- Multiple SensorTag connections to be achieved through Bluetooth pairing to a single receiver device such that the coach would not be required to pair up individual players with separate receiver devices (Laboratory testing)
- A minimum range of 35 meters was required for data streaming to cover the distance of a standard netball court (in situ testing)
- The coin cell battery powering the SensorTag was required to last a minimum of 2 hours of continuous streaming to sustain full netball gameplay (laboratory and in situ testing)

3.3 Methods

The methodology was divided into two concurrent trials to evaluate the listed hypotheses: laboratory testing for quality of data in a controlled environment, and in situ testing for range and data transfer capabilities of the SensorTag in a team environment.

3.3.1 Laboratory Testing

3.3.1.1 Motion Analysis Laboratory Setup:

Firstly, GRF measurements 6 degrees of freedom force plates (AMTI OR6-7) and accelerometers (Delsys Trigno Research+ Avanti™) were utilised in a motion analysis laboratory alongside two SensorTags. The AMTI OR6-7 Multi-Component Force Plates are considered gold standard due to the integration with the Vicon motion capture system and GRFs at up to 2000 Hz sampling rate with a measurement accuracy of $\pm 0.25\%$ (Appendix B). The force plates used to record GRFs produced through various simulated movements, such as sprinting, running, jogging, and jumping. The lower body of the participants were marked up with reflective markers, and the movements were visualized through Vicon Nexus 2.0 system.

Delsys Trigno Research+ Avanti™ sensors (Figure 8) were equipped with dual communication methods of Bluetooth BLE 4.2 and Wi-Fi to the base station, which communicated to the host computer with Vicon software (Delsys, 2019a). The onboard accelerometer could be tuned to the required $\pm 16g$ with a transmission range of up to 20 meters, assuming an optimal transmission environment. The rechargeable battery could provide functionality for 4 to 8 hours, hence was suitable for a laboratory testing session of up to 2 hours (Delsys, 2019b). The Trigno sensors were chosen as they could be synchronised with the Vicon software and timestamped to capture acceleration and force plate data. The method of system integration with system calibration, participant mark up, data collection and exporting are given in Appendix E, which was followed in every session. It must be noted that the 2018 study was conducted with Delsys Trigno wireless EMG sensors, which was the previous version of the Delsys Trigno sensors with the maximum sampling frequency of 150 Hz, $\pm 9g$ sensitivity and 20-meter range in situ (Corbo, 2018). The Trigno Avanti™ completely replaced the older model, and the newer model integrated higher accelerometer sensitivity ($\pm 16g$) and battery.

Image removed due to copyright restriction

Figure 8: Delsys Trigno Research+ Avanti™ (Tracklab, 2018)

3.3.1.2 SensorTag Setup

From the wide range of SensorTags available utilising technologies such as Zigbee, Wi-Fi, 6LoWPAN and BLE, the previous project concluded BLE to be the most efficient method of transmission due to the transmission range, battery lifetime and the ‘Internet of Things’ (IoT) development concept (Corbo, 2018). In particular, the chosen SensorTag was based on the CC2650 wireless Microcontroller (MCU), with BLE support to communicate with host devices (Figure 9). Hence the SensorTag could be paired with a central windows computer through interfacing with a receiving module, Silicon labs BLED112-V1 dongle, to allow data collection.

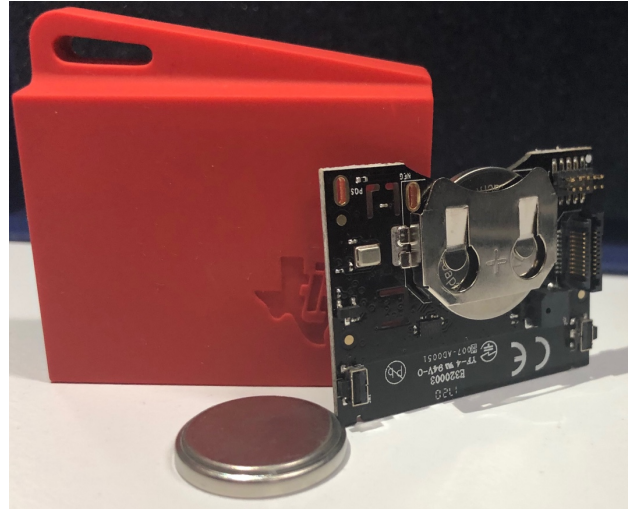


Figure 9: Texas Instruments SensorTag CC2650

The SensorTag could be directly programmed using the DevPack, which clipped onto the top of the PCB board of the SensorTag itself. The board was then connected to a computer using a micro-USB cable, and the firmware program for SensorTag was accessible to modify in Code Composer Studio (CCS). Any adjustments in the software needed to be individually updated through programming every individual sensor.

Although SensorTag can collect data at up to 400 Hz, it was not possible to stream data at that rate due to the hardware restrictions of coin cell battery used and BLE data transmission refresh rate. In addition, SensorTag did not have any onboard storage or processing capabilities, hence a decision to reduce the sampling frequency to 100 Hz was executed, as performed in other similar studies (Bailey *et al.*, 2017; Boyd *et al.*, 2011). By default, the SensorTag advertised at 10 Hz sampling frequency. The only method of changing the frequency was through software in CCS, where the streaming period variable *min_update_period* was changed to 10. This enabled the SensorTag to stream data every 10 milliseconds instead of default rate of updating every 100 milliseconds to achieve 10 Hz. The name of individual SensorTags and many other functionalities could also be modified through the CCS software and uploaded using the debugger DevPack.

Chapter 3: Testing and Validation of SensorTag

During netball gameplay, 14 players would be present on the field at any given time. Therefore, it was assessed to see whether multiple SensorTags were able to connect to a single master device for consistent streaming, thus reducing the number of devices the coach is required to maintain for all participants in the field. Bluetooth allows up to 7 ‘slave’ devices to connect to a ‘master’ at any given time depending on the capabilities of the host device, often requiring the use of receiver dongles such as the Silicon Labs BLED112-V1. When data is transferred between a master and a slave, the master chooses which slave device to address and switches rapidly (Darroudi and Gomez, 2017a).

Firstly, two SensorTags were powered on by pressing the power button to the side and ensuring that they were advertising connectivity by flashing green. A Surface Pro was used as the host device for the connection of multiple SensorTags with BLED112-V1 dongle paired to the device. The SensorTags were then paired to the device through the received dongle using *Bluetooth LE explorer* software. Upon completion of pairing, *SensorTag BLE Data Acquisition* software was used to enable the accelerometers of the connected SensorTags to display the data in x, y and z-axis of the accelerometer (Figure 10). Finally, the data were saved in a CSV format for post-analysis. The full breakdown instruction for data acquisition is provided in Appendix F.

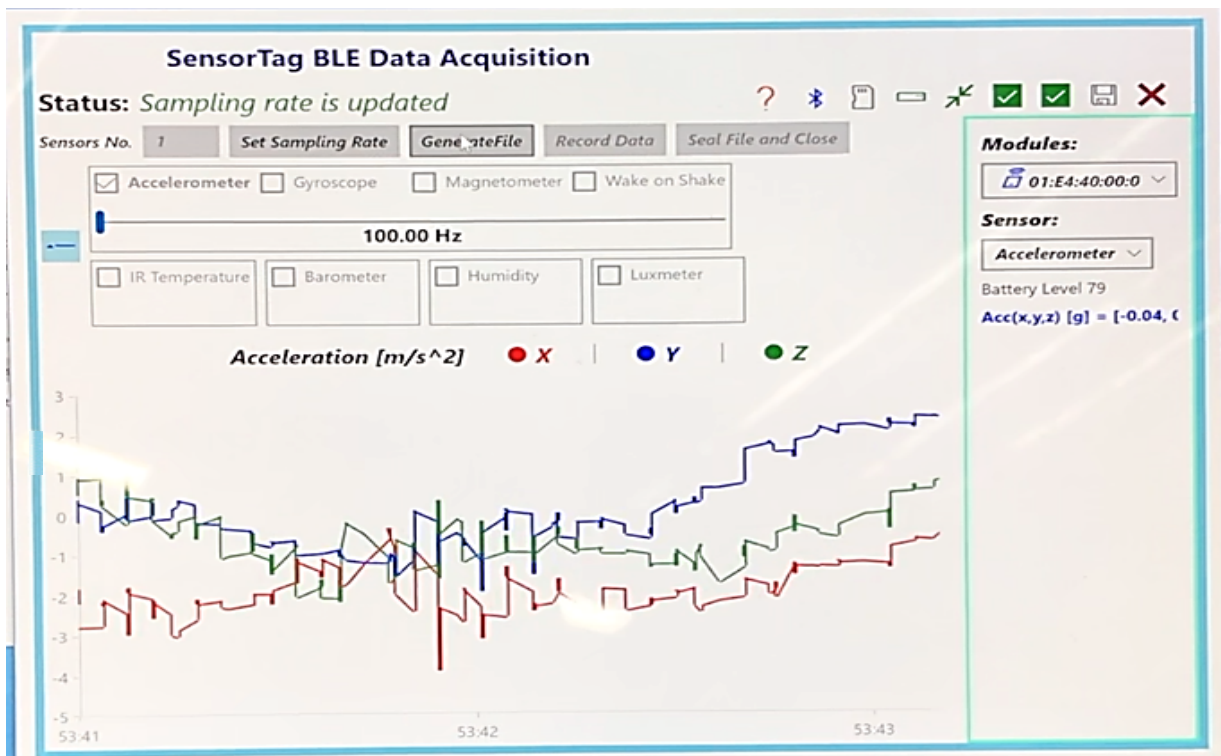


Figure 10: SensorTag BLE Data Acquisition application

3.3.1.3 Data Collection

During laboratory data collection, the Trigno accelerometers were used as a base measure for comparison with SensorTag and were set to collect data at $\pm 16g$. The participant was marked with 18 Vicon markers, 6 Trigno sensors and 2 SensorTags. The location chosen for the Vicon markers remained consistent, following the lower body marking guideline provided through Vicon (Appendix E). The Trigno sensors were attached to the participant to account for bilateral data collection of the lateral malleolus, shank and thigh for both left and right legs and secured with physio tapes. The positions of the Trigno sensors were selected based on the literature (Willemsen *et al.*, 1991a). From the previous study, the best placement for the accelerometer was found to be at the shank due to the presence of less soft tissues and hence minimising the interference of soft tissue oscillation (Corbo, 2018). Hence, two SensorTags were chosen for both the left and right shank of the participant and secured with physio tape (Figure 11). The axis orientation of the SensorTag and Trigno was maintained in reference to the anatomical plane of the body (Figure 12, Figure 13).



Figure 11: Participant lower body mark-up with Vicon reflective markers, 6 Delsys sensors and 2 SensorTags (Lateral Shank: right leg, Medial shank: left leg)

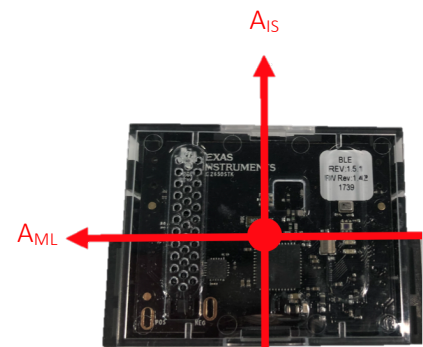


Figure 12: SensorTag axis orientation
(A_{IS} --Inferior/Superior axis; A_{ML} --
Medical/Lateral axis)



Figure 13: Trigno axis orientation
(A_{IS} --Inferior/Superior axis; A_{ML} --
Medical/Lateral axis)

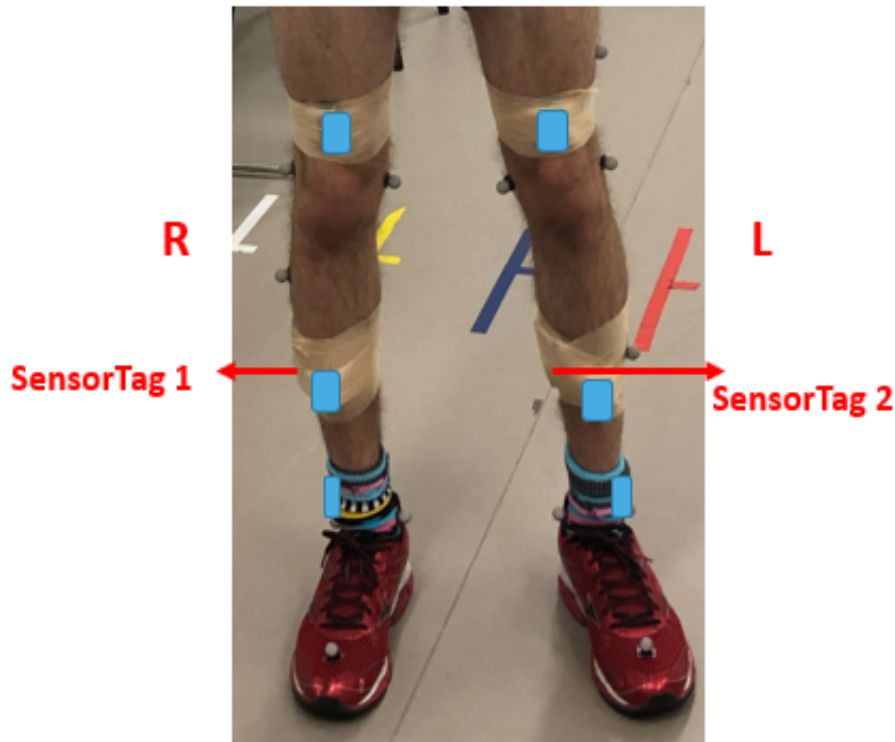


Figure 14: Two SensorTags (red) and 6 Delsys sensors (blue) positioning on the participant

The marked-up participant (Figure 14) was then required to do a range of netball simulated activities, such as walking, running, jogging, sprinting, jumping, two-foot landing, cutting, run on and change direction (Table 10). The participant was instructed to wait at the start line for the signal to begin the chosen activity, and continue over the force plates until the finish line (Figure 15). Although the force plates were used during testing, the data were not necessary for this study, and placement of the foot directly over a plate was not required. Each movement was completed at least 3 times and after each activity, both the SensorTag and Delsys data were saved in CSV format for post-processing.

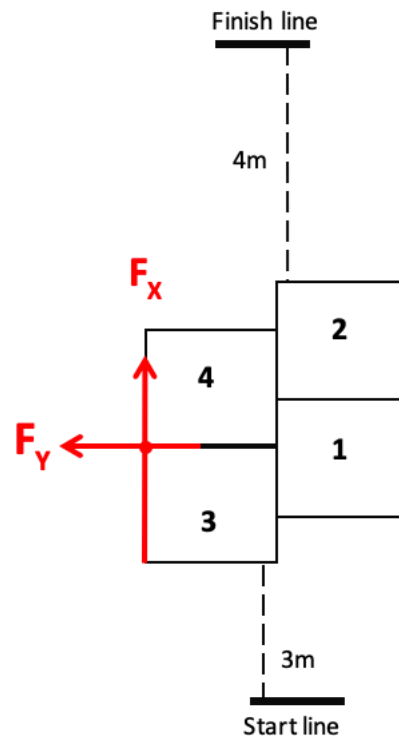


Figure 15: Force plate positioning

Chapter 3: Testing and Validation of SensorTag

Table 10: Game-based and simulated netball movements performed by each participant in the laboratory

(Corbo, 2018)

Movement	Trial Names	Procedure
General Game Activities		
Walk	Walk, Walk01, Walk02	Participants to: <ol style="list-style-type: none"> i. Stand at the start line as identified in Figure 15 ii. Walk at a comfortable, even pace towards the force plates, and continue walking over the force plates until the finish line (Figure 15)
Jog	Jog, Jog01, Jog02	Participants to: <ol style="list-style-type: none"> i. Stand at the start line. ii. Jog towards the force plates in a slow, non-purposeful run and continue over the force plates until the finish line.
Shuffle	Shuffle, Shuffle01, Shuffle02	Participants to: <ol style="list-style-type: none"> i. Stand at the start line. ii. Turn 90° clockwise on the spot and begin a shuffling motion across the force plates as if looking to receive a pass from the direction faced and continue shuffling until the finish line.
Run	Run, Run01, Run02	Participants to: <ol style="list-style-type: none"> i. Stand at the start line. ii. Run towards the force plates with elongated strides and continue running until the finish line.
Sprint	Sprint, Sprint01, Sprint02	Participants to: <ol style="list-style-type: none"> i. Stand at the start line. ii. Run with maximal effort or speed towards the force plates and continue sprinting until the finish line.
Jump	Jump, Jump01, Jump02	Participants to: <ol style="list-style-type: none"> i. Stand with left foot on force plate 2 and right foot on force plate 1 ii. Perform a maximal jump with a two-foot landing, simulating to catch a rebound following a shot at goal. iii. Ensure that the right foot strikes force plate 1 upon landing, whilst attempting to land as naturally as possible.
Cutting	Cut, Cut01, Cut02	Participants to: <ol style="list-style-type: none"> i. Stand at the start line. ii. Sprint towards the force plates and perform a cut with their right leg striking force plate 1 to change direction 45° to the left through force plate 4. Continue sprinting until finish upon change of direction. Movement should be performed as if attempting to dodge an opponent in competitive gameplay.

Chapter 3: Testing and Validation of SensorTag

Landing Conditions		
<i>For the Run-on, Pivot, and Two-foot simulations, the 'receiver' should stand at the finish line and give a chest pass with a flat trajectory. Subjects' approach speed to the catch should be similar to that required to beat an opponent in a competitive game-based situation.</i>		
Run-on	RO, RO01, RO02	<p>Participants to:</p> <ol style="list-style-type: none"> i. Stand at the start line. ii. Sprint toward the force plates and receive the oncoming pass by leaping with one leg and landing on the contralateral leg within the boundary of force plate 1. iii. After receiving and return the pass, continue running to the finish line. <p>Landing sequence: catch – land – step – pass (Otago, 2004)</p>
Pivot	Pivot, Pivot01, Pivot02	<p>Participants to:</p> <ol style="list-style-type: none"> i. Stand at the start line. ii. Sprint towards the force plates and receive the oncoming pass by leaping with one leg and landing on the contralateral leg on force plate 1. iii. After receiving the pass, the subject should pivot 180°, pass and sprint until start line. <p>Landing sequence: catch – land – pivot – pass (Otago, 2004)</p>
Two-foot	2F, 2F01, 2F02	<p>Participants to:</p> <ol style="list-style-type: none"> i. Stand at the start line. ii. Sprint towards the force plates and receive the oncoming pass by leaping with one leg and landing on two feet, ensuring that the right foot strikes force plate 1. iii. After receiving the pass, the subject should return the pass and run to the finish line. <p>Landing sequence: catch – land on two feet – step – pass (Otago, 2004)</p>
Step down: 460mm	460Step, 460Step01, 460Step02	<p>Place a 460mm high platform over force plate 3 and 4.</p> <p>Instruct subject to:</p> <ol style="list-style-type: none"> i. Passively step from the platform. ii. Complete a two-foot landing with the right foot completely within the boundaries of force plate 1.

3.3.2 In-Situ Testing

The laboratory testing did not accurately represent a real netball court, due to the difference in surface, size of space and other participants on the field. Therefore, another test was conducted at an indoor netball court with 3 participants. In this experiment, a single SensorTag was strapped to the right shank of a participant. The Trigno sensors were not used on the participant to simulate a more realistic situation. In addition, only 1 SensorTag was worn by the participant secured with physio taping on the right shank. The SensorTag setup was followed as described in *Section 3.3.1.2*. The positioning of the receiver device was maintained throughout the testing (Figure 16).

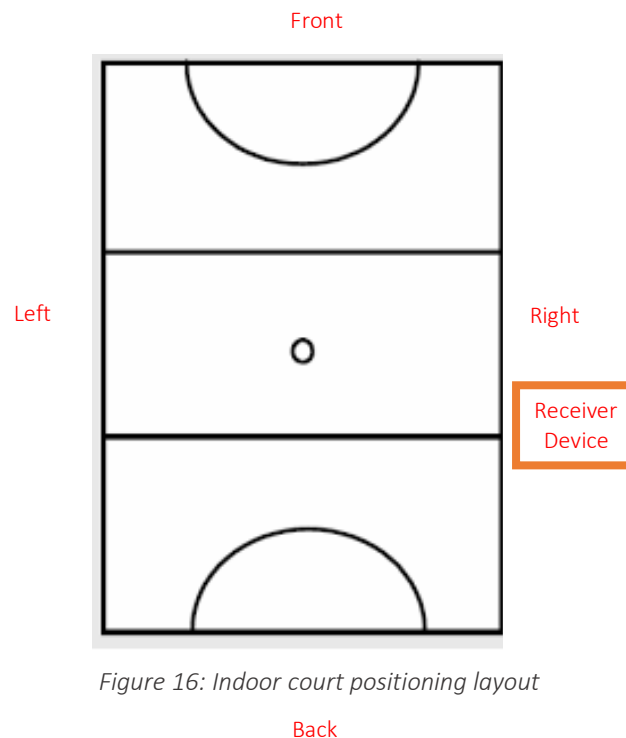


Figure 16: Indoor court positioning layout

The participant was then instructed to undertake these following manoeuvres:

- i. Walk from right to left in a straight line with back to the receiver device
- ii. Walk from left to right in a straight line towards the receiver device
- iii. Walk in back to front in a straight line with right side to the receiver
- iv. Walk from the front to back with the left side to the receiver
- v. Starting from the right position in front of the device, run around the edge of the court lines anticlockwise.

Chapter 3: Testing and Validation of SensorTag

Two other participants who were not wearing any sensors were also recruited; the additional participants were introduced to the court to ‘defend’ the previous participant. Data were collected through continuous streaming for 7 minutes during simulated play. The original participant was given instructions to play with the intent to score goals and the newly introduced participants were instructed to prevent the main participant from shooting goals. This test was different than the structured laboratory movements described in Table 10, to ensure data were captured in a more practical situation. Some of the movements observed include:

- i. Goal shooting and defending with the participants not directly blocking the line of sight of the receiver device
- ii. Goal shooting with a participant blocking the direct line of sight
- iii. Leaping to shoot goals and landing bilaterally with both feet on the ground

The data obtained from the continuous streaming was saved as CSV for post-processing.

3.4 Results

In the laboratory, at the end of every movement, the SensorTag was required to be reset by pressing the side button to continue data collection. During explosive movement such as sprinting, a complete dropout in signal connection was also observed, hence required re-pairing.

The Trigno sensors had a sampling frequency of 250 Hz whereas the maximum achievable sampling frequency was 100 Hz for SensorTag. The A_{IS} axis reading for both the Trigno and SensorTag were graphed together according to the same timestamp for each recorded movement. The dominant right leg was chosen for analysis, as it was the primary landing leg and observed the most loading during rapid impact. An example graph for a running trial lasting seven seconds for the right leg of the participant is provided (Figure 17).

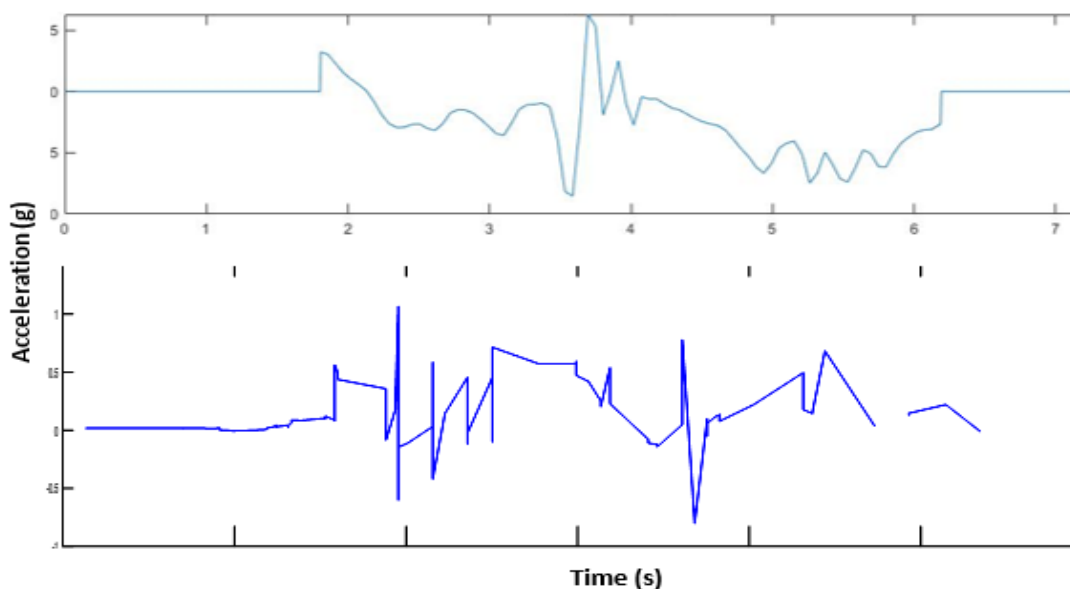


Figure 17: Participant running trial of 7 second duration(right leg) acceleration data (Top: Trigno, Bottom: SensorTag)

Comparing the results from both the Trigno and SensorTag accelerometer, a difference was noticed in terms of acceleration peak ranges. Trigno showed a range from -10 g to approximately +6 g. In contrast, SensorTag had an accelerometer range from -1 g t +1.5 g. As the acceleration was changed in software through CCS to ± 16 g prior data collection, it was assumed the range difference was due to the difference in positioning or possibly incorrect

Chapter 3: Testing and Validation of SensorTag

reading. Although the start and some peaks of the sensors could be matched, the results showed an inconsistent streaming rate across all movements. The loss in data were identified through the purely linear lines in data, which demonstrate a lack of points in data to create curves as observed in the Trigno data. Loss or dropout of Bluetooth connection was demonstrated through gaps in the data where no connection was made between the points (Figure 18).

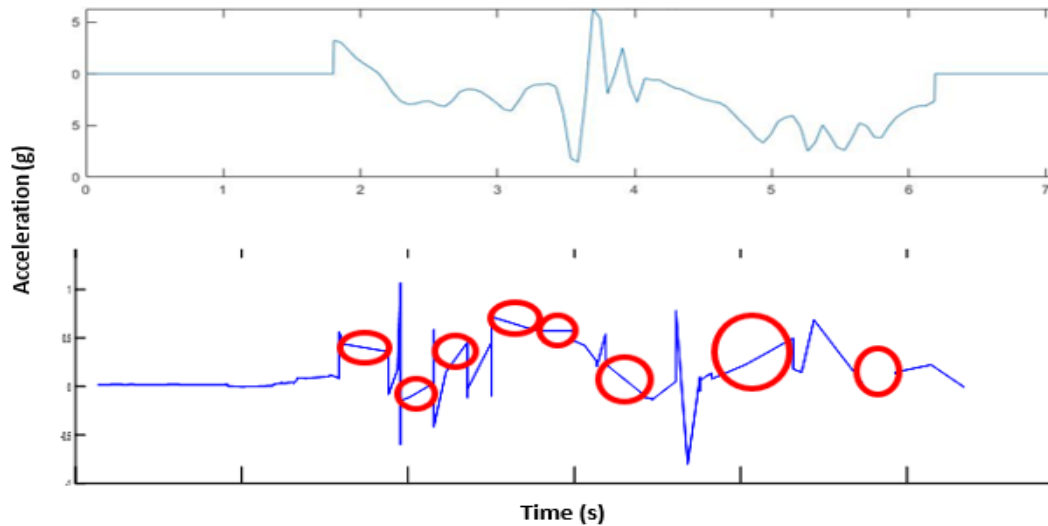


Figure 18: Loss of data and Bluetooth dropout (circled red) (Top: Trigno; Bottom: SensorTag; Movement: Running)

Figure 19 illustrates a jumping manoeuvre performed by the same participant and their resultant AIS acceleration recorded by both the Trigno (top) and SensorTag (bottom).

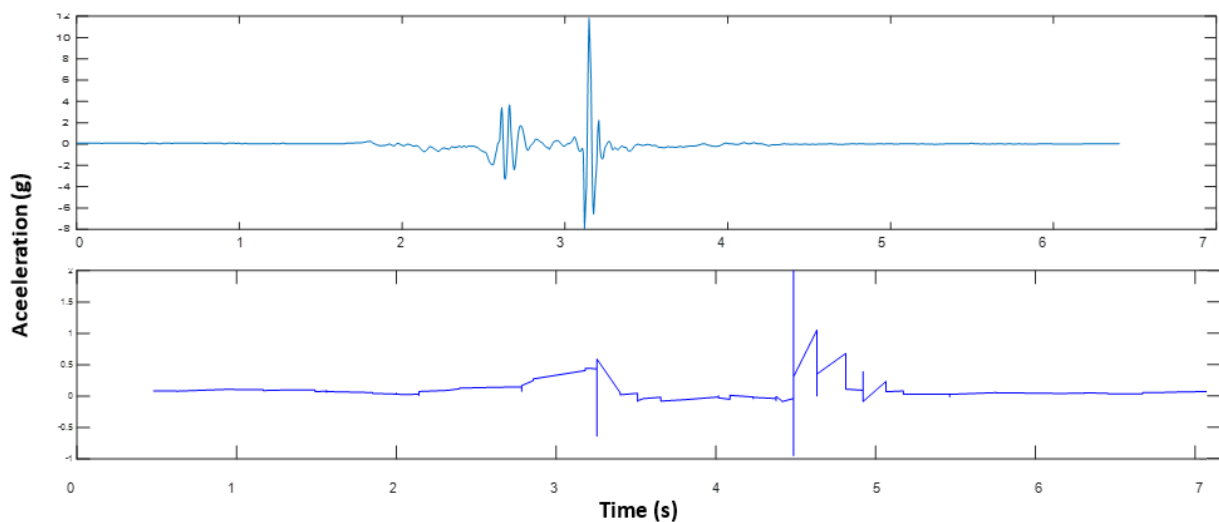


Figure 19: Participant jumping on the spot and landing (right leg) acceleration data (Top: Trigno; Bottom: SensorTag)

A delay was observed in data capture, and the peaks occurring during take-off and landing were further apart. Similar to the running activity, gaps were observed between data points resulting in purely linear lines.

Chapter 3: Testing and Validation of SensorTag

During the individual participant analysis, the range of the SensorTag was found to be inconsistent. Frequent loss of connection was observed with lags in between data capture, often requiring manual reset by hard pressing the SensorTag power button when attempting to reconnect for data capture. The range prior to dropout was between 3 meters and 15 meters.

The continuous activity with two additional participants had a total of 5.6 minutes of data (Figure 20), as the connection was then completely lost, and no additional data were recorded.

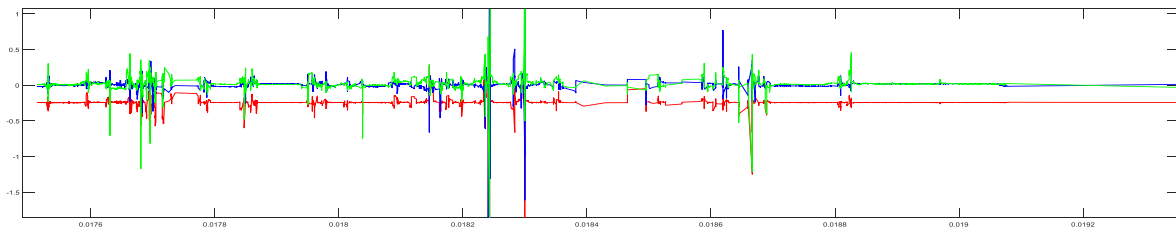


Figure 20: 5.6 minutes of continuous movement data(Acceleration of SensorTag in x (green), y (blue) and z (red) axis)

The graph provided an overall view of clusters of intense activities such as landing. The loss of data were observable when all three axes displayed a flat line from four minutes prior to the completion of continuous movements. The number of data points captured was compared against expected data points from 100 Hz streaming, to calculate the percentage of data loss.

At 100 Hz sampling frequency, the total number of expected data points per minute was calculated to be:

$$100 \text{ Hz} \times 60 \text{ (seconds)} = 6,000 \text{ data points/minute}$$

Therefore, during a 5.6-minute window, the expected data points are:

$$6,000 \frac{\text{data points}}{\text{minute}} \times 5.6 \text{ minutes} = 33,600 \text{ data points}$$

By assessing the CSV file produced from the experiment, in a 5.6-minute data reading, a total of 9488 data points was recorded, which represented:

$$\frac{9488 \text{ data points}}{33600 \text{ data points}} \times 100\% = 28.238\% \text{ of data}$$

As only 28.238% of the data were recorded, the total data loss during a 5.6-minute stream was:

$$100\% - 28.238\% = 71.762\%$$

Chapter 3: Testing and Validation of SensorTag

When assessing the continuous 5.6 minutes trial data with expected and actual data trendline, the number of data points remained unchanged from 3-minute mark up to the 5-minute mark, which was a drop out of connection in the middle of the data (Figure 21).

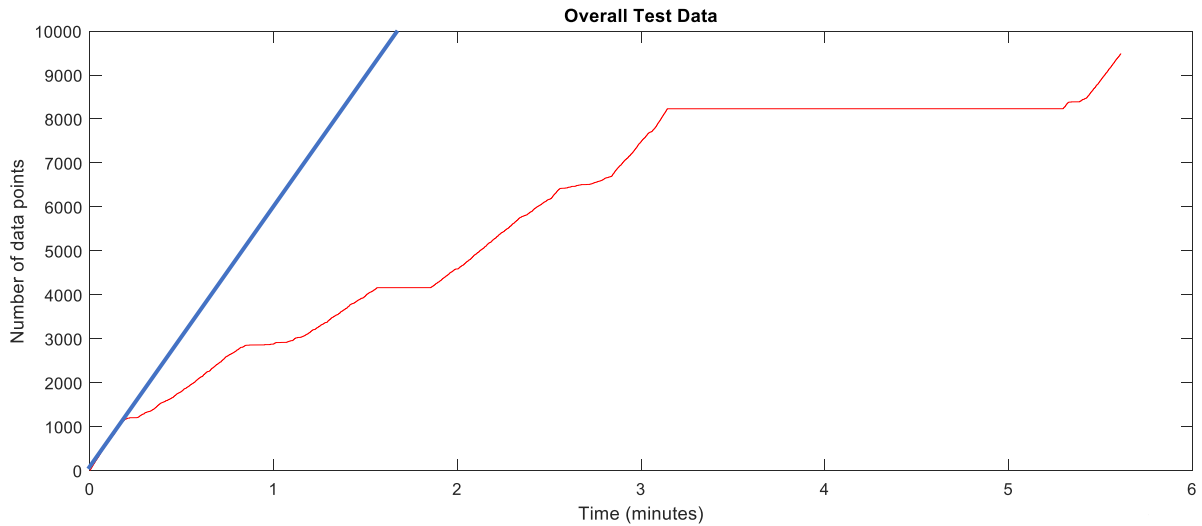


Figure 21: 5.6-minute trial of continuous activities displayed with number of data points against time (expected number of data points trend: blue; recorded number of data points: red)

The graph was expected to simulate the blue linear trendline with time proportional to the number of data points, reaching 33,600 data points instead of 9,488. Multiple other flat lines were also observed throughout the trial, further indicating short loss of data streaming. In addition, 1% battery loss was observed for every 2 minutes of streaming. Therefore, the total lifetime of a coin cell battery during continuous streaming:

$$2 \text{ minutes} \times 100 = 200 \text{ minutes or } 3.3 \text{ hours}$$

3.5 Discussion

The laboratory and in situ testings revealed similar findings in terms of limitation in sampling frequency, data loss, multiple device integration and connection interruption. SensorTag utilises BLE for communication, which is a feature of Bluetooth 4.0, most appropriately suited for short-range communications (Wang *et al.*, 2017). The main advantage of BLE compared with Bluetooth Classic is the reduced power consumption, making it suitable for use with coin cell batteries for wearable devices (Bluetooth, 2010).

During a typical BLE communication, a connection is established between the ‘slave’ and ‘master’ device, where the master can manage a maximum of 7 simultaneous connections with a slave device, and each slave can only connect to one master device. After the connection is established, the physical channel is divided into non-overlapping time units or connection events in which all packet of information is transmitted using the same data channel frequency. The data channel frequency is computed by using a frequency hopping algorithm, and the time between the start of two consecutive connections can range between 7.5 milliseconds to 4 seconds (Gomez *et al.*, 2012). Due to this, data can only be streamed every 7.5 milliseconds in the best-case scenario, with 100 Hz required for the transmission of data every 10 milliseconds. The battery life of the coin cell battery in a wearable device application with BLE is also significantly decreased from the expected 1 year lifetime, and as slave device is expected to operate at 100 Hz sampling frequency without remaining in sleep mode for substantial periods of time (Gomez *et al.*, 2012).

One of the key findings prior to testing was the sampling frequency limitation of the SensorTag. Due to the lack of onboard processing capabilities of SensorTag, the maximum sampling frequency achieved was 100 Hz and data required real-time streaming. The loss of 1% battery was observed for 2 minutes of streaming during laboratory and in situ testing, offering a maximum battery life of 3.3 hours assuming a brand-new battery and a consistent decrease rate. As coin cell batteries are not rechargeable, the battery on the device must be replaced after completion of each gameplay or training session (can last up to 2 hours), further adding to the cost, and maintenance of the device by the user and wastage.

Chapter 3: Testing and Validation of SensorTag

During laboratory testing, it was found that only two SensorTags could be connected to a master device at a time and still successfully collect data at the maximum achievable sampling frequency of 100 Hz, due to the refresh rate required for the master device to address each slave. The master can only address one slave at a time, and with an increased number of slaves, and at the maximum sampling frequency, the master cannot switch between the slaves fast enough, hence packets of data were missed. This was observed during laboratory testing, in movements such as running (Figure 18). The gaps in data were a direct result of switching to address another slave device.

However, when only a single SensorTag device was used, such as in situ testing, a 71.62% data loss was still observed. Bluetooth signals can be affected by an obstruction of the line of sight to the receiver (Juri *et al.*, 2016). The line of sight obstruction was caused by two other participants in the field who may have positioned themselves in front of the SensorTag during the game. This also incurred a frequent loss of connections, often requiring manual reset to begin recapture of data. Loss of bluetooth connection was less evident in the laboratory, as the laboratory was significantly smaller in size and no obstruction was present between the slave and the master device. Disruption of bluetooth originating from the obstruction of the line of sight between a transmitter (slave) and a receiver (master) has also been documented by literature (Juri *et al.*, 2016; Qureshi *et al.*, 2018; Zhao *et al.*, 2014).

The range of the SensorTag was also found to be inconsistent, ranging from 3 meters to 30 meters depending on the direct line of sight to the device. For example, if the participant had their back to the receiver with the transmitter at the front of the shank, the obstruction of the shank caused a signal dropout at a 3-meter distance. When a direct line of sight was maintained and the participant walked backwards in a straight line, the range was found to be 30 meters. During continuous streaming in situ, the range was significantly decreased, resulting in flat lines where no data were observed for a period of time (Figure 21).

BLE is mainly used for short-range communication such as a wearable smartwatch. Mukhopadhyay reported that Bluetooth had a reliable range of 10 m (Mukhopadhyay, 2015). A netball court is 30.5 meters, hence unreliable streaming of 3 meters to 30 meters is not sufficient for reliable capture of a full netball training or gameplay session. The older model of Delsys Trigno used in 2018 study utilised both Bluetooth and Wi-Fi, therefore was able to sustain longer ranges in situ (Corbo, 2018).

Chapter 3: Testing and Validation of SensorTag

The results also demonstrated the missing of short impulses due to significant data loss, in particular, Figure 19. The Trigno, which streamed at 250 Hz, displayed multiple peaks in acceleration data which are not present in the SensorTag data. If this device was to be used on the court, data will most likely be misrepresented due to the potential loss of key acceleration data. The validity of the SensorTag was determined through thorough consideration of the required specifications (Table 11).

Table 11: Specification comparison of SensorTag against the requirement

Specification	Requirement	SensorTag	Justification and validity of SensorTag
Size	~27 x 24 x 13 mm	46 x 32 x 7 mm	In situ testing conducted by 2018 study indicated that the dimensions of the Trigno sensors (as stated in requirement) was comfortable to wear and no change in technique was observed (Corbo, 2018). As the dimension of the SensorTag is approximate to Trigno, the size is valid
Battery life	≥ 2 hours	≤ 3.3 hours	A new battery would be required per device at the start of every gameplay lasting duration of 2 hours. Although SensorTag is sufficient, it requires battery change after every use (not ideal)
Onboard Processing	Required for reduced data transmission	Not available	Onboard processing would eliminate the need for post-processing. Raw data required for SensorTag post-processing
Sampling frequency	≥ 150 Hz	≤ 100 Hz	2018 study concluded the required sampling frequency captured peaks in acceleration as it occurred (Corbo, 2018). SensorTag did not meet the criteria
Multiple connections	7 players per master device	Limited with data loss (2-3)	Multiple connections would ensure the coach can monitor most players with a single master device without isolating 1 or 2 players per game

Chapter 3: Testing and Validation of SensorTag

<p>Range</p>	<p>$\approx 35 \text{ meters}$ $\leq 30 \text{ meters}$</p>	<p>Minimum 35 meters required to cover the longest (diagonal) distance across the netball court. SensorTag did not provide the required range unless a direct line of sight was maintained without the obstruction of other players. This is not practical for a team sport environment such as netball</p>
<p>Data loss</p>	<p>None 71.62%</p>	<p>Data loss at a low sampling frequency such as 100 Hz would misrepresent the movements due to potential loss of data peaks. SensorTag did not maintain a consistent connection, resulting in significant data loss</p>

Texas Instruments SensorTag CC2650 did not meet most of the required specifications of a practical and reliable wearable device. SensorTag also requires the use of CCS, which is not an open-source software, and thorough explanation of the variables and the firmware was not provided. The aims were not met as the BLE connection were not maintained in situ when other players were obstructing the line of sight between the sensor and the BLE receiver dongle, as concluded through in situ testing. Additionally, the minimum range of 35 meters was not achieved for data streaming to cover the distance of a standard netball court. Although multiple SensorTag connections were achieved through Bluetooth pairing to a single receiver device, data loss was observed during laboratory testing. Coin cell battery powering the SensorTag could maintain at least 2 hours of continuous streaming to sustain full netball gameplay, however, required a new battery at the beginning of every session. Overall, most of the requirements to satisfy the aim were not met and due to the hardware and software limitations, in particular, the restrictions of BLE, the SensorTag was not a viable solution to consider for further development.

CHAPTER 4:

DEVELOPMENT OF A

WEARABLE PROTOTYPE

4.1 Introduction

The characteristics of BLE were not suitable for the data transmission requirement of the wearable sensor as concluded from the findings of Chapter 3. Alternative methods of streaming, such as Wi-Fi and Zigbee were considered. Data transmission range, cost, availability, infrastructure, and support availability were considered when choosing the most appropriate method of streaming. This section will include the methodology and design decisions made to develop a working prototype wearable sensor using an alternative streaming method to BLE.

4.2 Aim

The primary aim of this phase was the development of a working prototype sensor, with reliable streaming and data processing. The hardware and software development according to the specified requirements were explored. An algorithm was created to conduct onboard processing of the device, such that the streaming frequency could be significantly reduced despite higher sampling rate when collecting and processing the data. A user interface was implemented for real-time display of data, and a protective casing was produced for fixation of the final prototype to the athlete. Based on the experience gained from the SensorTag validation (Chapter 4), the requirements to inform the hardware and software development process was modified to meet the aims of the study.

- A reliable streaming method was required with a sampling frequency of 150 Hz without any data loss.
- Onboard data processing was required to reduce streaming frequency. Data must be collected by the microprocessor of the sensor at a minimum 150 Hz, processed internally and the result must be streamed at 1 Hz frequency (1-second epoch).
- A user interface was required to display the processed data in real-time to subsequently log and store it in the host device for further analysis.
- The device was required to be portable and compact, such that it can be securely fixed and comfortable to wear for participants.
- All physical components forming the device must not be expensive (\leq AUD\$100)
- Movement data can be categorised into defined impact zones (Corbo, 2018)

4.3 Methods

The methodology describes both the hardware and software development to assess the listed hypotheses.

4.3.1 Hardware Development

4.3.1.1 Streaming method

The first phase in the development of a working prototype was to ensure an appropriate streaming method was chosen. Upon review of the literature and current commercially available devices, it was found that Wi-Fi was very commonly used in various wearable devices (Adesida *et al.*, 2019; Li *et al.*, 2016; Mukhopadhyay, 2015). The Trigno sensors previously used in the study (Chapter 3) utilised Wi-Fi to communicate with the base station and transfer a large amount of data at 250 Hz as BLE only wasn't sufficient (Delsys, 2019b). When connected to a router as a central point, multiple client Wi-Fi devices can stream data to the host depending on the specifications of the router. A Wi-Fi device can provide 20-30 times the range of a BLE device, hence it was deemed sufficient for the range required in the project (Mukhopadhyay, 2015).

4.3.1.2 Hardware Specifications

Esp8266 is a low-cost Wi-Fi microchip with the internet protocol suite (TCP/IP stack) and onboard microcontroller capabilities (Espressif Systems, 2013). The microcontroller achieves significantly low power consumption due to onboard power-saving architecture and a maximum clock speed of 160 MHz. The Real-Time Operating System (RTOS) and Wi-Fi stack allow 80% of processing capabilities for custom programming and development as required by the user (Espressif Systems, 2019). This single chip integrates onboard processing and data streaming capabilities, therefore was chosen as one of the key components for the project. A brief specification of ESP8266 microchip is given in Appendix G.

Esp8266 gained significant popularity in terms of development boards, due to the inclusion of onboard USB to UART bridge (facilitates host communication) and a Micro-USB connector with a 3.3-volt voltage regulator, which can provide power to the board and connectivity to the software development computer (Espressif Systems, 2013). Various commercially available development boards integrated the ESP8266 microchip to increase functionality and

Chapter 4: Development of a Wearable Prototype

compatibility with open source software, such as the Arduino IDE. For the hardware development of a portable and working prototype, a list of specifications was created such that the most appropriate ESP8266 development board could be chosen and any adjustments could be made.

A digital accelerometer was required that could maintain a high sampling rate, and the output was to be directly read by the ESP8266 microcontroller. The resolution, sensitivity and the number of axes required were also considered to ensure the accelerometer met the standard of the 2018 study. To ensure the device was wearable, it was chosen to be powered using a portable battery. Coin cell batteries were not considered viable as Wi-Fi requires higher power consumption than BLE (Darroudi and Gomez, 2017b). Lithium-ion Polymer (LiPo) batteries were chosen due to their thin, light and powerful nature with large capacity. A 400 mAh battery could provide up to 1.9 Watt-hour (Wh) when used at full extent, which would be sufficient for the length of 2 hours (Adafruit, 2019a). LiPo batteries are also rechargeable, therefore a LiPo battery charger with protective circuitry was required. The full list of components and the reasoning for the specifications were summarised (Table 12).

Table 12: Hardware specification for working prototype

Part	Specifications	Justification
Accelerometer:	Sensitivity: $\pm 16 g$	2018 study concluded the maximum observed magnitude of accelerometer signal falls in this range (Corbo, 2018)
	Sampling Frequency: $\geq 150 \text{ Hz}$	2018 study concluded the required sampling frequency captured peaks in acceleration as it occurred (Corbo, 2018)
	Resolution: 10 bits	The output of 1024 step, sufficient for the expected output
	Output type: Digital	ESP8266 microcontroller only accepted digital inputs. If analogue output was chosen, additional microcontroller such as Arduino Nano would be required
	Axis: 3 (x, y, z)	Although 2018 study only obtained data measured in A_{IS} axis, 3 axes would provide further information for future research

Chapter 4: Development of a Wearable Prototype

ESP8266 WI-FI module	USB Serial Chip	Required for direct communication with the module with Micro USB cable
	Transmission range: ≈ 35 meters	Minimum 35 meters required to cover the longest(diagonal) distance across the netball court
	Onboard processing memory	The allocated memory for onboard processing must allow data capture and calculation in a 1-second epoch and real-time
Lithium Polymer (LiPo) Battery	Battery life: ≥ 2 hours	Typical netball gameplay can last the maximum duration of 2 hours
	Rechargeable	The battery must be recharged and reused, to reduce waste and running cost of the unit
	Size: 35.5 x 16.6 x 7.6mm	Compact size will ensure it fits with the device
	Protection circuitry	LiPo batteries are damaged when the voltage drops below 20% capacity, a circuitry is required to cut off power when the battery is low
LiPo Battery charger	LED: indicate charging	Visual confirmation of power for the user
	USB and battery power	Upon connection of a MicroUSB cable, the device must switch over to USB for power while charging the LiPo battery
	Voltage regulator	5V USB power must be converted to 3.3V for the safety of LiPo battery
Target size	PCB board: ~27 x 24 x 13 mm	In situ testing conducted by 2018 study indicated that the dimensions of the Trigno sensors (as stated in requirement) was comfortable to wear and no change in technique was observed (Corbo, 2018)
	Outside shell: Wider to fit the battery	A bigger enclosure will be required for storage of the battery
Software Compatibility	Open Source: Arduino	Open Source Arduino IDE was chosen as the preferred programming IDE as more support was available and a large suite of components support Arduino

Chapter 4: Development of a Wearable Prototype

4.3.1.3 Component Selections

Adafruit Feather Huzzah ESP8266 (Feather) is a development board with ESP8266 microcontroller onboard processing capabilities and is directly programmable using Arduino IDE (Figure 22). This board also incorporates a USB Serial chip, allowing fast development with 921,600 baud rate. The board has auto-reset, hence no manual reset is required when updating software (Adafruit, 2019b).

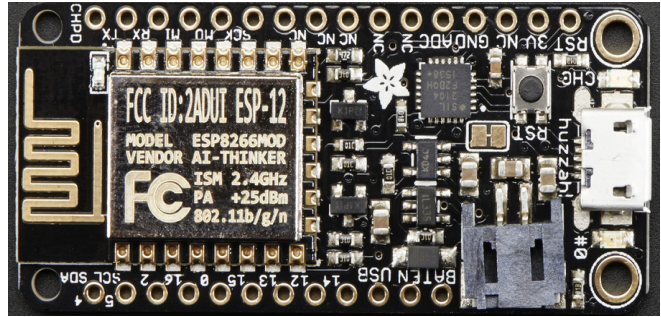


Figure 22: Adafruit Feather Huzzah with ESP8266

The Feather also harbours a 3.7V LiPo battery connector with built-in battery charger, with dual power capability when connected to power through micro-USB. The charging of LiPo battery is indicated by a LED, with a voltage regulator to ensure 5V is converted to 3.3V for board safety. Finally, the PCB size of the board is 51 x 23 x 8 mm; considered adequately compact to meet the sizing requirement (Adafruit, 2019b). After consideration of the device against Table 12, the specifications of the ESP8266 WI-FI module, LiPo battery charger, target size, and software compatibility were met.

As the Feather did not have an onboard accelerometer, the ADXL345 from Analog Devices was explored. The ADXL345 is a small, low power, thin, and 3 axes digital MEMS accelerometer with 13-bit resolution (Analog Devices, 2009). This accelerometer can measure up to $\pm 16 g$, with sampling rate reaching up to 3200 Hz (Analog Devices, 2009). It measures both static accelerations resulting from gravity and the dynamic acceleration resulting from motion or shock, allowing the device to detect tilt as well. The power consumption of the device is proportional to the sampling frequency, therefore can be adjusted accordingly. Therefore, the ADXL345 met all the expected specifications of an accelerometer (Table 12). To integrate the ADXL345 accelerometer directly to the Feather, breakout boards with pinouts for connections were required, and the SparkFun ADXL345 breakout board was chosen (Figure 23).

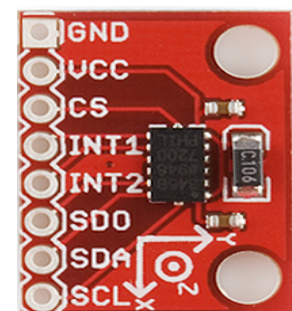


Figure 23: Sparkfun
ADXL345

Chapter 4: Development of a Wearable Prototype

Finally, a 400 mAh LiPo battery with customised dimensions 35.5 x 16.6 x 7.6mm was chosen, such that it could fit directly on top of the Feather while providing sufficient power to the Feather and accelerometer. This battery met the remaining specifications (Table 12) as it was rechargeable and has a built-in protective circuitry to cut off power if capacity reaches damagingly low levels.

4.3.1.4 Component Wiring

After choosing the required components, the Feather, accelerometer and battery were connected using Serial Peripheral Interface (SPI) communication protocol (Figure 24). The detailed pinouts of the Feather are provided in Appendix I.

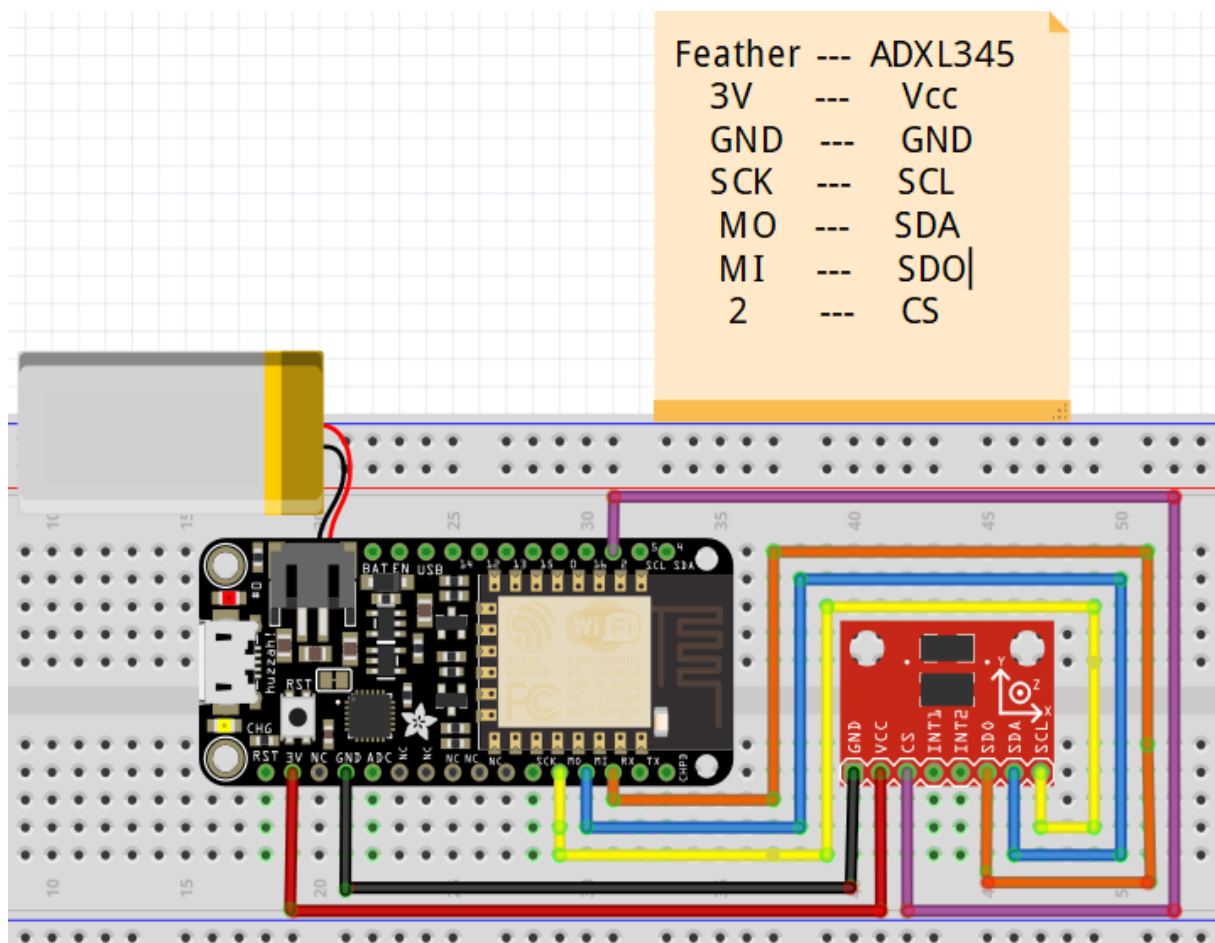


Figure 24: Arrangement of components and wiring

Chapter 4: Development of a Wearable Prototype

Due to the accelerometer unit attached to the Feather, the battery was fixed to the side to prevent wire damage. The Feather was further secured with a cable tie, to ensure the unit was as rigid as possible (Figure 27). Electrical tape was used to wrap around the wire connection of the LiPo battery to reduce potential wire damage (Figure 28).



Figure 27: Feather and battery secured inside casing (without cover)



Figure 28: Final prototype (with cover and taping)

4.3.2 Software Development

4.3.2.1 Data Acquisition

The WebSocket Protocol allows two-way communication between the client and the host, providing a mechanism for a browser-based application that requires the communication between client and host without relying on opening multiple HTTP connections (Wang, Salim, Moskovits, *et al.*, 2013). The protocol allows efficient real-time data transfer between client and host.

As mobile applications require frequent software updates, for the purpose of the project, utilising Websockets to establish a connection between the ESP8266 of the Feather board and a laptop was decided as the better alternative for data acquisition. The WebSocket interface was developed by Lucas Kleiss and integrated into the Arduino IDE (Kleiss, 2019).

4.3.2.2 Calculation of Accelerometer Amplitude Variable

As the ESP8266 board had onboard processing capabilities, data could be collected and processed onboard at a high sampling rate but streamed only at 1-second epoch (1 Hz). Data processed in a 1-second epoch was shown to produce the most consistent correlation with peak VGRF (Corbo, 2018). The low streaming rate reduces the chances of significant data loss and preserves battery capacity. The main algorithm and the header function developed in the Arduino IDE is provided in Appendix J (Kleiss, 2019).

The header function included the required ESP8266, ADXL345, WebSocket, Domain Name Systems (DNS), serial and web server libraries, to ensure the processed data could be directly sent to the web interface (Appendix J). The main program included the setups required for establishing a connection with the WebSocket server and accelerometer data capture. From the previous study, it was concluded that the A_{IS} amplitude had the most consistent and highest correlation to VGRF (Corbo, 2018). Therefore, A_{IS} amplitude in a 1-second epoch was calculated for x, y and z-axis.

The sampling frequency was not set to a specific value, rather the maximum achievable sampling frequency during a 1-second period was monitored to deduce the absolute minimum and maximum value occurring within that period. After performing this calculation, using the

Chapter 4: Development of a Wearable Prototype

‘sliding window technique’, the A_{IS} amplitude will be continuously calculated for every second of data captured.

For example, for the time window of 3 to 4 seconds, the absolute maximum and minimum acceleration value were calculated (Figure 29). The maximum and minimum were then added together, to create the A_x amplitude variable. This calculation was performed on all axes simultaneously. Every second of data collection, three amplitude variables were produced from the three axes.

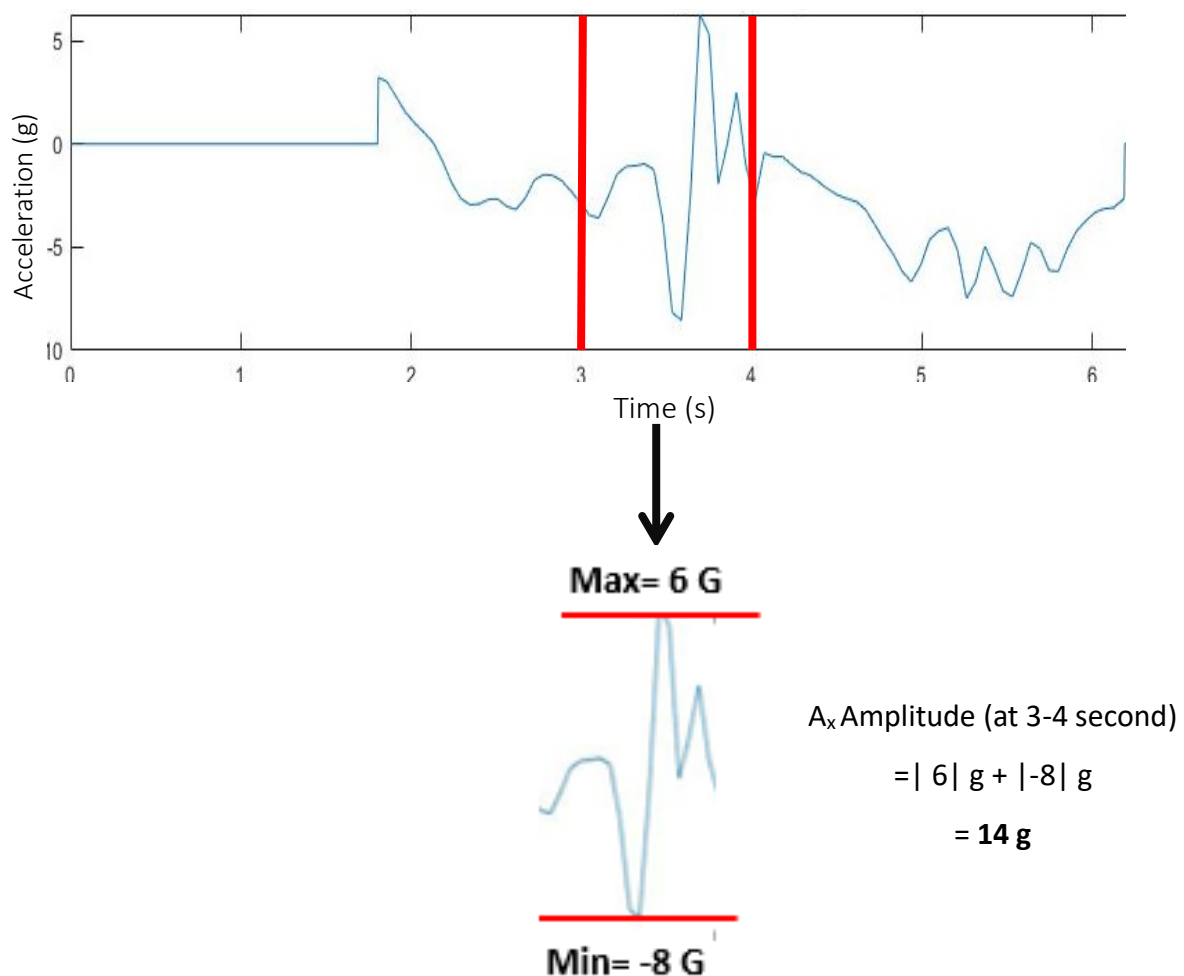


Figure 29: Acceleration amplitude calculation (x axis) 1 second epoch

4.3.2.3 Web Interface

The final phase of the software development was creating a web-based user interface such that the data could be visualised and recorded for further analysis. The ESP8266 chip was set as an access point, such that a laptop could directly connect using Wi-Fi. The web interface was integrated along with Websockets in Arduino IDE (Kleiss, 2019).

The calculated accelerometer amplitude and sampling frequency at which the data were captured was streamed directly to the web interface at 1 Hz. The data could also be logged with individual file names by activating *start logging*, and hence saved for post-processing. The saved logs could be accessed through accessing *view logs*. The interface presented both graphical and serial format for graphing (Figure 30).

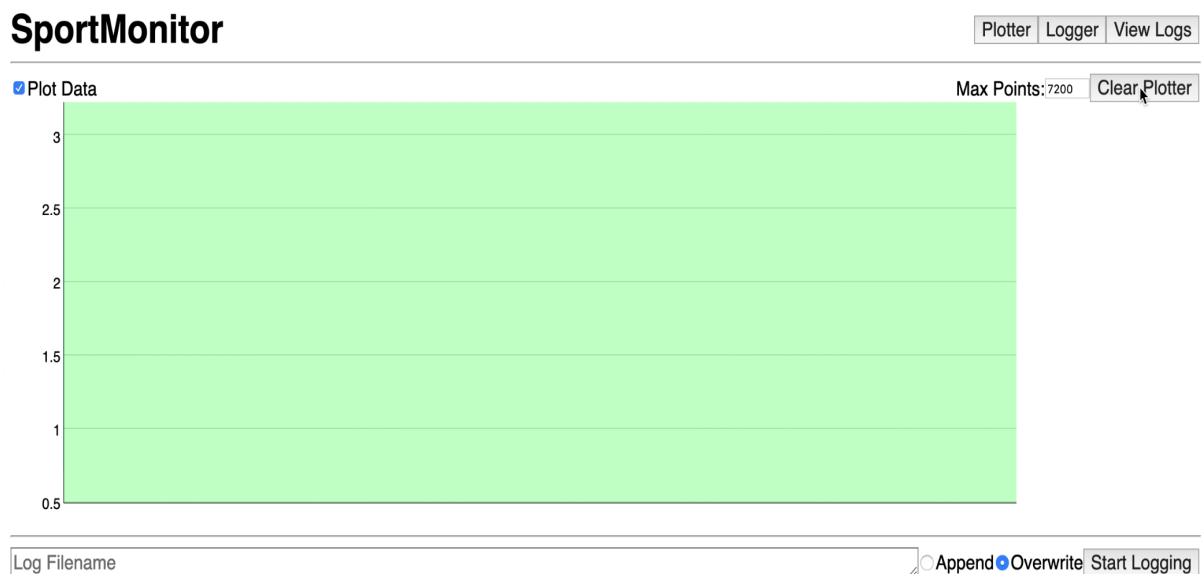


Figure 30: Web Interface

The previous study had also classified low, moderate and high impact zones of activity based on the A_{IS} amplitude: low zone was below 6g, the moderate zone was between 6 g to 17 g and high impact zone was above 17g of acceleration (Corbo, 2018). To provide better visualisation of the impact zones, the plot was divided into green, amber and red zones according to the A_{IS} amplitude zones (Figure 31).

SportMonitor

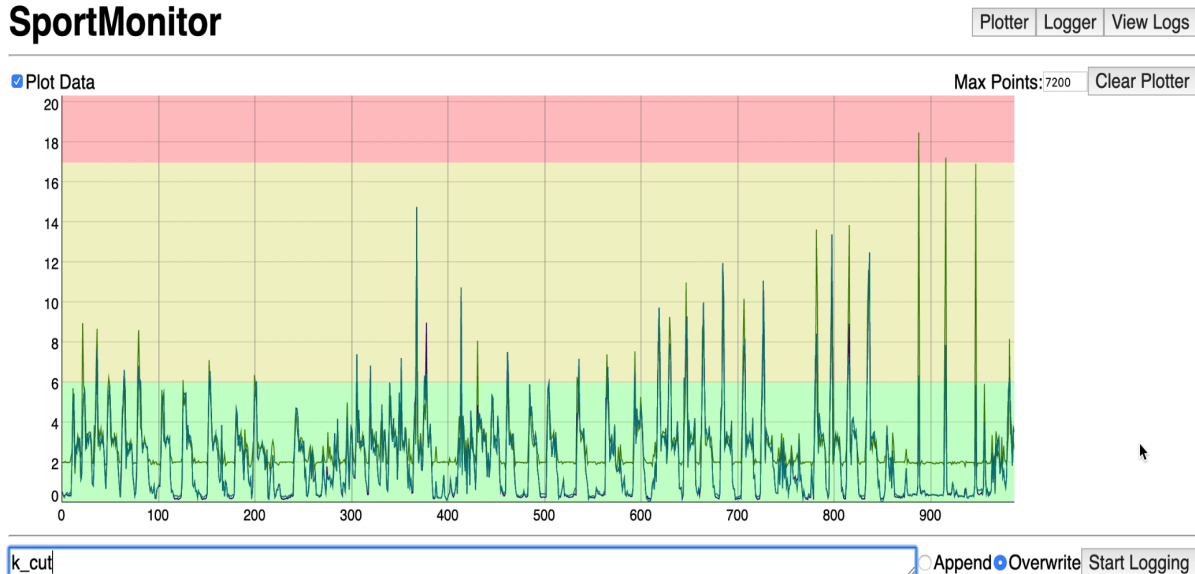


Figure 31: Activity impact zones during multiple activities (1000 second window)

Figure 32 was a recorded log named *k_walk03* which could be accessed through *view logs* after recording, displaying the acceleration amplitude in x, y and z-axis and sampling frequency (SF) at which the data were calculated on the 1-second epoch respectively:

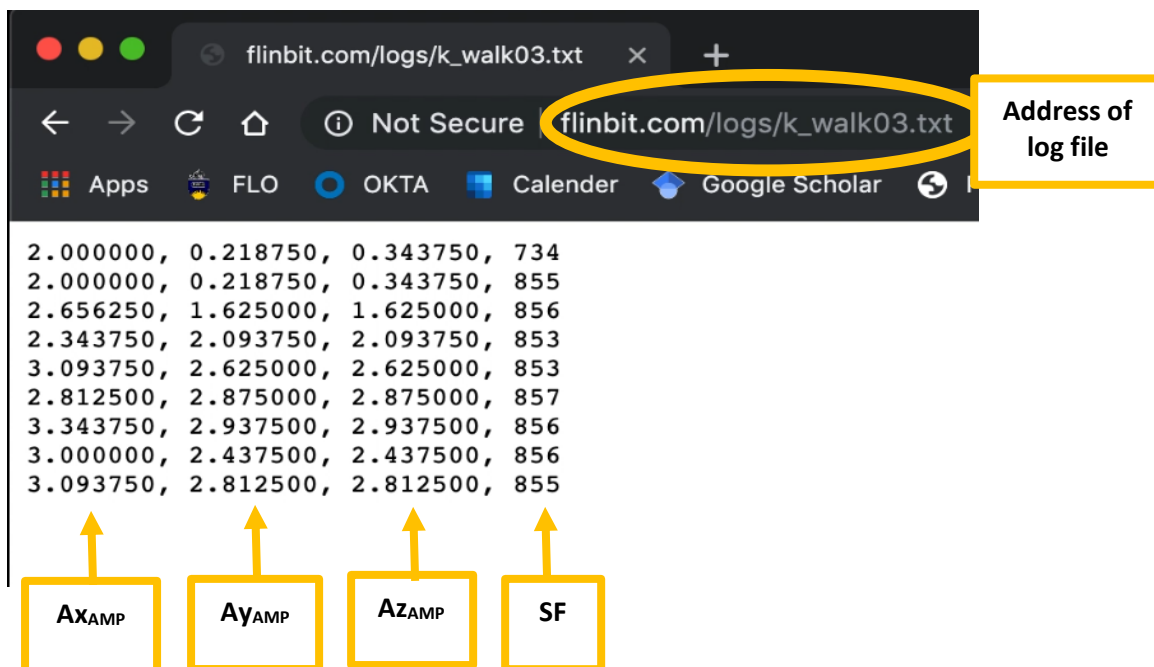


Figure 32: Example of activity log

Chapter 4: Development of a Wearable Prototype

4.4 Results

The final prototype device utilised Wi-Fi as a streaming method and could achieve an average sampling frequency of 850 Hz while processing data in x, y and z-axis in every 1-second epoch. Assuming access to a 3D printer, streaming device and soldering facility, the chosen components were available for purchase online, and the total cost of the unit was AUD\$65 (Table 13).

Table 13: Component cost

Component	Cost (AUD)
Adafruit Feather Huzzah ESP8266	\$25.00 (Adafruit, 2019b)
Sparkfun ADXL345 breakout board	\$28.00 (Sparkfun, 2019)
LiPo battery (400mAh)	\$12.00 (Adafruit, 2019b)
Total Cost: \$65	

Real-time streaming of processed data were achieved through Websockets, and the software development was conducted through the Arduino IDE. As the data were processed on board, the streaming frequency was reduced to 1 Hz, hence the chance of data loss was significantly reduced. The user interface provided visual feedback of changing impact zones depending on amplitude changes. Figure 33 demonstrates a participant jogging with the Feather prototype secured on the dominant shank with physio tape, and the Feather categorised the activity in the moderate impact zone (amber).

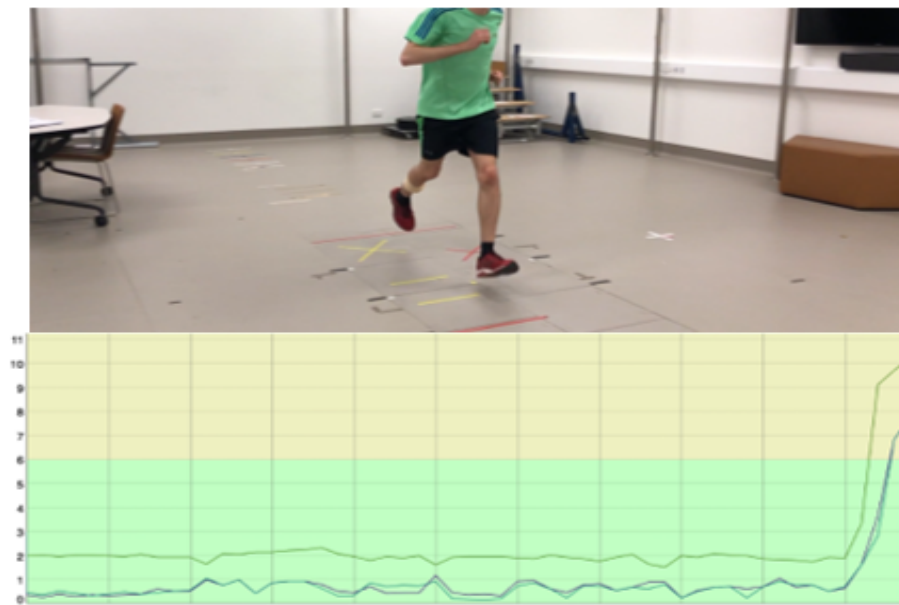


Figure 33: Activity: Slow walk (green), followed by jogging (amber) (Top: participant; bottom: Feather sensor data display)

Chapter 4: Development of a Wearable Prototype

In contrast, Figure 34 demonstrates the same participant performing a sprint and sudden change in direction, which showed the amplitude in the high impact zone (red).

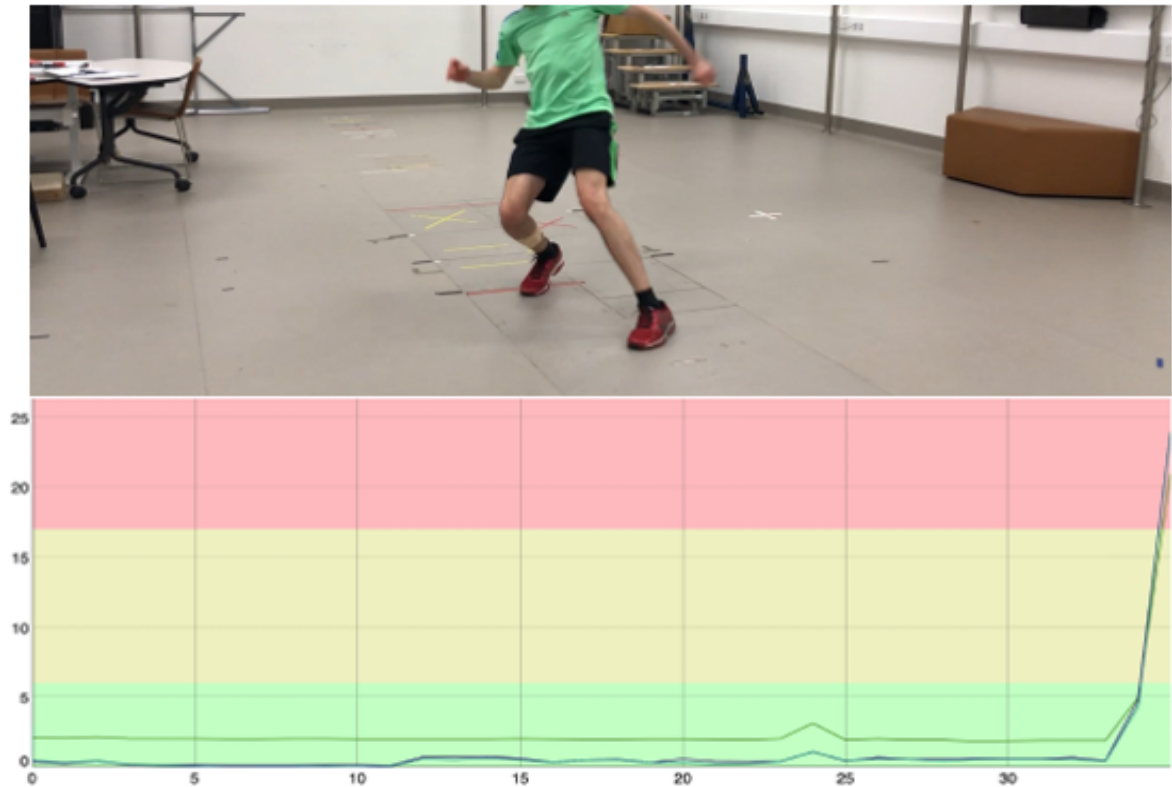


Figure 34: Activity: Sprint and rapid change in direction (red) (Top: participant; bottom: Feather sensor data display)

There was no data loss or connection interruption observed when testing the Feather prototype. The changing impact zone provided a visual indication of impact zones depending on the intensity of the activity.

4.5 Discussion

One of the key factors in the development of a prototype was ensuring an alternative streaming method to BLE was selected that had a larger range and minimal interruption when collecting data. Wi-Fi was chosen as the alternate streaming method, in particular, the ESP8266 chip.

ESP8266 chip is a highly durable and integrated a 32-bit Tensilica processor, standard digital peripheral interfaces, power amplifier, antenna switches, low noise receive amplifier, filters and power management modules (Espressif Systems, 2019). Particularly suited for wearable devices, ESP8266 chip achieves low power consumption with a combination of several registered technologies and three modes of operation: active mode, sleep mode and deep sleep mode. This allows battery-powered designs to run longer. The onboard L106 32-bit RISC processor, combined extra-low power consumption with reaching a maximum clock speed of 160 MHz (Espressif Systems, 2019). Due to the Wi-Fi stack and the Real-Time Operating System (RTOS), approximately 80% of the processing power was available for user application development, hence allowing the onboard processing required for data processing.

The components were chosen to be a combined price of AUD\$65, which met the low-cost criteria of below AUD\$100. The component cost could be further reduced if the components were sourced directly from the supplier based in China. When assembling the components, the accelerometer was connected using the SPI protocol. There were two methods of serial communication available: SPI and I2C. SPI communication is faster, and consumes less power compared to I2C. I2C allows multiple masters and multiple slave connections, whereas SPI allows multiple slaves but a single master configuration. In SPI, communication is always started by the master and a synchronised communication protocol is maintained due to the shared clock between master and slave (Wang, Salim and Moskovits, 2013). After comparison, due to power consumption, speed, and lack of requirement of multiple master devices, SPI was chosen as the main communication protocol for development.

The prototype hardware was kept rigid through securing the accelerometer breakout board to the Feather and securing the Feather directly to the 3D printed case. The battery was removed when the device was not in use. The prototype could then be secured to the shank of the participant with physio tape.

Chapter 4: Development of a Wearable Prototype

Websockets was used to display the result to the user, instead of a mobile application, for future development and maintenance simplicity. Websockets allows communication through multiple clients if a router is used as the central host, therefore future development of connecting multiple athletes to the same central device could be achieved using Websockets.

The accelerometer data were collected and processed in a 1-second epoch by the microcontroller, which achieved an average sampling frequency of 850 Hz. Research had indicated that with a higher sampling frequency, shorter impulses in acceleration during rapid movements could be captured (Camomilla *et al.*, 2018). The streaming frequency was reduced to 1 Hz, and no loss in data were observed. The Feather prototype was compared against the specifications from Chapter 3 (Table 14).

Table 14: Feather prototype comparison with specifications

Specification	Requirement	Feather Prototype	Validity of Prototype
Size	~27 x 24 x 13 mm	68 x 47 x 15 mm	Although the dimensions are larger than required due to the outside cover, it was worn by participants and deemed comfortable. Future works could reduce the size by printing a smaller casing
Battery life	≥ 2 hours	~ 3.5 hours	The 400 mAh battery would provide 3.5 hours of power to the device at full capacity. Rechargeable battery provides prolonged usage
Onboard Processing	Required for reduced data transmission	Available	Amplitude is calculated onboard, reduced streaming rate to 1 Hz
Sampling frequency	≥ 150 Hz	~850 Hz	Exceeded the required criteria due to onboard processing
Multiple connections	7 players to one master device)	1, but multiple can be integrated	Maximum 24 client connections can be made using a Wi-Fi router

Chapter 4: Development of a Wearable Prototype

Range	≈ 35 meters	~ 50 meters	Exceeded required range due to inherent characteristics of Wi-Fi and lower streaming rate
Data loss	None	None	No data loss was observed

In addition to meeting the design criteria (Table 14), the Feather was also used to directly identify low, moderate and high impact activities as demonstrated in Section 4.4. The results indicated that real-time feedback according to the movements, and consistently high sampling frequency were achieved, and that the lower streaming frequency significantly reduced the likelihood of data loss. The easy to visualise interface provides coaches with a fast and effective way to assess individual athletes. However, further testing must be conducted to ensure the zones could be effectively identified for different activities for different participants.

The Feather prototype equipped with ESP8266 provided a reliable method of data streaming with the average sampling frequency of 850 Hz. The onboard processing capabilities eliminated the requirement for post-processing while ensuring no data loss. The processed data in 1-second epoch was displayed in real-time to the user through a Websocket based interface. The user interface had capabilities such that data can be logged and stored in the host device for further analysis. The physical components forming the device cost AUD\$65, which met the requirement of \leq AUD\$100 . A 3D printed casing ensured the circuitry and battery of the device were protected. Movement data could be categorised into impact zones (Corbo, 2018). Overall, all the objectives were met, and the Feather prototype was considered a viable solution for further development of pilot data collection.

CHAPTER 5:

CORRELATION AND

FEASIBILITY STUDY USING

WEARABLE PROTOTYPE

Chapter 5: Correlation and Feasibility Study using Wearable Prototype

5.1 Introduction

In the previous study, it was concluded that fixing an accelerometer to the shank and collecting A_{IS} amplitude over a 1-second epoch could be used to deduce an impact dose (Corbo, 2018). A pilot validation study was required using a range of participants, and laboratory-based force plates and accelerometers (Chapter 3). The correlation was found to be strongest when comparing A_{IS} amplitude at the shank with the VGRF obtained by the force plates (Corbo, 2018). The laboratory findings provided a strong theoretical foundation for understanding the correlation of A_{IS} amplitude obtained from the Feather prototype. This section includes the methodology and results from the pilot correlation and feasibility study. To determine whether the Feather prototype that was developed in Chapter 4 could be used to deduce the impact dose measure of participants in the laboratory environment.

5.2 Aim

The primary aim of this phase was to collect pilot data of participants performing simulated laboratory-based netball activities within a laboratory setting. The data were then analysed to validate the effectiveness of impact dose measured through the A_{IS} amplitude at the shank. The main objectives of the correlation and feasibility study investigated are listed below:

- The acceleration amplitude collected at the shank in the inferior superior axis was required to be correlated with VGRF. The impact zone identified through the 2018 study will remain consistent amongst participants.
- The accelerometer sensitivity of $\pm 16 g$ would be sufficient to record the acceleration of lower limbs during netball specific movements in the laboratory.
- The sampling rate would be sufficient, and no data loss would be observed during simulated movements
- The battery of the prototype would be sufficient for a 2-hour laboratory trial.

Chapter 5: Correlation and Feasibility Study using Wearable Prototype

5.3 Methods

The methodology details the laboratory protocols and data extraction for pilot data collection for each participant.

5.3.1 Participant Selection

Three participants were chosen for the pilot validation study, who were provided with an information pack consisting of an information sheet and a consent form (Appendix K). The participant details were collected for further analysis (Table 15).

Table 15: Pilot study participant details

Attributes	Participant 1	Participant 2	Participant 3
Gender	Male	Female	Male
Height	177 cm	156 cm	179 cm
Age	31	22	22
Sporting involvement	Hockey	None	Squash, tennis, soccer, volleyball, athletics (middle-distance sprints, long jump, triple jump)
Previous injuries	Ligament tear of Achilles, partial ligament tear of Achilles, occasional discomfort	None	None
Pre-existing factors affecting the lower limb	None	Asymmetric hip, prosthetic left foot	None

The three participants were from varied backgrounds and did not have current or previous netball engagement. All participants had a dominant right leg, hence the placement of the Feather prototype was chosen to be at the right shank.

Chapter 5: Correlation and Feasibility Study using Wearable Prototype

5.3.2 Data Collection

The testing was conducted in the Flinders University Motion Analysis and Rehabilitation Laboratory, utilising the AMTI OR6-7 force plates integrated to Vicon Nexus 2.0 software. The laboratory was configured as described in *Section 3.3* for data collection at the start of every session. The lower limb of the participant was marked up with reflective Vicon markers (*Section 3.3*). Alongside the Feather prototype sensor, 4 Trigno sensors were chosen as secondary measures (Figure 35). The placement of the Feather sensor was chosen to be at the dominant (right) shank of the participant, as it had been shown to provide the best correlation (Corbo, 2018). The Trigno sensors were placed on the lateral malleolus and shank for both dominant (right) and non-dominant legs.

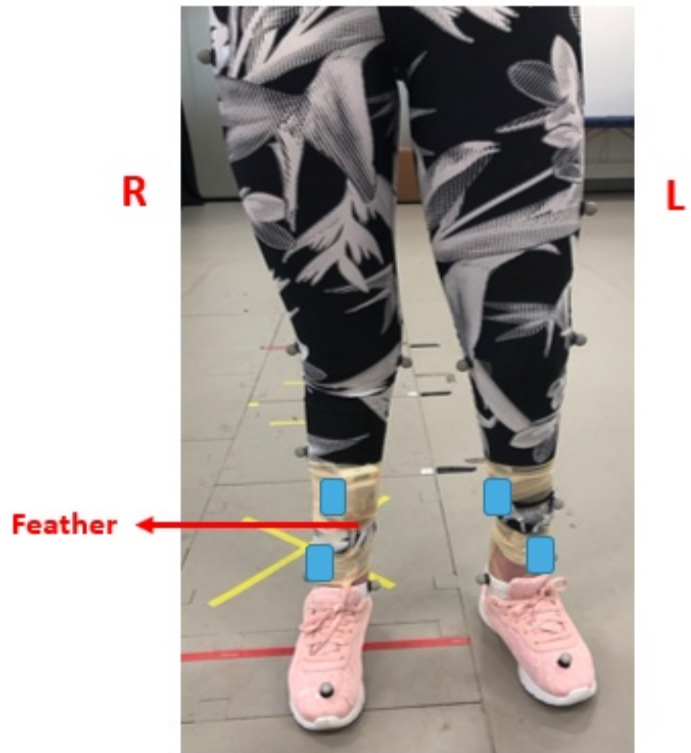


Figure 35: Participant 2 with the Feather prototype sensor (Right shank) and four Trigno sensors (Blue: Trigno; Red: Feather prototype)

To begin each trial, a T-pose stance of the participant was collected (Appendix E), where the participant was to maintain in a static position with their right foot on plate 2 and left foot on plate 1. This position was required to calculate the mass of the participant, such that force data could be normalized. Next, the game-based laboratory protocols of netball simulated movements outlined in Table 10 (*Section 3.3.1.3*) were replicated by each participant during a laboratory data collection session. Three valid trials were collected per movement, per participant. As the Feather was not synchronised with the Vicon software, both Vicon and Feather data capture were manually activated at the same time. After each trial of a single movement, the data were saved for both the Feather and Trigno with the same name, for ease of data processing. Additionally, a video camera was used to record the timing of data collection, such that any delay between Vicon and Feather in data capture could be identified and appropriately accounted for.

Chapter 5: Correlation and Feasibility Study using Wearable Prototype

5.3.3 Data Export and File Processing

After each trial, Vicon was used to review and reconstruct the trial movement to ensure the participants' grounded foot landed completely within the boundaries of the force plates, such that the trial would be valid. A document was kept recording the relevant plates of each movement, and any observations that could potentially impact the data for that movement. Any other factors that had the potential to impact the accuracy of the result, such as the participant modifying their movement in an attempt to ensure proper landing within the boundaries of the force plates, were recorded so the trial data could be discarded. After validating the trial, ie, ensuring proper foot contact and natural movement of the participant, the data were exported as a CSV file and converted to XLS format for MATLAB processing. The logged data from the Feather prototype was also downloaded as a CSV file. After completion of the whole movement protocol, the data file for each trial was modified to create new XLS files with each movement, where the force plate, Trigno data and Feather data were combined with corresponding column numbers for all movements. This was required for data processing, as one column across all movement files would represent the same variable. The Trigno files were not analysed but were kept in the document for future comparison.

5.3.4 Data Analysis

At the conclusion of data collection, 90 combined files were obtained from 90 trials (3 participants by 3 repetitions by 10 movements). MATLAB was used to analyse individual participant data and plot the A_{IS} amplitude with VGRF for every movement, and calculate the correlation using linear regression (Appendix L). Firstly, the main function of the MATLAB algorithm, *main.m*, was used to extract the movement files for a participant, accepting any number of movements and number of trials. Using the Tpose file, *mass.m* calculated the mass of the participant and returned this value back to *main.m*. Within *main.m*, a colour vector was then formed, with a different colour assigned to each movement and ensuring all trials of a movement corresponded exactly to the same colour. For each trial file, *extractFeature.m* extracted the force plate data and normalised according to the bodyweight of the participant. Peak force (BW) and corresponding A_{IS} amplitude was then extracted, depending on the boundaries of heel strike and toe-off occurrence (Figure 36).

Chapter 5: Correlation and Feasibility Study using Wearable Prototype

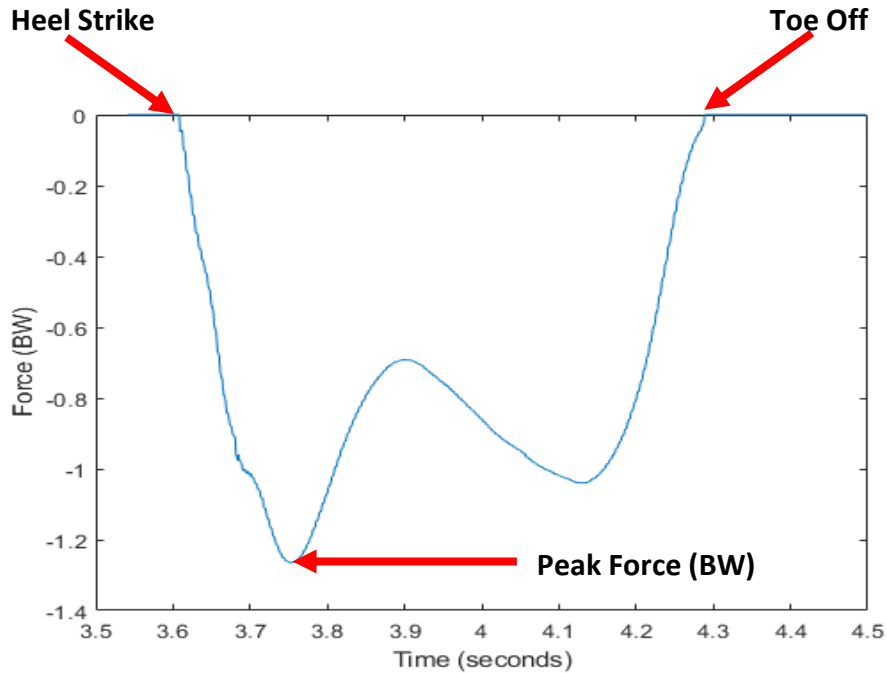


Figure 36: Example walk data (Participant 3) demonstrating peak force (BW), heel strike and Toe off from normalised force data (z axis: vertical ground reaction force)

For movements such as jump, 2F, and 440step, no toe-off was present in the data as the activity concluded with both feet of the participant remaining on the force plate (Figure 37). For these movements, toe-off was defined as the point at which VGRF (F_z) reached -0.5 BW at a plateau, and muscle stabilisation and balance was achieved. The calculated peak force (BW) and acceleration amplitude (A_{IS}) was returned to *main.m* and stored in the trial struct variable.

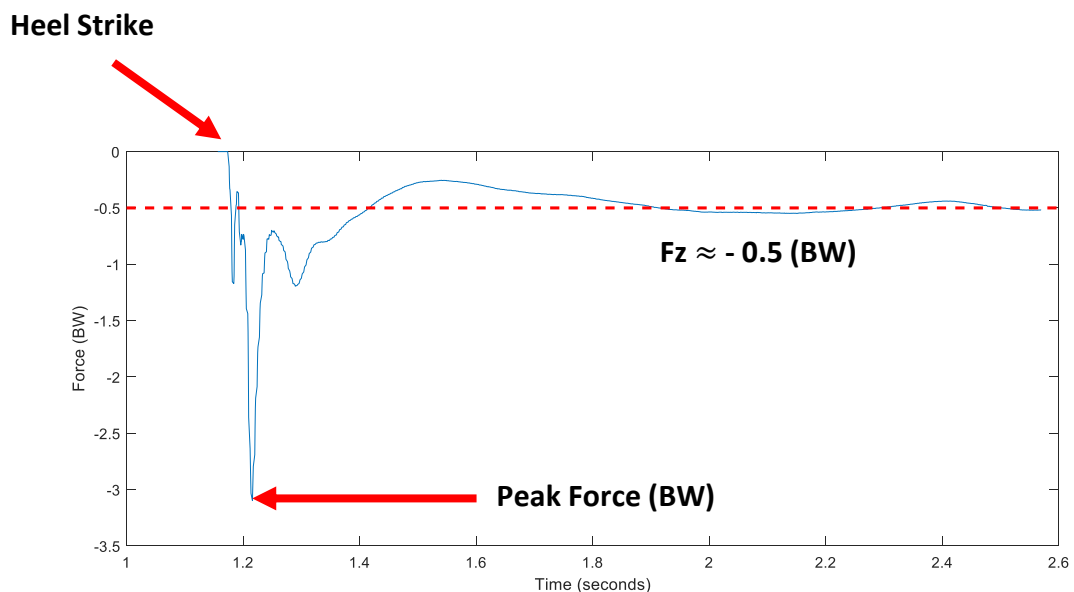


Figure 37: Example 440 step data (Participant 3) demonstrating peak force (BW), heel strike and plateau force from normalised force data (z axis: vertical ground reaction force)

Chapter 5: Correlation and Feasibility Study using Wearable Prototype

The structs formed from extracting features of every trial files for each specific movement was then stored into a vector containing all trials of the same movements, using *vector.m*, and outputted back into *main.m*. A single structure was then formed with all movement vectors, such that any required variables could be identified as the analysis continued. Next, *correlate.m* was used for processing the movement vectors, and plotted as required using the *plotFeatures.m* function. Finally, *main.m* utilised *tabulate.m* to create an XLS spreadsheet with all the calculated peak VGRF (BW) and corresponding A_{IS} amplitude for every individual participant. Therefore, seven functions were used to analyse the Feather prototype variables with VGRF for each participant (Figure 38).

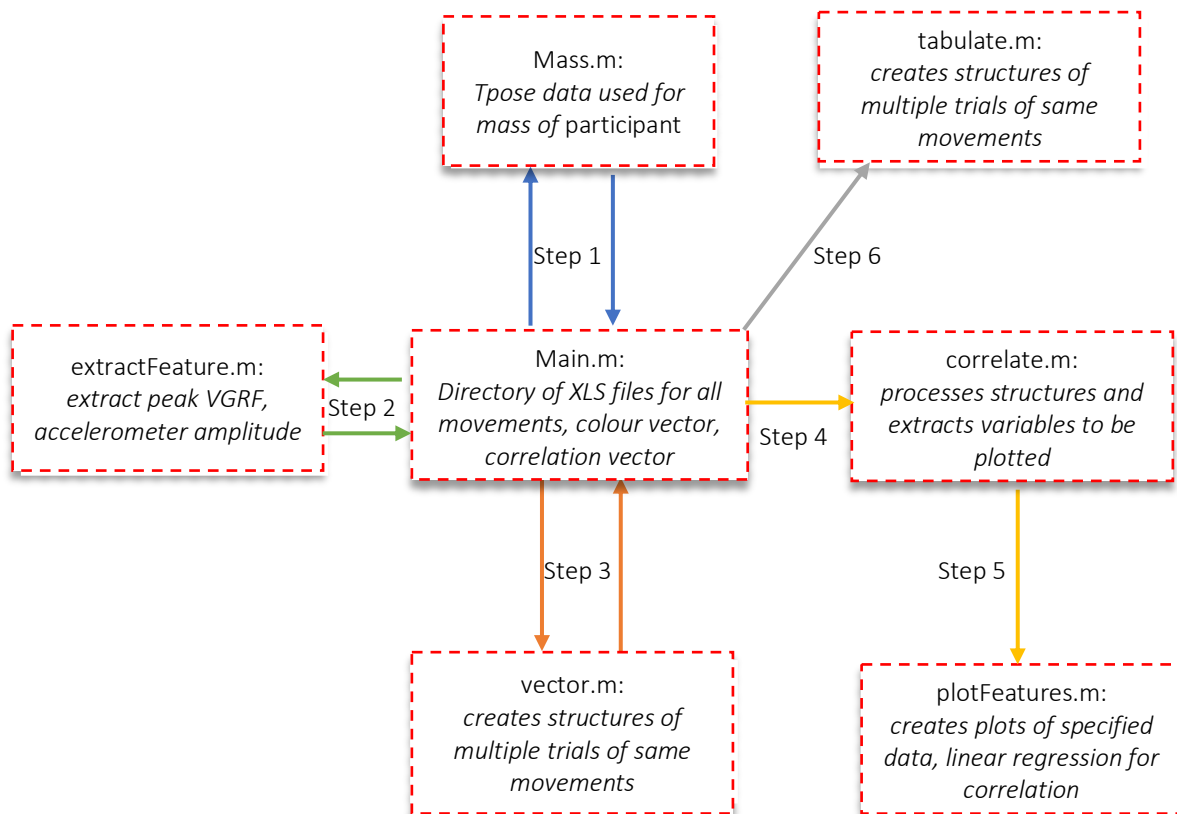


Figure 38: MATLAB dataflow for individual analysis

Chapter 5: Correlation and Feasibility Study using Wearable Prototype

5.4 Results

Linear regression was used to correlate the individual participant results (Figure 39, Figure 40, Figure 41). The movements were differentiated using coloured markers.

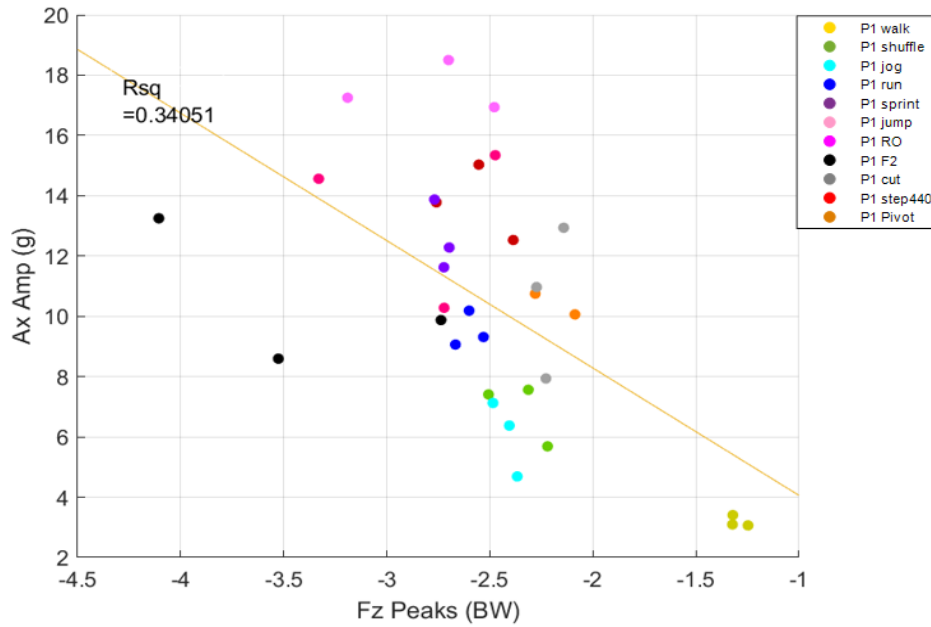


Figure 39: A(IS) amplitude (shank) vs Fz (VGRF) correlation: Participant 1

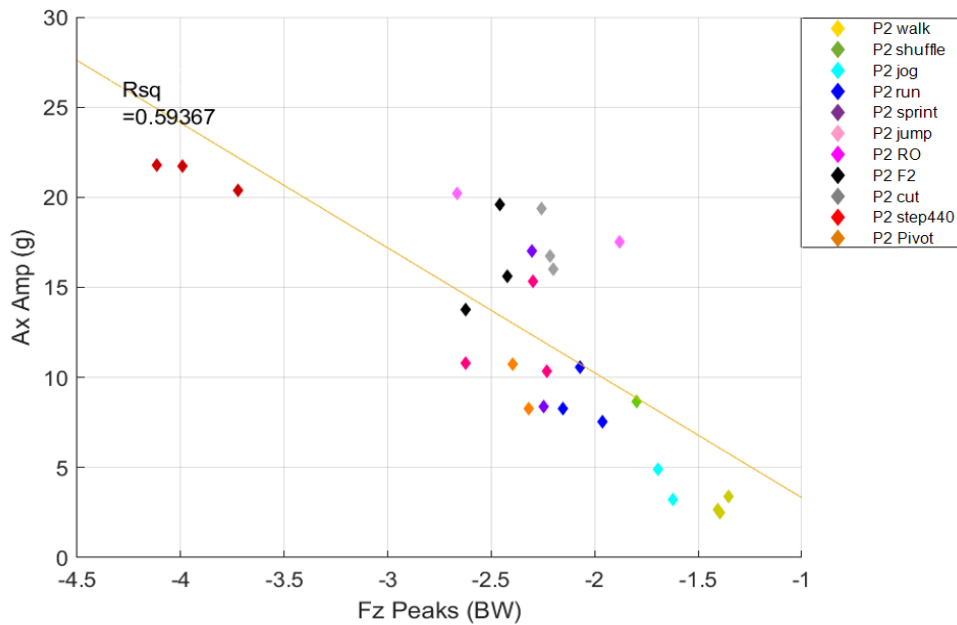


Figure 40: A(IS) amplitude (shank) vs Fz (VGRF) correlation: Participant 2

Chapter 5: Correlation and Feasibility Study using Wearable Prototype

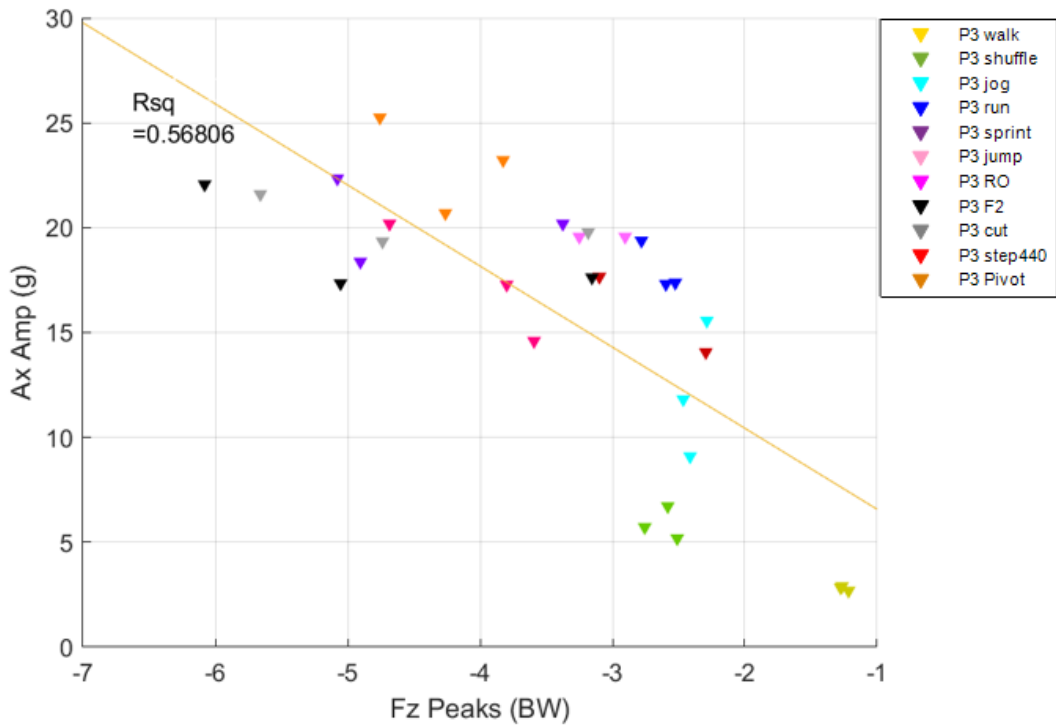


Figure 41: A_{IS} amplitude(shank) vs Fz (VGRF) correlation: Participant 3

Participant 1, 2 and 3 displayed an R^2 value of 0.34, 0.59 and 0.57 respectively. The average peak VGRF and A_{IS} amplitude for the Feather secured at the dominant (right) shank were presented for each movement (Figure 42, Figure 43).

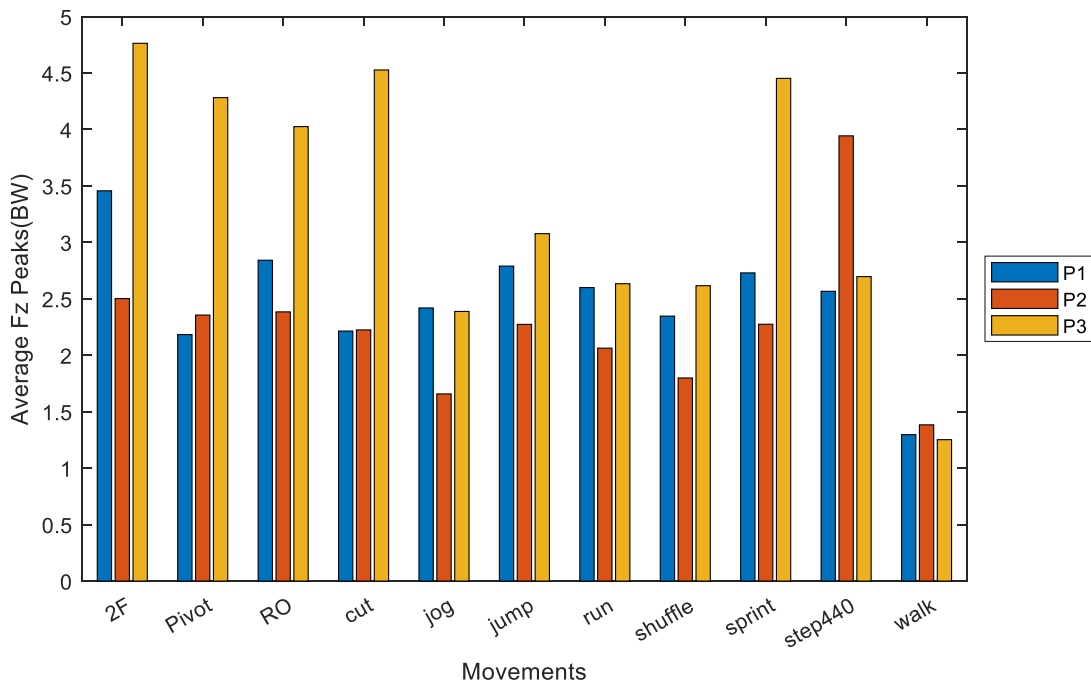


Figure 42: Average Fz peak VGRF (BW) based on movements for participant 1, 2 and 3

Chapter 5: Correlation and Feasibility Study using Wearable Prototype

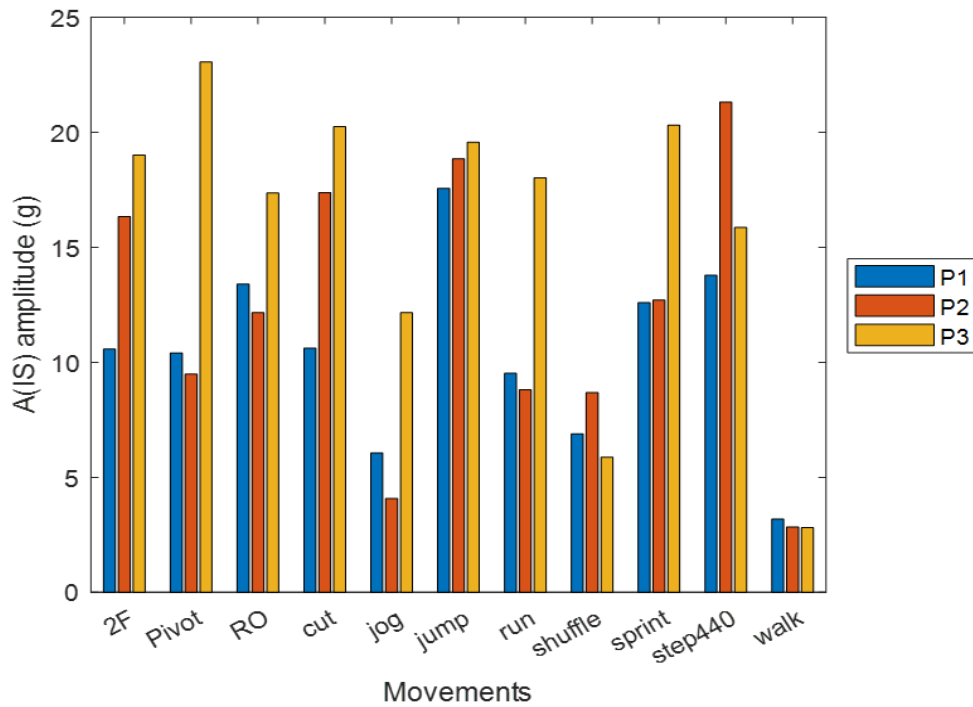


Figure 43: Average A(IS) amplitude at the shank for movements for of each participant

Due to the difference in the participant's athletic abilities, physique and previous injuries, variance in individual VGRF peak force and A_{IS} amplitude measured at the shank was observed. Each participant demonstrated varying peak force and A_{IS} amplitudes during high-intensity activities, with an example movement for participant 3 provided in Figure 44.

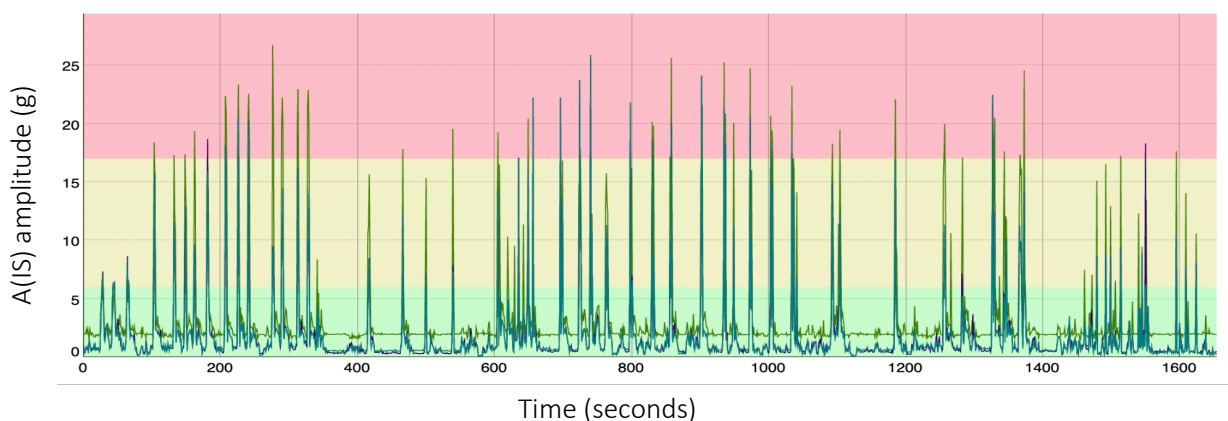


Figure 44: Continuous data collection of participants 3 undertaking laboratory movement protocols (duration of 28 minutes; movements include run, sprint, jump, 2F, pivot, 460step, Run-on and cut; excludes: walk, jog and shuffle)

Chapter 5: Correlation and Feasibility Study using Wearable Prototype

The individual participants were then combined, and linear regression was used to indicate an overall correlation between the peak VGRF and A_{IS} amplitude for each movement (Figure 45). The steep gradient fit of the linear line indicated clear zoning of different movements according to the impact, hence separating data into low, moderate and high impact zones (Corbo, 2018). Walking was classified in the low impact zone, and jumping was classified in the high impact zone for all participants consistently. However, participant 3 displayed higher A_{IS} amplitude and peak force compared to participants 1 and 2. The impact zones were applied according to the previous study, and the overall correlation provided an R^2 value of 0.53. Discrepancies in peak forces for sprint, cut, run-on, pivot and 2F were observed between all three participants.

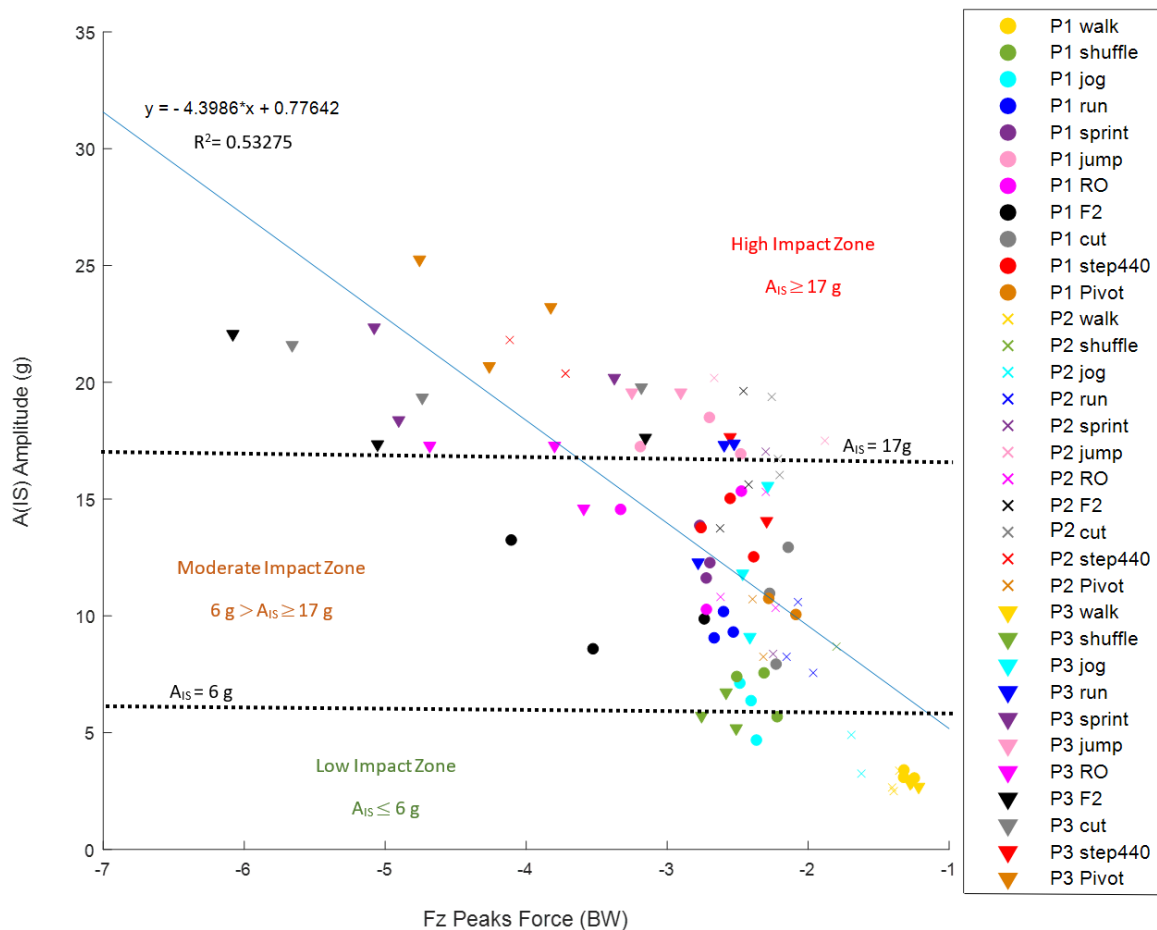


Figure 45: A_{IS} amplitude (g) vs F_z peak VGRF (BW) correlation with three impact zones combined with three participants

5.5 Discussion

The use of AMTI OR6-7 force plates and the Feather prototype developed in Chapter 4 allowed the investigation of re-correlating the peak VGRF with A_{IS} amplitude, using linear regression. The correlation and feasibility study findings were then used to validate the impact zones when accelerometer data were collected from the shank according to a previous study (Corbo, 2018).

5.5.1 Individual Participant Analysis

The laboratory correlation and feasibility study conducted with three participants demonstrated varied results in peak VGRF and A_{IS} amplitude. A clear correlation was observed for participant 2 (Figure 40) and participant 3 (Figure 41), whereas participant 1 (Figure 39) displayed a trend at which the peak VGRF was not clearly correlated with A_{IS} amplitude.

During the laboratory trial, it was observed that participant 1 was landing with greater knee flexion and the lower limb appeared less stiff compared to other participants. During the movement protocols, participant 1 was visibly not demonstrating explosive movements with maximal efforts, due to previous right leg injuries and the potential fear of re-injury. Although A_{IS} amplitude showed an increasing trend with increased activity intensity, the VGRF for the participant did not increase significantly. Participant 1 had a history of knee ligament related injuries in recent years on their right leg (Table 15).

A recent study involving 36 athletes with a history of ACL injuries performing movements such as jump landings, identified that individuals with higher fear of re-injury demonstrated lower peak knee, hip, and trunk flexion hence increased lower limb stiffness in landing (Trigsted *et al.*, 2018). Furthermore, studies have shown that subjects can consciously alter the landing stiffness to reduce the force observed by the affected limb in an attempt to shield themselves from further injuries (Arampatzis *et al.*, 2002; Devita and Skelly, 1992; Dufek and Bates, 1990; Zhang *et al.*, 2000). Butler *et al* identified that soft landings would induce lower VGRF due to conscious bending of the knee and reduced stiffness (Butler *et al.*, 2003). Participant 1 was visibly landing and changing direction (i.e. Pivot, cut) with caution, contributing to a potential decline in resulting VGRF during high impact movements. In comparison, low impact movement such as walking produced low VGRF as expected and high impact movement such as '2F' produced the highest VGRF. 'Jump' displayed the highest A_{IS}

Chapter 5: Correlation and Feasibility Study using Wearable Prototype

amplitude, but the resulting VGRF was reduced due to soft landing. However, all three trials were very consistent, and the previously injured right leg produced higher VGRF than left, potentially due to slightly increased stiffness from injury discomfort (Figure 46).

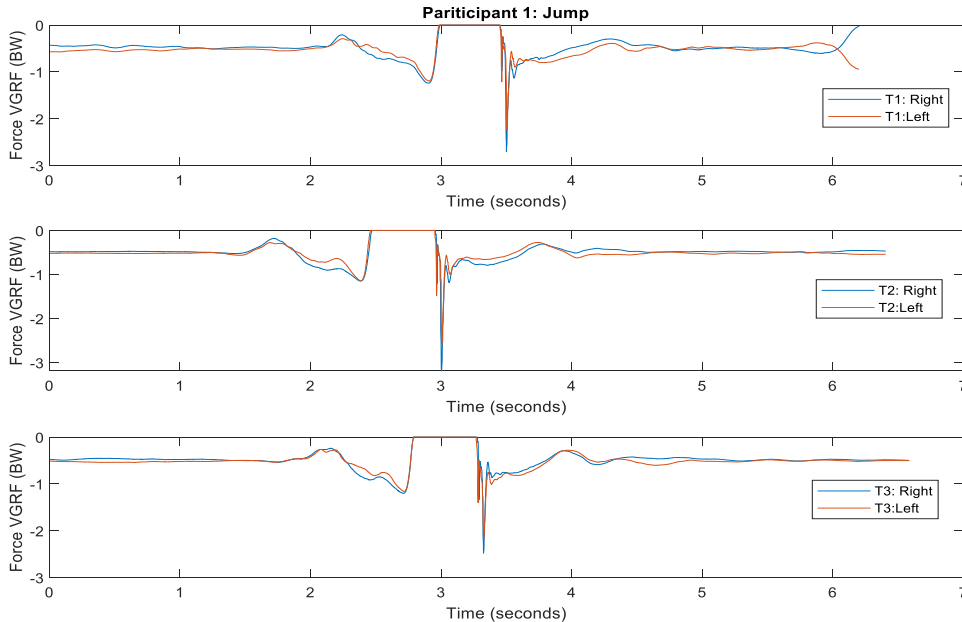


Figure 46: Jump trial comparison: Participant 1 Vertical Ground Reaction Force (VGRF) vs Time across three trials

Participant 2 was a female participant with no previous sporting involvement and a prosthetic left foot and hip asymmetry, with notable asymmetry in force distribution between dominant (right) and non-dominant (left) limb was observed through the movement trials (Figure 47).

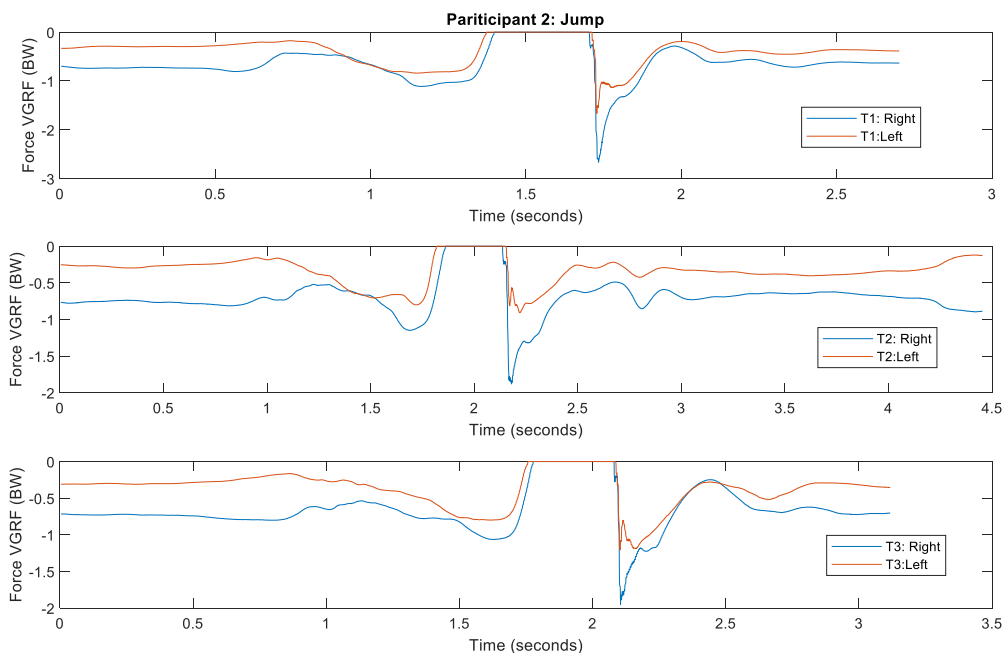


Figure 47: Jump trial comparison: Participant 2 Vertical Ground Reaction Force (VGRF) vs Time across three trials

Chapter 5: Correlation and Feasibility Study using Wearable Prototype

The peak VGRF observed by the dominant leg of participant 2 was much higher than the non-dominant leg, due to the asymmetry. However, a clearer trend was observed between the peak VGRF and the A_{IS} amplitude. Compared to participant 1, when stepping off a 440 mm platform, participant 2 produced the largest force and A_{IS} amplitude rather than cut movement. Movements requiring a sudden change of direction such as pivot, and cut generated a reduced amount of peak VGRF, as it was more difficult for the participant to rapidly change movements due to the left foot prosthetic. The low impact movements such as walking were also found to produce the lowest VGRF. The force distributions for participant 2 ranged between -1 BW to -4.2 BW, same as participant 1. The trials for individual movements were also very consistent, and the most consistent trend was produced from participant 2 regardless of the hip asymmetry.

Finally, participant 3 was an athletic male individual with an extended history of sporting involvements. The individual was observed to exert his maximal efforts during laboratory trials and confirmed to be comfortable doing so due to no previous injuries. The confidence in his movements and involvement with high impact sports may have contributed to the peak VGRF being much higher than participant 1 and 2, with a much more scattered distribution of VGRF and A_{IS} amplitude (Figure 41), and consistency across trials (Figure 48).

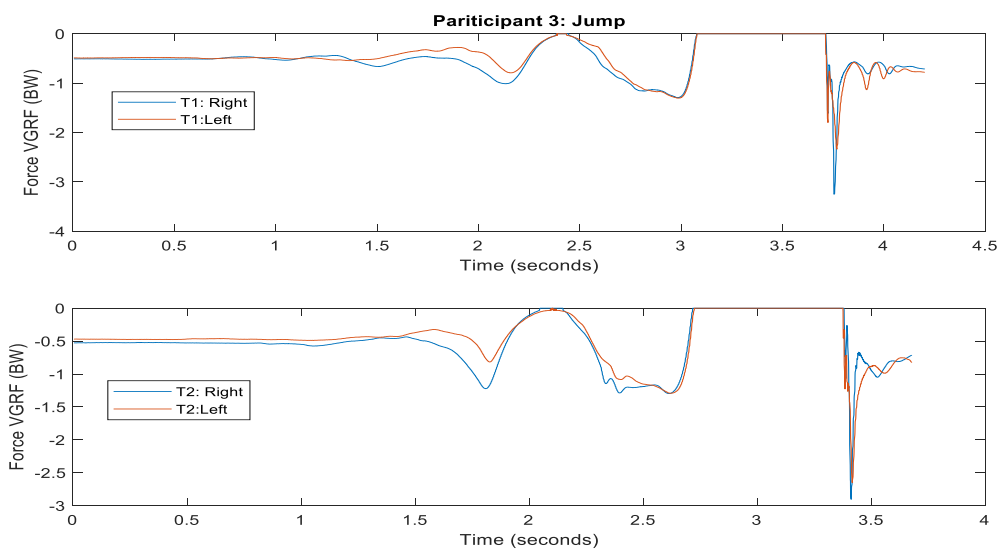


Figure 48: Jump trial comparison: Participant 3 Vertical Ground Reaction Force (VGRF) vs Time across two trials. Participant 3 displayed a peak VGRF distribution ranging from -1 BW up to -6.1 BW, the peak VGRF occurring during 'cut' and '2F'. Although the movement '2F' was also indicative of producing higher VGRF in participant 1, an almost 2 BW in magnitude increase in VGRF was observed in participant 3.

Chapter 5: Correlation and Feasibility Study using Wearable Prototype

5.5.2 Combined Analysis: Impact Zone and Feather Feasibility

For the combined correlation of all three varied participants (Figure 45), the R^2 value was not high enough to reliably estimate VGRF, however, a distribution of activities could be allocated into low, moderate and high impact zones, similar to the previous study (Appendix O). Walking was most consistent across all three participants, being classified in the “low” impact zone of below 6 g A_{IS} amplitude. Some movements produced by participants 1 and 2 were classed into the “moderate” zone, even when they may be considered as high impact, due to their less explosive nature of landing impacted by previous injuries or the current conditions of their lower limb. Data from participant 3 was consistently classified in the “high” impact zone, as expected from the heavy-footed and explosive nature of play. Moderate activities for all participants included ‘jogging’ and ‘running’, and trials for each participant were clustered in similar ranges. ‘Jump’ was a high impact activity for all three participants, but most other movements varied according to the efforts and forces exerted by the participants.

Although variance amongst participants was evident from the data, all trial data remained consistent according to the individual participant movements, validating the A_{IS} amplitude calculated by the Feather prototype was collecting reliable data. The range of A_{IS} amplitude for the previous study was found to be up to 25 g, which remained consistent with the maximum A_{IS} amplitude calculated by the Feather to be approximately at 25 g (Appendix O).

From preliminary data collection in the laboratory, the findings indicated that the Feather prototype was effective in correlating impact zones according to the A_{IS} amplitude measured at the shank. The impact zones identified in 2018 study were maintained, and the findings provided an overall estimate of VGRF according to individual participants.

Chapter 5: Correlation and Feasibility Study using Wearable Prototype

5.5.3 Limitations

One of the key limitations of this study was the restriction of movement due to the laboratory dimensions. Participant 3 reported finding it almost impossible to reach their absolute maximum speed during movements such as sprinting due to the 3-meter run-up before completing a movement in a 4-meter space. The restricted space may have contributed to a lowered intensity of high impact movements. Additionally, the laboratory protocols also required the landing to occur completely on the force plates. Although, participants were encouraged to land as naturally as possible without purposely adjusting their jump to land on the plates, subconscious awareness of the landing area may have affected the usual landing techniques of the participants. The effects of the laboratory dimensions could be mitigated through conducting a similar trial in situ on a netball court. The open conditions and lack of force plates would allow players to naturally conduct their movements. However, in situ testing without any force plates, A_{IS} amplitude would not be able to be directly correlated with VRF, hence laboratory tests as conducted were required.

Additionally, the participants chosen had different backgrounds and introduced a large variance to the data due to personal history and experiences. In addition, while all participants were required to wear sporting shoes, the make and age of the shoe was not consistent due to the limited project budget. The difference in footwear could have directly impacted on the magnitude of VGRG and landing technique. An important stakeholder for this project is the Contax Premier League Netball Group, with the coaches and players having significant interest in the project outcomes. In future testing, netball players from the Contax group could be used to collect further laboratory data and validate the impact zone for athletes of similar expertise. The increased sample size of participants will also provide stronger evidence regarding the placement of the sensor and correlation of the impact zones.

The larger size of the Feather prototype casing may have protruded further than intended and must be reduced to fit the size of the Feather prototype. Due to the size of the LiPo battery, the case was designed to be larger than required. The prototype was, however, comfortable to wear as reported by participants but was not ideal to wear on a netball court due to the protrusion. The exact placement of the Feather prototype on the shank could have varied between participants, contributing to minor discrepancies, as a recent study has shown that orientation placement errors can reduce VGRF estimation accuracy (Tan *et al.*, 2019).

Chapter 5: Correlation and Feasibility Study using Wearable Prototype

Finally, it should be noted that there could have been noise present in the raw acceleration data as the attachment of the accelerometer to the Feather board may have not been completely rigid during high impact motion. The potential of this systematic error was minimised through securing the boards with cable ties and securing the outer shell with sufficient electrical tape prior to data collection. The use of physio tape to secure the prototype to the shank provided comfort to the user while also restricting any undesirable movements. However, this method of fixation could have potentially introduced motion artefact leading to a higher A_{IS} amplitude than expected. Multiple trials were conducted and continuous verbal confirmations regarding the ‘feel’ of the device were received from each participant to ensure the prototype was not sliding and remained rigidly affixed.

Despite the limitations of the study, the Feather prototype was effective in collecting A_{IS} amplitude data from participants in real-time. The maximum achievable A_{IS} amplitude from the accelerometer sensitivity range of $\pm 16 g$ was 32g, whereas the maximum observed amplitude from all participants was approximately 25g, meaning that the accelerometer sensitivity was sufficient. Laboratory testing demonstrated a variance in data amongst different participants as expected, and a correlation was observed between VGRF and A_{IS} amplitude from the Feather prototype placed at the shank. Due to the onboard processing and increased range of Wi-Fi, no data loss was observed in the laboratory, however further testing in situ would be required to clarify the range with other participants on court. The battery of the prototype was also sufficient for a continuous trial of two participants lasting approximately three hours. The impact zones identified through this study were consistent with previous work, although variance was observed for the same movements across participants due to varied abilities, age, sports history and efforts.

CHAPTER 6:
CONCLUSION

6.1 Summary of Findings

Literature throughout the past 30 years has documented the high occurrence of lower limb injuries in netball due to high speed, strength and repeated explosive loading (Hopper, 1986; Hopper *et al.*, 1995; Hume and Steele, 2000; Otago and Peake, 2007; Saunders and Otago, 2009). Recent sports surveys conducted by ASC reported a 22% increase in dropouts due to injury or poor health acquired by netball gameplay (ASC, 2019a). As the top team sport for girls between 14 to 16 years old, the frequency of lower limb injuries can lead to a reduction in sporting activity, increased need for medical treatment, and adverse social and economic effects for young athletes. The current active injury countermeasures are primarily subjective training practices, that fail to quantify the loading of lower limbs. Laboratory-based wearable devices for impact monitoring can be used, however these are expensive and generally inaccessible to sub-elite players. Due to the lack of active monitoring of the lower limb impact forces in training and games, preventative measures cannot be taken, leading to a significantly higher risk of chronic injuries.

A review of the literature identified the growing popularity of wearable devices, such as low cost, portable and widely available IMUs, in particular, accelerometers-based units to measure general energy expenditure and lower-limb shock attenuation (Adesida *et al.*, 2019; Camomilla *et al.*, 2018). Additionally, studies have also demonstrated that accelerometer based variables could be used to represent VGRF experienced by the lower limb during movement protocols (Corbo, 2018; Tan *et al.*, 2019). When an accelerometer was placed on a participants shank, the A_{IS} amplitude in a 1-second epoch correlated to the VGRF when netball simulated movements were performed (Corbo, 2018). However, the accelerometer used in the study (Delsys Trigno Avanti Research+ sensors) were laboratory-based, expensive and contained no onboard processing capabilities, hence it was not a viable solution for sub-elite netball participants. Therefore, the primary objective of this project was to contribute to the design and development of an inexpensive and compact accelerometer-based wearable device that could quantify lower limb related impact dose experienced during training and competitive netball gameplay.

Firstly, the commercially available IMU manufactured by Texas Instruments, the SensorTag CC2650, was evaluated against laboratory-based AMTI OR6-7 force plates and Delsys Trigno Avanti™ Research+ sensors. During laboratory and in situ testing, SensorTag demonstrated a 71.62% data loss at 100Hz (maximum sampling frequency), resulting in poor representation of A_{IS} amplitude in a 1-second epoch. The effective range of the SensorTag was also found to be inconsistent, varying from 3 meters to 30 meters depending on direct line of sight to the device. BLE is primarily used for short-range communication, such as a wearable smartwatch, and has a reported reliable range of 10 metres (Mukhopadhyay, 2015). A netball court is 30.5 meters, hence an unreliable streaming range between 3 meters to 30 meters is not sufficient for capture of a full netball training session or game. Frequent Bluetooth connection dropouts were also observed during the obstruction of the line of sight. Overall, the SensorTag did not meet the required specifications of a practical and reliable wearable device.

An alternative objective was to create a Wi-Fi enabled working prototype with a user interface, such that the A_{IS} amplitude data could be displayed to the user. The Feather prototype equipped with ESP8266 provided a reliable method of data streaming with an average sampling frequency of 850 Hz. The onboard processing capabilities eliminated the requirement for post-processing, and no data loss was observed. The A_{IS} amplitude at the shank was calculated in a 1-second epoch and was displayed in real-time to the user through a Websocket-based user interface with data logging capabilities. The prototype components combined to a total cost of AUD\$65, which met the low-cost requirement of \leq AUD\$100 compared to the approximate cost estimate of AUD\$20k for laboratory-based accelerometers such Delsys Trigno Avanti™ Research+ sensors (set of 16 with base station).

The Feather prototype was then validated through a laboratory-based correlation and feasibility study. The relationship between A_{IS} amplitude and VGRF, obtained from AMTI OR6-7 force plates, was used to identify low, moderate and high impact zones. Three participants with varied athletics and injury backgrounds were assessed in the netball specific validation study. A notable increase in A_{IS} amplitude was observed for combined participant data with the increased VGRF. Low impact movements such as ‘walking’ correlated to peak VGRF between 1.1 BW to 1.5 BW amongst all three participants with A_{IS} amplitude below 6 g. In contrast, high impact movements such as ‘jumping’ corresponded to a peak VGRF between 2 BW to 3.75 BW, with A_{IS} amplitude of above 17g. The percentage of time spent in each of the impact zones within netball gameplay could be presented as a measure of impact dose.

Chapter 6: Conclusion

It must be noted that factors such as fear of reinjury, a prosthetic foot, no previous history of injury and experience in high-intensity sports resulted in a large variation in peak VGRF between participants for individual high impact movements but remained consistent for each participant. This study validated the consistency of Feather prototype to process data in real-time, however future data collection is required from a larger sample size to further validate the impact zones and subsequent impact dose during netball gameplay.

6.2 Future Recommendations

The primary aim of this project was to develop an inexpensive and reliable wearable device that could be worn by athletes during netball gameplay to categorise impact zones to subsequently infer impact dose. The Feather prototype was successful at deducing impact zones across a range of participants in laboratory-based movement simulations. Based on the preliminary testing findings, the immediate goal would be to repeat the laboratory protocol (*Section 5.3.2*) of the prototype fixed at the shank with participants from Contax Premier League Netball Group, who are major stakeholders to the project. The larger pool of participants will assist in further validation on the impact zone specified through 2018 and the current study (Appendix B, Figure 45).

Upon further validation and adjustments made to the impact zones if required, in situ testing should be conducted to deduce impact dose in full netball gameplay. Any interruption in data streaming and gameplay should be noted for immediate adjustments in development. The feedback regarding the size of the sensor and comfort should facilitate the ideal method of fixation of the device.

In the development of the prototype, a proof-of-concept approach was taken to find the best components for the project, such as ESP8266, LiPo battery, and ADXL345 digital accelerometer. As the current attachment between the Feather and ADXL345 breakout board is not completely rigid, future development must consider the redesign of the PCB to incorporate core components in a compact size. Furthermore, micro-SD cards should also be integrated, such that offline processed data storage could be achieved.

The current method of streaming incorporates Websockets, which can allow reading from multiple sensors if a central device, such as a Wi-Fi router, is used. Alternatively, a web-based application could be implemented that incorporates multiple-device streaming through a central router and display through a graphical user interface for individual players, hence significantly reducing the time required for the setup of multiple devices during gameplay.

As the findings of this study presented that individual kinematics such as varied landing techniques and previous injuries could have an effect on the impact zone and corresponding

peak VGRF, further study must be conducted to demonstrate long term implication of individual technique variability and impact dose with injury correlation.

The literature has documented the need for active injury prevention in netball with increased participant dropout rate due to injuries sustained during gameplay. With the popularity of the game amongst young athletes, the consequences of the injuries directly impact their mental, physical and social wellbeing, with many requiring extensive surgeries and restricted activities for extended periods. The findings of this project demonstrate the viability of an inexpensive wearable device to categorise netball specific movements into impact zones, such that impact dose could be deduced. By acting on future recommendations, the device could be integrated into netball training and gameplay, aiding coaches to identify 'at risk' players and techniques and modify training regimes accordingly to counteract the risks, ensuring proactivity rather than reactivity in injury monitoring.

REFERENCES

Reference List

- Adafruit. (2019a), “Lithium Ion Polymer Battery - 3.7v 500mAh”, *Adafruit.Com*, available at: <https://www.adafruit.com/product/1578> (accessed 12 October 2019).
- Adafruit. (2019b), “Adafruit HUZZAH ESP8266 breakout”, *Adafruit.Com*, available at: <https://learn.adafruit.com/adafruit-feather-huzzah-esp8266/overview> (accessed 12 October 2019).
- Adafruit. (2019c), “3D Printed Case for Adafruit Feather”, *Adafruit.Com*, available at: <https://learn.adafruit.com/3d-printed-case-for-adafruit-feather/parts> (accessed 13 October 2019).
- Adesida, Y., Papi, E. and McGregor, A.H. (2019), “Exploring the role of wearable technology in sport kinematics and kinetics: A systematic review”, *Sensors (Switzerland)*, available at: <https://doi.org/10.3390/s19071597>.
- AIHW. (2013), *Australian Institute of Health and Welfare Canberra Hospital Care for Australian Sports Injury*, available at: www.aihw.gov.au (accessed 22 July 2019).
- American Heart Association. (2019), “About American Heart Association”, available at: <https://www.heart.org/> (accessed 29 July 2019).
- AMTI. (2012), *OR6-7 Brochure*, available at: <https://amti.biz/select-product/PDFs/Biomechanics-force-platforms/OR6-7-brochure.pdf>.
- Analog Devices. (2009), “ADXL345 Datasheet”, *Sparkfun.Com*, available at: https://www.sparkfun.com/datasheets/Sensors/Accelerometer/ADXL345.pdf?_ga=2.22211132.668792845.1570872450-555196528.1567469728 (accessed 12 October 2019).
- Arampatzis, A., Brüggemann, G.P. and Klapsing, G.M. (2002), “A three-dimensional shank-foot model to determine the foot motion during landings”, *Medicine and Science in Sports and Exercise*, available at: <https://doi.org/10.1097/00005768-200201000-00020>.
- ASC, A.S.C. (2016), *Summary of Key National Findings, AusPlay Participation Data for the Sport Sector*.
- ASC, A.S.C. (2018), *Children’s Participation in Organised Physical Activity Outside of School Hours*, available at: https://www.clearinghouseforsport.gov.au/__data/assets/pdf_file/0012/796827/AusPlay_focus_Children_Participation.pdf (accessed 14 July 2019).
- ASC, A.S.C. (2019a), *Results by Sport*, available at: <https://www.clearinghouseforsport.gov.au/research/smi/ausplay/results/sport> (accessed 10 April 2019).

- ASC, A.S.C. (2019b), *Basketball State of Play Report*.
- Bailey, J.A., Gastin, P.B., Mackey, L. and Dwyer, D.B. (2017), “The player load associated with typical activities in elite netball”, *International Journal of Sports Physiology and Performance*, available at:<https://doi.org/10.1123/ijsp.2016-0378>.
- Bamberg, S.J.M., Benbasat, A.Y., Scarborough, D.M., Krebs, D.E. and Paradiso, J.A. (2008), “Gait analysis using a shoe-integrated wireless sensor system”, *IEEE Transactions on Information Technology in Biomedicine*, IEEE, Vol. 12 No. 4, pp. 413–423.
- Besier, T. (2019), *The Importance of Measuring Lower Limb Cumulative Load in Sport: A Mechanobiological Approach*, New Zealand.
- Best, G. (2016), “034 EPIDEMIOLOGY AND INCIDENCE OF INJURY IN ELITE NETBALL PLAYERS-AN INJURY AUDIT OF THE 2016 NETBALL SUPERLEAGUE SEASON”, available at:<https://doi.org/10.1136/bjsports-2016-097372.34>.
- Bluetooth, S.I.G. (2010), “Specification of the Bluetooth System-Covered Core Package version: 4.0”, June.
- Borresen, J. and Lambert, M.I. (2009), “The quantification of training load, the training response and the effect on performance”, *Sports Medicine*, Springer, Vol. 39 No. 9, pp. 779–795.
- Boyd, L.J., Ball, K. and Aughey, R.J. (2011), “The reliability of MinimaxX accelerometers for measuring physical activity in Australian football”, *International Journal of Sports Physiology and Performance*, Vol. 6 No. 3, pp. 311–321.
- Butler, R.J., Crowell, H.P. and Davis, I.M.C. (2003), “Lower extremity stiffness: Implications for performance and injury”, *Clinical Biomechanics*, available at:[https://doi.org/10.1016/S0268-0033\(03\)00071-8](https://doi.org/10.1016/S0268-0033(03)00071-8).
- Camomilla, V., Bergamini, E., Fantozzi, S. and Vannozzi, G. (2018), “Trends supporting the in-field use of wearable inertial sensors for sport performance evaluation: A systematic review”, *Sensors (Switzerland)*, Vol. 18 No. 3, available at:<https://doi.org/10.3390/s18030873>.
- Corbo, E. (2018), *The Design and Development of a Wearable Device to Assess Lower-Limb Impact Dose during Competitive Netball Play*, Flinders University.
- Cormack, S.J., Smith, R.L., Mooney, M.M., Young, W.B. and O’Brien, B.J. (2014), “Accelerometer Load as a Measure of Activity Profile in Different Standards of Netball Match Play”, *IJSP-*Journal.Com ORIGINAL INVESTIGATION International Journal of Sports Physiology and Performance**, Vol. 9, pp. 283–291.

- Cummins, C., Orr, R., O'Connor, H. and West, C. (2013), "Global positioning systems (GPS) and microtechnology sensors in team sports: a systematic review", *Sports Medicine*, Springer, Vol. 43 No. 10, pp. 1025–1042.
- Cumps, E., Verhagen, E. and Meeusen, R. (2007), "Prospective epidemiological study of basketball injuries during one competitive season: Ankle sprains and overuse knee injuries", *Journal of Sports Science and Medicine*.
- Cunniffe, B., Proctor, W., Baker, J.S. and Davies, B. (2009), "An evaluation of the physiological demands of elite rugby union using global positioning system tracking software", *The Journal of Strength & Conditioning Research*, LWW, Vol. 23 No. 4, pp. 1195–1203.
- Darroudi, S.M. and Gomez, C. (2017a), "Bluetooth Low Energy Mesh Networks: A Survey", *Sensors*, Multidisciplinary Digital Publishing Institute, Vol. 17 No. 7, p. 1467.
- Darroudi, S.M. and Gomez, C. (2017b), "Bluetooth Low Energy Mesh Networks: A Survey", *Sensors*, Multidisciplinary Digital Publishing Institute, Vol. 17 No. 7, p. 1467.
- Delsys. (2019a), *Trigno Wireless Biofeedback Systems*, available at: <https://www.delsys.com/downloads/USERSGUIDE/trigno/wireless-biofeedback-system.pdf> (accessed 6 October 2019).
- Delsys. (2019b), *Trigno Wireless Biofeedback Systems*.
- Devita, P. and Skelly, W.A. (1992), "Effect of landing stiffness on joint kinetics and energetics in the lower extremity", *Med Sci Sports Exerc*, Citeseer, Vol. 24 No. 1, pp. 108–115.
- Dufek, J.S. and Bates, B.T. (1990), "The evaluation and prediction of impact forces during landings", *Medicine and Science in Sports and Exercise*.
- Elvin, N.G., Elvin, A.A., Arnoczky, S.P. and Torry, M.R. (2007), "The correlation of segment accelerations and impact forces with knee angle in jump landing", *Journal of Applied Biomechanics*, available at: <https://doi.org/10.1123/jab.23.3.203>.
- Espressif Systems. (2013), *ESPRESSIF SMART CONNECTIVITY PLATFORM: ESP8266*, available at: https://cdn-shop.adafruit.com/datasheets/ESP8266_Specifications_English.pdf.
- Espressif Systems. (2019), *ESP8266EX Datasheet*, available at: https://www.espressif.com/sites/default/files/documentation/0a-esp8266ex_datasheet_en.pdf.
- Ferrari, A., Rocchi, L., van den Noort, J. and Harlaar, J. (2013), "Toward the use of wearable inertial sensors to train gait in subjects with movement disorders", *Converging Clinical*

- and Engineering Research on Neurorehabilitation*, Springer, pp. 937–940.
- Ferreira, M. and Spamer, E. (2011), “Biomechanical, anthropometrical and physical profile of elite university netball players and the relationship to musculoskeletal injuries”, *South African Journal for Research in Sport, Physical Education and Recreation*, available at:<https://doi.org/10.4314/sajrs.v32i1.54100>.
- Finch, C., Da Costa, A., Stevenson, M., Hamer, P. and Elliott, B. (2002), “Sports injury experiences from the Western Australian sports injury cohort study”, *Australian and New Zealand Journal of Public Health*, available at:<https://doi.org/10.1111/j.1467-842X.2002.tb00348.x>.
- Finch, C.F. (Caroline F.. (1995), *The Feasibility of Improved Data Collection Methodologies for Sports Injuries*, edited by Williams, F., Ozanne-Smith, J., Centre, M.U.A.R., Foundation, V.H.P. and (Australia), N.S.R.C., Clayton, Vic. : Monash University Accident Research Centre, Clayton, Vic.
- Flood, L. and Harrison, J.E. (2009), “Epidemiology of basketball and netball injuries that resulted in hospital admission in Australia, 2000-2004”, *Medical Journal of Australia*.
- Fong, D.T.P. and Chan, Y.Y. (2010), “The use of wearable inertial motion sensors in human lower limb biomechanics studies: A systematic review”, *Sensors (Switzerland)*, Vol. 10 No. 12, pp. 11556–11565.
- Foster, C. (1998), “Monitoring training in athletes with reference to overtraining syndrome”, *Medicine and Science in Sports and Exercise*, WILLIAMS & WILKINS, Vol. 30, pp. 1164–1168.
- Fox, A., Spittle, M., Otago, L. and Saunders, N. (2013a), “Activity profiles of the Australian female netball team players during international competition: Implications for training practice”, *Journal of Sports Sciences*, Routledge , Vol. 31 No. 14, pp. 1588–1595.
- Fox, A., Spittle, M., Otago, L. and Saunders, N. (2014), “Offensive agility techniques performed during international netball competition”, *International Journal of Sports Science and Coaching*, available at:<https://doi.org/10.1260/1747-9541.9.3.543>.
- Fox, A.S., Spittle, M., Otago, L. and Saunders, N. (2013b), “Descriptive analysis of landings during international netball competition: Enhancing ecological validity of laboratory testing environments”, *International Journal of Performance Analysis in Sport*, available at:<https://doi.org/10.1080/24748668.2013.11868681>.
- Gomez, C., Oller, J. and Paradells, J. (2012), “Overview and evaluation of bluetooth low energy: An emerging low-power wireless technology”, *Sensors (Switzerland)*, available at:<https://doi.org/10.3390/s120911734>.

- Grana, W.A. (1994), “Acute ankle injuries”, *Clinical Practice of Sports Injury Prevention and Care*. Oxford: Blackwell Scientific Publications, pp. 217–227.
- Haddad, M., Stylianides, G., Djaoui, L., Dellal, A. and Chamari, K. (2017), “Session-RPE Method for Training Load Monitoring: Validity, Ecological Usefulness, and Influencing Factors ”, *Frontiers in Neuroscience* .
- Halson, S.L. (2014), “Monitoring Training Load to Understand Fatigue in Athletes”, *Sports Medicine*, available at:<https://doi.org/10.1007/s40279-014-0253-z>.
- Hamill, J., Derrick, T.R. and Holt, K.G. (1995), “Shock attenuation and stride frequency during running”, *Human Movement Science*, Vol. 14 No. 1, pp. 45–60.
- Hausler, J., Halaki, M. and Orr, R. (2016), “Application of global positioning system and microsensor technology in competitive rugby league match-play: a systematic review and meta-analysis”, *Sports Medicine*, Springer, Vol. 46 No. 4, pp. 559–588.
- Hewett, T.E., Stroupe, A.L., Nance, T.A. and Noyes, F.R. (1996), “Plyometric training in female athletes: Decreased impact forces and increased hamstring torques”, *American Journal of Sports Medicine*, available at:<https://doi.org/10.1177/036354659602400611>.
- Hides, J., Mendis, D., Parker, A. and Smith, M. (2018), “Injury surveillance in female community netball players”, *Journal of Science and Medicine in Sport*, Vol. 21, p. S47.
- Hopper, D. (1986), “A Survey of Netball Injuries and Conditions Related to These Injuries”, *Australian Journal of Physiotherapy*, available at:[https://doi.org/10.1016/S0004-9514\(14\)60656-5](https://doi.org/10.1016/S0004-9514(14)60656-5).
- Hopper, D. and Elliott, B. (1993), “Lower Limb and Back Injury Patterns of Elite Netball Players”, *Sports Medicine: Evaluations of Research in Exercise Science and Sports Medicine*, available at:<https://doi.org/10.2165/00007256-199316020-00006>.
- Hopper, D., Elliott, B. and Lalor, J. (1995), “A descriptive epidemiology of netball injuries during competition: a five year study”, *British Journal of Sports Medicine*, available at:<https://doi.org/10.1136/bjism.29.4.223>.
- Hopper, D., Lo, S.K., Kirkham, C. and Elliott, B. (1992), “Landing patterns in netball: analysis of an international game”, *British Journal of Sports Medicine*, available at:<https://doi.org/10.1136/bjism.26.2.101>.
- Hopper, D.M., McNair, P. and Elliott, B.C. (1999), “Landing in netball: Effects of taping and bracing the ankle”, *British Journal of Sports Medicine*, available at:<https://doi.org/10.1136/bjism.33.6.409>.
- Hume, P.A. and Steele, J.R. (2000), “A preliminary investigation of injury prevention strategies in netball: Are players heeding the advice?”, *Journal of Science and Medicine*

- in Sport*, available at:[https://doi.org/10.1016/S1440-2440\(00\)80007-9](https://doi.org/10.1016/S1440-2440(00)80007-9).
- IFNA. (2011), “About IFNA”, available at:
<https://web.archive.org/web/20110308132327/http://www.netball.org/IFNA.aspx>
 (accessed 9 July 2019).
- INF, I.N.F. (2018), *Rules of Netball*, available at:
https://netball.com.au/sites/default/files/2019-06/2019reprint_INF_Netball_Rules_Book_2018_Print_Ready_Artwork.pdf (accessed 17 July 2019).
- Jaiyesimi, B.G. (2018), “EFFECTS OF A BAREFOOT INTERVENTION PROGRAMME ON THE LANDING KINETICS AND KINEMATICS OF NETBALL PLAYERS”.
- Jobling, I. and Barham, P. (1991), “The development of netball and the All-Australia Women’s Basketball Association (AAWBBA)”, *Sporting Traditions*, Australian Society for Sports History, Vol. 8 No. 1, pp. 29–48.
- Juri, A., Arslan, T. and Fengzhou, W. (2016), *Obstruction-Aware Bluetooth Low Energy Indoor Positioning*, available at:<https://doi.org/10.33012/2016.14866>.
- Kearney, S. (2019), “NetballSmart – Netball New Zealand Injury Prevention Programme. Engage and make a difference”, *Journal of Science and Medicine in Sport*, Vol. 22, p. S90.
- Kennedy, B., Appleby, B. and Piggott, B. (2011), “An investigation of the heart-rate profile of elite netball match play”, *Journal of Science and Medicine in Sport*, available at:<https://doi.org/10.1016/j.jsams.2011.11.194>.
- Kleiss, L. (2019), “SportMonitor”, *Github.Com*, available at:
https://github.com/LAK132/SportMonitor?fbclid=IwAR0SdNZlxYN4J1H4TF_0GGw4jgHJ-D3UTnU1C7X8o8cG9sgUj0pJ6ZwpBqM.
- Kovács, I., Tihanyi, J., Devita, P., Rácz, L., Barrier, J. and Hortobágyi, T. (1999), “Foot placement modifies kinematics and kinetics during drop jumping”, *Medicine and Science in Sports and Exercise*, available at:<https://doi.org/10.1097/00005768-199905000-00014>.
- Langeveld, E., Coetzee, F.F. and Holtzhausen, L.J. (2012), “Epidemiology of Injuries in Elite South African Netball Players”, *South African Journal for Research in Sport Physical Education and Recreation*.
- Langsdon, R. (2015), “Strange technology allows us all to train like champions”, *Planet Innovation*, available at: <https://planetinnovation.com/perspectives/strange-technology-allows-us-train-like-champions/> (accessed 20 October 2019).

- Li, R.T., Kling, S.R., Salata, M.J., Cupp, S.A., Sheehan, J. and Voos, J.E. (2016), “Wearable Performance Devices in Sports Medicine”, *Sports Health*, available at:<https://doi.org/10.1177/1941738115616917>.
- Lysholm, J. and Wiklander, J. (1987), “Injuries in runners”, *The American Journal of Sports Medicine*, SAGE Publications Inc STM, Vol. 15 No. 2, pp. 168–171.
- McClay, I.S., Robinson, J.R., Andriacchi, T.P., Frederick, E.C., Gross, T., Martin, P., Valiant, G., et al. (2016), “A Profile of Ground Reaction Forces in Professional Basketball”, *Journal of Applied Biomechanics*, available at:<https://doi.org/10.1123/jab.10.3.222>.
- McGrath, A.C. and Ozanne-Smith, J. (1998), *ATTACKING THE GOAL OF NETBALL INJURY PREVENTION: A REVIEW OF THE LITERATURE*, available at: https://www.monash.edu/__data/assets/pdf_file/0004/217426/muarc130.pdf (accessed 23 July 2019).
- McGrath, A.C. and Ozanne-Smith, J. (1998), *Attacking the Goal of Netball Injury Prevention: A Review of the Literature*.
- McKay, G.D., Goldie, P.A., Payne, W.R. and Oakes, B.W. (2001), “Ankle injuries in basketball: Injury rate and risk factors”, *British Journal of Sports Medicine*, available at:<https://doi.org/10.1136/bjism.35.2.103>.
- McKay, G.D., Payne, W.R., Goldie, P.A., Oakes, B.W. and Stanley, J.J. (1996), “A comparison of the injuries sustained by female basketball and netball players.”, *Australian Journal of Science and Medicine in Sport*.
- McKenzie, C.R., Whatman, C., Brughelli, M. and Borotkanics, R. (2019), “The effect of the NetballSmart Dynamic Warm-up on physical performance in youth netball players”, *Physical Therapy in Sport*, available at:<https://doi.org/10.1016/j.ptsp.2019.03.005>.
- McLachlan, F. (2016), “The Silent Game: A Critical Reading of the History of Netball in Australia”, *The International Journal of the History of Sport*, Routledge, Vol. 33 No. 17, pp. 2153–2168.
- McLellan, C.P., Lovell, D.I. and Gass, G.C. (2011), “Biochemical and endocrine responses to impact and collision during elite rugby league match play”, *The Journal of Strength & Conditioning Research*, LWW, Vol. 25 No. 6, pp. 1553–1562.
- McManus, A., Stevenson, M.R. and Finch, C.F. (2006), “Incidence and risk factors for injury in non-elite netball”, *Journal of Science and Medicine in Sport*, available at:<https://doi.org/10.1016/j.jsams.2006.03.005>.
- Mills, P.M., Morrison, S., Lloyd, D.G. and Barrett, R.S. (2007), “Repeatability of 3D gait

- kinematics obtained from an electromagnetic tracking system during treadmill locomotion”, *Journal of Biomechanics*, Elsevier, Vol. 40 No. 7, pp. 1504–1511.
- Mothersole, G.A., Cronin, J.B. and Harris, N.K. (2013), “Key prerequisite factors influencing landing forces in netball”, *Strength and Conditioning Journal*, available at:<https://doi.org/10.1519/SSC.0b013e318289b79e>.
- Mukhopadhyay, S.C. (2015), “Wearable sensors for human activity monitoring: A review”, *IEEE Sensors Journal*, available at:<https://doi.org/10.1109/JSEN.2014.2370945>.
- Muro-De-La-Herran, A., Garcia-Zapirain, B. and Mendez-Zorrilla, A. (2014), “Gait analysis methods: An overview of wearable and non-wearable systems, highlighting clinical applications”, *Sensors*, Multidisciplinary Digital Publishing Institute, Vol. 14 No. 2, pp. 3362–3394.
- Myklebust, H., Gløersen, Ø. and Hallén, J. (2015), “Validity of ski skating center-of-mass displacement measured by a single inertial measurement unit”, *Journal of Applied Biomechanics*, Vol. 31 No. 6, pp. 492–498.
- Netball Australia. (2019), “About the KNEE Program”, *Netball Australia*, available at: <https://knee.netball.com.au/about/> (accessed 28 July 2019).
- Nigg, B.M. and Yeadon, M.R. (1987), “Biomechanical aspects of playing surfaces”, *Journal of Sports Sciences*, Taylor & Francis Group, Vol. 5 No. 2, pp. 117–145.
- Otago, L. (1983), “A game analysis of the activity patterns of netball players”, *Sports Coach*, Vol. 7 No. 1, pp. 24–28.
- Otago, L. (2004), “Kinetic analysis of landings in netball: Is a footwork rule change required to decrease ACL injuries?”, *Journal of Science and Medicine in Sport*, available at:[https://doi.org/10.1016/S1440-2440\(04\)80047-1](https://doi.org/10.1016/S1440-2440(04)80047-1).
- Otago, L. and Peake, J. (2007), “The role of insurance data in setting priorities for netball injury prevention strategies”, *Journal of Science and Medicine in Sport*, available at:<https://doi.org/10.1016/j.jsams.2006.05.016>.
- Polar. (2018), “Polar H10 | Heart rate monitor chest strap | Polar Australia”, available at: https://www.polar.com/au-en/products/accessories/h10_heart_rate_sensor?gclid=EAIaIQobChMI6eKi5PjQ4QIV2CMrCh2yAwvQEAKYAYABEgKIUFd_BwE (accessed 15 April 2019).
- Qureshi, U.M., Umair, Z., Duan, Y. and Hancke, G.P. (2018), “Analysis of Bluetooth Low Energy (BLE) Based Indoor Localization System with Multiple Transmission Power Levels”, *IEEE International Symposium on Industrial Electronics*, available at:<https://doi.org/10.1109/ISIE.2018.8433787>.

- Sabatini, A.M. (2011), “Estimating three-dimensional orientation of human body parts by inertial/magnetic sensing”, *Sensors*, Molecular Diversity Preservation International, Vol. 11 No. 2, pp. 1489–1525.
- Sant’Anna, A., Wickström, N., Eklund, H., Zügner, R. and Tranberg, R. (2012), “Assessment of gait symmetry and gait normality using inertial sensors: in-lab and in-situ evaluation”, *International Joint Conference on Biomedical Engineering Systems and Technologies*, Springer, pp. 239–254.
- Saunders, N. and Otago, L. (2009), *Elite Netball Injury Surveillance: Implications for Injury Prevention*, *Journal of Science and Medicine in Sport - J SCI MED SPORT*, Vol. 12, available at: <https://doi.org/10.1016/j.jsams.2008.12.148>.
- Saunders, N., Otago, L. and Peoples, J. (2018), *Down to Earth A Practical Guide to Safe and Effective Landing in Netball*, available at: http://www.flamesnetball.com.au/wp-content/uploads/2013/05/safe_landing.pdf (accessed 28 July 2019).
- Schepers, H.M., Van Asseldonk, E.H.F., Buurke, J.H. and Veltink, P.H. (2009), “Ambulatory estimation of center of mass displacement during walking”, *IEEE Transactions on Biomedical Engineering*, IEEE, Vol. 56 No. 4, pp. 1189–1195.
- Simpson, M.J., Jenkins, D.G., Leveritt, M.D. and Kelly, V.G. (2019), “Physical profiles of elite, sub-elite, regional and age-group netballers”, *Journal of Sports Sciences*, available at: <https://doi.org/10.1080/02640414.2018.1553269>.
- Singapore Sports Council. (2017), “Bettering your netball positional play - ActiveSG”, available at: <https://www.myactivesg.com/Sports/Netball/Training-Method/Develop-Your-Game/Bettering-your-netball-positional-play> (accessed 17 July 2019).
- Sitler, M., Ryan, C.J., Hopkinson, L.W., Wheeler, L.J., Santomier, J., Kolb, L.R. and Polley, C.D. (1994), “The efficacy of a prophylactic knee brace to reduce knee injuries in football: a prospective, randomized study at West Point”, *The American Journal of Sports Medicine*, Sage Publications, Vol. 18 No. 3, pp. 310–315.
- Smithers, M. and Myers, P.T. (1985), “Injuries in sport: A prospective casualty study”, *Medical Journal of Australia*, John Wiley & Sons, Ltd, Vol. 142 No. 8, pp. 457–461.
- Sparkfun. (2019), “SparkFun Triple Axis Accelerometer Breakout - ADXL345”, *Sparkfun.Com*, available at: <https://www.sparkfun.com/products/9836> (accessed 12 October 2019).
- Sports Ball Blog. (2018), “Know your WA from your GK – Netball Positions Explained”, available at: <https://www.sportsballshop.co.uk/sportsballblog/know-your-wa-from-your-gk-netball-positions-explained/> (accessed 17 July 2019).

- Steele, J.R., Milburn, P. (1987), “Ground reaction forces on landing in netball”, *Journal of Human Movement Studies*, Vol. 13, pp. 399–410.
- Steele, J.R. (1990a), “Biomechanical Factors Affecting Performance in Netball: Implications for Improving Performance and Injury Reduction”, *Sports Medicine*, available at: <https://doi.org/10.2165/00007256-199010020-00003>.
- Steele, J.R. (1990b), “Injuries and the veteran netball player: minimising risks”, *Commonwealth International Conference Physical Education Sport Health Dance Recreation Leisure, 1990a*, Vol. 164.
- Steele, J.R. and Lafortune, M.A. (1989a), “A Kinetic Analysis of Footfall Patterns at Landing in Netball”, *ISBS - Conference Proceedings Archive*, available at: <https://ojs.ub.uni-konstanz.de/cpa/article/view/3494> (accessed 25 July 2019).
- Steele, J.R. and Lafortune, M.A. (1989b), “The relationship between technique and ground reaction forces at landing in netball”, *Journal of Biomechanics*, Vol. 22 No. 10, p. 1085.
- Steele, J.R. and Milburn, P.D. (1988), “Effect of Different Synthetic Sport Surfaces on Ground Reaction Forces at Landing in Netball”, *International Journal of Sport Biomechanics*, Vol. 4 No. 2, pp. 130–145.
- Suárez-Arrones, L.J., Portillo, L.J., González-Ravé, J.M., Muñoz, V.E. and Sanchez, F. (2012), “Match running performance in Spanish elite male rugby union using global positioning system”, *Isokinetics and Exercise Science*, IOS Press, Vol. 20 No. 2, pp. 77–83.
- Tan, T., Chiasson, D.P., Hu, H. and Shull, P.B. (2019), “Influence of IMU Position and Orientation Placement Errors on Ground Reaction Force Estimation”, *Journal of Biomechanics*, Elsevier, p. 109416.
- Tao, W., Liu, T., Zheng, R. and Feng, H. (2012), “Gait analysis using wearable sensors”, *Sensors*, Molecular Diversity Preservation International, Vol. 12 No. 2, pp. 2255–2283.
- Tay, A., Yen, S.C., Li, J.Z., Lee, W.W., Yogaprakash, K., Chung, C., Liew, S., et al. (2013), “Real-time gait monitoring for Parkinson Disease”, *2013 10th IEEE International Conference on Control and Automation (ICCA)*, IEEE, pp. 1796–1801.
- Taylor, T. (2001), “Gendering Sport : The Development of Netball In Australia”, *Sporting Traditions*.
- Taylor, T. and Darcy, S. (2001), *School of Leisure, Sport and Tourism Working Paper Series UTS: BUSINESS Working Paper No 2 Netball in Australia: A Social History*, available at: <http://datasearch.uts.edu.au/business/publications/lst/index.cfm> (accessed 12 July 2019).

- Texas Instruments. (2015), “TIDC-CC2650STK-SENSORTAG SimpleLink™ multi-standard CC2650 SensorTag™ kit reference design”, available at: <http://www.ti.com/tool/TIDC-CC2650STK-SENSORTAG> (accessed 4 October 2019).
- Texas Instruments. (2016), *CC2650 SimpleLink™ Multistandard Wireless MCU Datasheet*, available at: <http://www.ti.com/lit/ds/symlink/cc2650.pdf>.
- Thomas, C., Ismail, K.T., Simpson, R., Comfort, P., Jones, P.A. and Dos’ Santos, T. (2019), “Physical Profiles of Female Academy Netball Players by Position”, *Journal of Strength and Conditioning Research*, available at: <https://doi.org/10.1519/JSC.0000000000001949>.
- Tracklab. (2018), “Delsys Trigno Research+ - Tracklab”, available at: <https://tracklab.com.au/products/emg/delsys-trigno-research/> (accessed 6 October 2019).
- Trigsted, S.M., Cook, D.B., Pickett, K.A., Cadmus-Bertram, L., Dunn, W.R. and Bell, D.R. (2018), “Greater fear of reinjury is related to stiffened jump-landing biomechanics and muscle activation in women after ACL reconstruction”, *Knee Surgery, Sports Traumatology, Arthroscopy*, Vol. 26 No. 12, pp. 3682–3689.
- Venter, R.E., Opperman, E. and Opperman, S. (2011), “The use of Global Positioning System (GPS) tracking devices to assess movement demands and impacts in Under-19 Rugby Union match play: Sports technology”, *African Journal for Physical Health Education, Recreation and Dance*, AFAHPER-SD, Vol. 17 No. 1, pp. 1–8.
- Wang, V., Salim, F. and Moskovits, P. (2013), *The Definitive Guide to HTML5 WebSocket*, Vol. 1, Springer.
- Wang, V., Salim, F., Moskovits, P., Wang, V., Salim, F. and Moskovits, P. (2013), “The WebSocket Protocol”, *The Definitive Guide to HTML5 WebSocket*, available at: https://doi.org/10.1007/978-1-4302-4741-8_3.
- Wang, Z., Yang, Z. and Dong, T. (2017), “A review of wearable technologies for elderly care that can accurately track indoor position, recognize physical activities and monitor vital signs in real time”, *Sensors (Switzerland)*, available at: <https://doi.org/10.3390/s17020341>.
- Warden, S.J., Hinman, R.S., Watson, M.A., Avin, K.G., Bialocerkowski, A.E. and Crossley, K.M. (2008), “Patellar taping and bracing for the treatment of chronic knee pain: A systematic review and meta-analysis”, *Arthritis & Rheumatism*, John Wiley & Sons, Ltd, Vol. 59 No. 1, pp. 73–83.
- Watt, G.M. and Finch, C.F. (1996), “Preventing Equestrian Injuries”, *Sports Medicine*, Springer International Publishing, Vol. 22 No. 3, pp. 187–197.

- Willemsen, A.T.M., Frigo, C. and Boom, H.B.K. (1991a), “Lower Extremity Angle Measurement with Accelerometers—Error and Sensitivity”, *IEEE Transactions on Biomedical Engineering*, available at:<https://doi.org/10.1109/10.137284>.
- Willemsen, A.T.M., Frigo, C. and Boom, H.B.K. (1991b), “Lower extremity angle measurement with accelerometers - error and sensitivity analysis”, *IEEE Transactions on Biomedical Engineering*, Vol. 38 No. 12, pp. 1186–1193.
- WOO and L-Y., S. (1990), “Fundamental studies in knee ligament mechanics”, *Knee Ligaments*, Raven press, pp. 115–134.
- Young, C.M., Gastin, P.B., Sanders, N., Mackey, L. and Dwyer, D.B. (2016), “Player load in elite netball: Match, training, and positional comparisons”, *International Journal of Sports Physiology and Performance*, available at:<https://doi.org/10.1123/ijsp.2015-0156>.
- Zhang, S., Derrick, T.R., Evans, W. and Yu, Y.J. (2008), “Shock and impact reduction in moderate and strenuous landing activities”, *Sports Biomechanics*, Vol. 7 No. 2, pp. 296–309.
- Zhang, S.N., Bates, B.T. and Dufek, J.S. (2000), “Contributions of lower extremity joints to energy dissipation during landings”, *Medicine and Science in Sports and Exercise*, available at:<https://doi.org/10.1097/00005768-200004000-00014>.
- Zhao, X., Xiao, Z., Markham, A., Trigoni, N. and Ren, Y. (2014), “Does BTLE measure up against wifi? A comparison of indoor location performance”, *20th European Wireless Conference, EW 2014*.
- Zulkarnain, J. and Khairullina, K. (2019), “The pilot study on Down to Earth (D2E) injury prevention program among varsity netball players”, *Gazzetta Medica Italiana Archivio per Le Scienze Mediche*, Vol. 178 No. 4, available at:<https://doi.org/10.23736/S0393-3660.18.03766-X>.

APPENDICES

Appendix A: SBREC Application Modification Request

The Ethics application (8017) modification requests made during 2019 are provided:

MODIFICATION (No.3) APPROVAL NOTICE

Project No.: **8017**

Project Title: Design and Implementation of a Wearable Device to Measure Lower-Limb Mechanical Load during Competitive Netball Play

Principal Researcher: Anika Talukder

Email: talu0010@flinders.edu.au

Modification Approval Date:	26 March 2019	Ethics Approval Expiry Date:	1 December 2019
-----------------------------	---------------	------------------------------	-----------------

I am pleased to inform you that the modification request submitted for project 8017 on the 13 March 2019 has been reviewed and approved by the SBREC Chairperson. A summary of the approved modifications is listed below. Any additional information that may be required from you will be listed in the second table shown below called 'Additional Information Required'.

Approved Modifications	
Extension of ethics approval expiry date	
Project title change	
Personnel change	X
Research objectives change	
Research method change	
Participants – addition +/- change	
Consent process change	
Recruitment process change	
Research tools change	
Document / Information Changes	X
Other (if yes, please specify)	

RESPONSIBILITIES OF RESEARCHERS AND SUPERVISORS

1. Participant Documentation

Please note that it is the responsibility of researchers and supervisors, in the case of student projects, to ensure that:

- all participant documents are checked for spelling, grammatical, numbering and formatting errors. The Committee does not accept any responsibility for the above mentioned errors.
- the Flinders University logo is included on all participant documentation (e.g., letters of Introduction, information Sheets, consent forms, debriefing information and questionnaires – with the exception of purchased research tools) and the current Flinders University letterhead is included in the header of all letters of introduction. The Flinders University international logo/letterhead should be used and documentation should contain international dialling codes for all telephone and fax numbers listed for all research to be conducted overseas.
- the SBREC contact details, listed below, are included in the footer of all letters of introduction and information sheets.

This research project has been approved by the Flinders University Social and Behavioural Research Ethics Committee (Project Number 'INSERT PROJECT No. here following approval'). For more information regarding ethics approval of the project the Executive Officer of the Committee can be contacted by telephone on 8201 3116, by fax on 8201 2035 or by email human.researchethics@flinders.edu.au.

2. Annual Progress / Final Reports

Please be reminded that in order to comply with the monitoring requirements of the [National Statement on Ethical Conduct in Human Research \(2007-Updated 2018\)](#) an annual progress report must be submitted each year on **20 June** (approval anniversary date) for the duration of the ethics approval.

If the project is completed *before* ethics approval has expired please ensure a final report is submitted immediately. If ethics approval for your project expires please submit either (1) a final report; or (2) an extension of time request and an annual report.

Student Projects

The SBREC recommends that current ethics approval is maintained until a student's thesis has been submitted, reviewed and approved. This is to protect the student in the event that reviewers recommend some changes that may include the collection of additional participant data.

Your next report is due on **20 June 2019** or on completion of the project, whichever is the earliest.

The report template is available from the [Managing Your Ethics Approval](#) SBREC web page.

Please retain this notice for reference when completing annual progress or final reports.

3. Modifications to Project

Modifications to the project must not proceed until approval has been obtained from the Ethics Committee. Such proposed changes / modifications include:

- change of project title;
- change to research team (e.g., additions, removals, principal researcher or supervisor change);
- changes to research objectives;
- changes to research protocol;
- changes to participant recruitment methods;
- changes / additions to source(s) of participants;
- changes of procedures used to seek informed consent;
- changes to reimbursements provided to participants;

- changes / additions to information and/or documentation to be provided to potential participants;
- changes to research tools (e.g., questionnaire, interview questions, focus group questions);
- Extensions of time.

To notify the Committee of any proposed modifications to the project please complete and submit the *Modification Request Form* which is available from the [Managing Your Ethics Approval](#) SBREC web page. Download the form from the website every time a new modification request is submitted to ensure that the most recent form is used. Please note that extension of time requests should be submitted prior to the Ethics Approval Expiry Date listed on this notice.

Change of Contact Details

Please ensure that you notify the Executive Officer if either your mailing or email address changes to ensure that correspondence relating to this project can be sent to you. A modification request is not required to change your contact details.

4. **Adverse Events and/or Complaints**

Researchers should advise the [Executive Officer](#) immediately on 08 8201-3116 or human.researchethics@flinders.edu.au if:

- any complaints regarding the research are received;
- a serious or unexpected adverse event occurs that effects participants;
- an unforeseen event occurs that may affect the ethical acceptability of the project.

MODIFICATION (No.4) APPROVAL NOTICE

Project No.:

8017

Project Title:

Design and Implementation of a Wearable Device to Measure Lower-Limb Mechanical Load during Competitive Netball Play

Principal Researcher:

Ms Anika Talukder

Email:

tal0010@flinders.edu.au

Modification

27 August 2019

Ethics Approval Expiry

Date:

1 December 2019

Approval Date:

I am pleased to inform you that the modification request submitted for project 8017 on the 26 August 2019 has been reviewed and approved by the Chairperson of the Committee. A summary of the

approved modifications are listed below. Any additional information that may be required from you will be listed in the second table shown below called 'Additional Information Required'.

Approved Modifications	
Extension of ethics approval expiry date	
Project title change	
Personnel change	
Research objectives change	
Research method change	
Participants – addition +/- change	X
Consent process change	
Recruitment process change	
Research tools change	
Document / Information Changes	
Other (if yes, please specify)	

Additional Information Required
None.

RESPONSIBILITIES OF RESEARCHERS AND SUPERVISORS

5. Participant Documentation

Please note that it is the responsibility of researchers and supervisors, in the case of student projects, to ensure that:

- all participant documents are checked for spelling, grammatical, numbering and formatting errors. The Committee does not accept any responsibility for the above mentioned errors.
- the Flinders University logo is included on all participant documentation (e.g., letters of Introduction, information Sheets, consent forms, debriefing information and questionnaires – with the exception of purchased research tools) and the current Flinders University letterhead is included in the header of all letters of introduction. The Flinders University international logo/letterhead should be used and documentation should contain international dialling codes for all telephone and fax numbers listed for all research to be conducted overseas.
- the SBREC contact details, listed below, are included in the footer of all letters of introduction and information sheets.

This research project has been approved by the Flinders University Social and Behavioural Research Ethics Committee (Project Number 'INSERT PROJECT No. here following

approval'). For more information regarding ethics approval of the project the Executive Officer of the Committee can be contacted by telephone on 8201 3116, by fax on 8201 2035 or by email human.researchethics@flinders.edu.au.

6. Annual Progress / Final Reports

In order to comply with the monitoring requirements of the *National Statement on Ethical Conduct in Human Research 2007 (updated 2018)*; please be reminded that; an annual progress report must be submitted each year on the **20 June** (approval anniversary date) for the duration of the ethics approval using the report template available from the [Managing Your Ethics Approval](#) web page.

Please note that no data collection can be undertaken after the ethics approval expiry date listed at the top of this notice. If data is collected after expiry, it will not be covered in terms of ethics. It is the responsibility of the researcher to ensure that annual progress reports are submitted on time; and that no data is collected after ethics has expired.

If the project is completed *before* ethics approval has expired please ensure a final report is submitted immediately. If ethics approval for your project expires please either submit (1) a final report; or (2) an extension of time request (using the modification request form).

Next Report Due Date:

20 June 2019

Final Report Due Date:

1 December 2019

Student Projects

For student projects, the SBREC recommends that current ethics approval is maintained until a student's thesis has been submitted, assessed and finalised. This is to protect the student in the event that reviewers recommend that additional data be collected from participants.

7. Modifications to Project

Modifications to the project must not proceed until approval has been obtained from the Ethics Committee. Such proposed changes / modifications include:

- change of project title;
- change to research team (e.g., additions, removals, researchers and supervisors)
- changes to research objectives;
- changes to research protocol;
- changes to participant recruitment methods;
- changes / additions to source(s) of participants;
- changes of procedures used to seek informed consent;
- changes to reimbursements provided to participants;
- changes to information / documents to be given to potential participants;
- changes to research tools (e.g., survey, interview questions, focus group questions etc);
- extensions of time (i.e. to extend the period of ethics approval past current expiry date).

To notify the Committee of any proposed modifications to the project please complete and submit the *Modification Request Form* which is available from the [Managing Your Ethics Approval](#) SBREC web page. Download the form from the website every time a new modification request is submitted to ensure that the most recent form is used. Please note that extension of

Change of Contact Details

If the contact details of researchers, listed in the approved application, change please notify the Committee so that the details can be updated in our system. A modification request is not required to change your contact details; but would be if a new researcher needs to be added on to the research / supervisory team.

8. Adverse Events and/or Complaints

Researchers should advise the [Executive Officer](#) immediately on 08 8201-3116 or human.researchethics@flinders.edu.au if:

- any complaints regarding the research are received;
- a serious or unexpected adverse event occurs that effects participants;
- an unforeseen event occurs that may affect the ethical acceptability of the project.

Appendix B: Vicon AMTI OR6-7 Force Plate Specifications

Figure 49 is extracted from *OR6-7 Brochure* (AMTI, 2012):



Figure 49: Vicon AMTI OR6-7 Force Platforms Specifications

Appendix C: Texas Instruments SensorTag Specifications

Figure 50 is an extract of *CC2650 SimpleLink Multistandard Wireless MCU* datasheet (Texas Instruments, 2016):

***Image
removed due
to copyright
restriction***

Figure 50: Texas Instruments SensorTag CC2650 Specifications

Appendix D: Delsys Trigno Research+ Specifications

Figure 51 and Figure 52 are extracted from *Trigno Wireless Systems User's Guide* (Delsys, 2019a)

RF Frequency Band	2400-2483 MHz (ISM band)
Dimension	27 x 37 x 13 mm
Mass	14 g
Temperature Range ⁽¹⁾	5 - 45 degrees Celsius
EMG Signal Input Range	11mV / 22mV r.t.i.
EMG Signal Bandwidth	20-450 Hz / 10-850 Hz
EMG Contact Dimensions	5x1 mm
Contact Material ⁽²⁾	99.99% silver
Accelerometer Range	±2g, ±4g, ±8g, ±16g
Accelerometer Bandwidth	24 Hz – 470Hz (configurable in software)
Gyroscope Range	±250 dps, ±500 dps, ±1000dps, ±2000dps
Gyroscope Bandwidth	24Hz – 360 Hz (configurable in software)
Magnetometer Range	±4900 uT
Magnetometer Bandwidth	50 Hz
Inter-Sensor Delay	< 1 sample period (Base Station only)
Intra-Channel Delay	< 1-2 sample period
Analog Output Range	± 5 V (Base Station only)
Analog Output Bandwidth (Ch. 1-16)	DC-500 Hz (Base Station Only)
Analog Output Bandwidth (Ch. 17-64)	DC-50 Hz (Base Station Only)
Analog Output Group Delay (Ch. 1-16)	48 ms (Base Station Only)
Analog Output Group Delay (Ch. 17-64)	96 ms (Base Station Only)

1) Exposure beyond these temperature limits may damage the rechargeable battery.
 2) Sensor skin contacts are made from pure silver and should not be used if allergic reactions to silver are expected or found to occur.

Figure 51: Delsys Trigno Avanti Research+ Specification

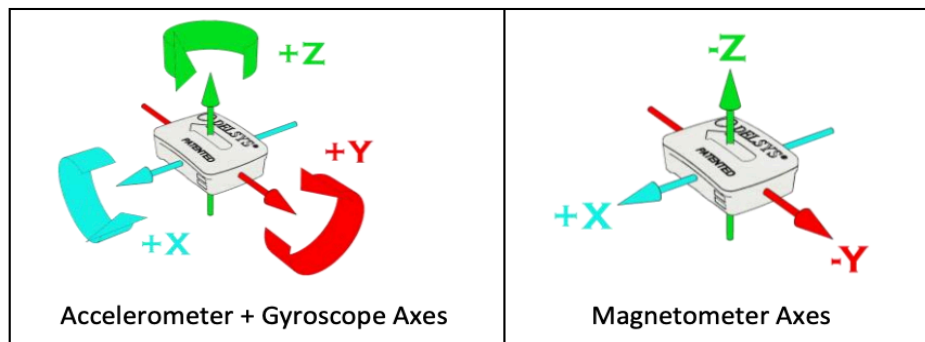


Figure 10: Trigno Sensors are fitted with an internal Inertial Measurement Unit (IMU) that will output 3 DOF acceleration data as well as 3 DOF rotational data as oriented in the figure (left). An onboard magnetometer measures compass heading and can be used to calculate orientation along with the accelerometer and gyroscope data.

Figure 52: Delsys Trigno Research+ Axis'

Appendix E: Vicon Protocols

The methodology for data collection using Vicon is provided below (Corbo, 2018)

SYSTEM CALIBRATION

Calibrating the system is to be completed prior to each day of testing. The following steps occur within the VICON software.

1. Calibrate the cameras
 - a. Click 'start' under 'calibrate cameras' within the 'system preparation' tab of the 'tools' area
 - b. Turn the calibration wand on and walk up and back across the area being used, whilst waving the calibration wand in figure 8 at different locations in front of the body (i.e. feet, torso, head)
 - c. Calibration is complete when all red triangles on the camera views on the calibration screen have turned green
 - d. All image errors should be below 0.15. Repeat calibration process if more than one image error is above 0.1.
2. Set volume origin
 - a. Leave and calibration wand on and place it at the junction of force plates 3 and 4
 - b. Adjust the height of the feet of the wand to level the wand, as indicated by the level on the wand
 - c. Click 'start', 'set origin' under 'set volume origin' within the 'system preparation' tab of the 'tools' area

DATA ACQUISITION CONFIGURATION

Configuration of data acquisition is to be completed prior to each day of testing.

1. Add the force plates
 - a. Right-click 'devices', 'add digital device', 'add AMTI Gen5/optima device – BETA9+dbg'
 - b. Set the orientation of each force plate
 - i. Click '#1 [1000Hz] (AMTI OR67 V1.0)' (force plate 1), 'show advanced'
 - ii. Fill the 'Position' and 'Orientation' input boxes as according to 'Rehabilitation and Motion Analysis Laboratory – 2016 Configuration' sheet in the Motion Analysis Lab
 - iii. Repeat steps i and ii for force plates 2, 3 and 4
2. Add the Delsys sensors
 - a. Open the 'Trigno Control Utility' program
 - b. Right-click 'devices', 'add digital device', 'add Delsys Trigno System'
3. Create a data location
 - a. In the 'communications' area, navigate to investigator's data location (i.e. their full name)
 - b. Click the 'new patient' button (black stick person) and name using the date
 - c. Click the 'create new session button' (grey pack man) and name using movement
4. Create a new subject
 - a. Click the 'subjects' tab in the 'resources' area
 - b. Add a subject 'Ai' by clicking the 'create a new subject from labelling skeleton' button
 - c. Select 'Pluggingait Lowerbody Ai' from the dropdown box
 - d. Enter appropriate patient measurements

Steps 5 and 6 should be repeated for every new subject used during data collection. It only needs to be completed once for every new subject.

SUBJECT MARK-UP

Subject mark-up should be repeated for every new subject used during data collection, before each of their data collection sessions.

5. Ensure that the subject is wearing tight-fitting exercise clothing, which does not interfere with the sensor positioning. The subject should be wearing sporting sneakers, and the make and age of the shoe should be recorded.
6. Use the large dots to mark-up the subject as according to Figure 53 and the 'Pluggingait Lowerbody Ai'. This should be completed with gloves on and using double-sided tape to stick the markers directly onto the body.
7. Remove EMG sensors 1 – 14 from the Trigno charging station and press the small black button. The green light on each sensor should begin to flash approximately once per second when a successful wireless connection is established, and they are ready for data collection. The 'Trigno Control Utility' program can also be used to check successful connections.
8. Ensure to note down which sensors are applied to the leg. Place 1 Delsys directly below the modified sensor, followed by one in the non-dominant leg, one in lateral malleolus and 1 in knee. Record the name and location of each sensor and respective orientation.
9. Apply the EMG sensors using the provided Trigno double-sided tape in the listed locations. A length of sporting tape should also be used to encompass the limb and each sensor once to improve fixation. All positions are applicable to both left and right legs for bilateral data collection.

Trigno EMG Sensor Positions

- Upper thigh (6 cm proximal to the centre of thigh, defined as the midpoint between the greater trochanter and patella) (Willemsen *et al.*, 1991b)
- Lower thigh (6 cm distal to centre of thigh, defined as the midpoint between the greater trochanter and patella) (Willemsen *et al.*, 1991b)
- Upper shank (5 cm proximal to the centre of shank, defined as the midpoint between the patella and the medial malleolus) (Willemsen *et al.*, 1991b)
- Lower shank (5 cm distal to centre of shank, defined as the midpoint between the patella and the medial malleolus) (Willemsen *et al.*, 1991b)
- Medial malleolus
- Lateral malleolus
- Posterior calcaneus (Fong and Chan, 2010)

Note: Where possible, these sensor positions were chosen to minimise the interference of soft tissue oscillations (Hamill *et al.*, 1995; Zhang *et al.*, 2008). It should be noted that upper and lower thigh are most susceptible to this interference.



Figure 53 - Plugingait Full Body Marker Positions

DATA COLLECTION

Data collection is to be completed by at least two different subjects.

10. Mark the floor as necessary to guide movements.
11. Begin data collection by navigating to the 'Capture' tab of the 'Tools' menu.
12. Tick the 'Auto Increment Trial Number' checkbox and untick the 'Permit Overwrite of Existing Files' checkbox.
13. Ensure that the system is functioning as expected. Step 12 should be completed once for each subject on each new day of testing.
 - a. Fill the 'Trial Name' as 'T-Pose' and ask the subject to stand with one foot on force plate one and the other on force plate two, facing the TV screen.
 - b. Press the 'start' button, wait 5 seconds, get the subject to perform a jump on spot jump to mark the start of activity prior undertaking required task, and press the 'stop' button.
 - c. Ensure that all markers are visible.
 - d. If the alignment is correct, the dots will automatically fill with green, red and blue lines.
14. Complete 3 successful trials of each movement
 - a. Data collection is begun and ended by clicking the 'start'/'stop' button
 - b. Each movement should have an appropriate 'Trial Name', with VICON simply auto-incrementing each movement by appropriately adding a number to the end of the 'Trial Name' or movement name. For example, 'Run, Run01, Run02...'
 - c. Ensure that each movement is sufficiently rehearsed prior to data collection (i.e. at least 2 rehearsals per movement).

REVIEWING DATA

15. Double-click on the file to be reviewed in Vicon and run the 'reconstruct and label' pipeline to create dots and planes.
16. Use the 'playback bar' to trim the data such that only the beginning until the end of the movement is captured.
17. Export the data as a '.csv' file by clicking 'settings', 'Export as .csv', 'ASCII Data part 1', 'VICON data'. Name data files with subject name, movement and movement number.
18. Repeat steps 15 - 17 for all data files collected.

Appendix F: SensorTag Data Acquisition Setup

SensorTag data acquisition steps are listed below:

1. Power all SensorTag on, make sure they are flashing green. Change batteries if needed.
2. Connect one of the Bluetooth low energy dongles to the desired windows device. Ensure it was registered by accessing “Bluetooth and other devices”
3. Go to Microsoft Store and download “Bluetooth LE explorer” and “SensorTag Data Acquisition”
4. Pair the desired SensorTag devices to the computer using Bluetooth LE Explorer. Once a new device pairing is happening, the screen will prompt you to allow the pairing. Allow it and check into “Bluetooth and other devices” setting to see whether it has been registered.
5. After pairing, go into SensorTag Data Acquisition and, depending on the number of SensorTag chosen, ie:3, input “3” in the “SensorTag no” field. Click “search and connect”
6. Choose the accelerometer sensor and “enable sensor”
7. There should be three SensorTag popping up on the “Modules” section. If they don’t, check the batteries and make sure the lights are flashing.
8. Choose the accelerometer by going into “Sensor”. An accelerometer graph should appear with x, y and z coordinates
9. Set the Sampling rate to 100 Hz. Make sure you select every module and choose 100 Hz for all of the devices.
10. “Record data”, each of the SensorTag will automatically register the movements and collect data
11. You can also pause recording by pressing “pause recording”
12. Once done, “Seal file and send data”. Once you “generate the file”, it should prompt you to choose the type of file. Choose “CSV” and the bottom option from the dropdown menu.
13. The App will automatically quit, the file in CSV format can be found under Music folder, and into a subfolder called “BLEdata”. The device logs could also be found here
14. Tested on iMac and Surface pro on 13th June, both functioned as expected.

Appendix G: ESP8266 Specifications

Figure 54 is an extract of *ESP8266EX Datasheet* (Espressif Systems, 2019)



Figure 54: Esp8266 Specification

Appendix H: ADXL345 Specifications

Figure 55 is an extract of *ADXL345* datasheet (Analog Devices, 2009)



Figure 55: ADXL345 Specifications

Appendix I: Adafruit Feather Huzzah ESP8266 Pinout

Figure 56 is extracted from *Adafruit Feather Huzzah ESP8266* (Adafruit, 2019b)



Figure 56: Adafruit Feather Huzzah ESP8266 pinout diagram

Appendix J: Data Acquisition Arduino Code

The following Arduino header and main function received significant contributions from Lucas Kleiss and calculated and streamed the A_{IS} amplitudes in real-time in 1-second epoch (Kleiss, 2019). The full folder containing HTML for website and user interface can be found in the GitHub folder.

Header Function:

```
//
// Serial
//

extern String SerialInputString;
extern bool SerialInputComplete;
bool SerialEvent();

//
// WiFi
//

#include <ESP8266WiFi.h>

extern char AP_SSID[];
extern char AP_Password[];
extern int AP_Channel;

extern IPAddress AP_IP;
extern IPAddress AP_Gateway;
extern IPAddress AP_Subnet;

//
// DNS
//

#include <DNSServer.h>

extern const uint16_t DNSPort;
extern DNSServer DNS;

//
// Web Server
//

#include <ESP8266WebServer.h>

extern const uint16_t ServerPort;
extern ESP8266WebServer Server;

void ServerHandleRequest();
void ServerHandleHotspotDetectHtml();
```



```

void ServerHandleNCSITxt();
void ServerHandleConnectTestTxt();
void ServerHandleSuccessTxt();
void ServerSendFile(const String &path);
void ServerSendDirectory(const String &path);
void ServerStartLogging(const String &fname, const bool overwrite);
void ServerStopLoggin();

//
// Web Sockets
//

#include <WebSockets.h>
#include <WebSocketsServer.h>
#include <WebSocketsClient.h>

extern const uint16_t SocketPort;
extern WebSocketsServer Socket;

//
// SPIFFS
//

#include <FS.h>

extern File LogFile;
extern const String LogDir;

//
// Tokeniser
//

bool IsWhitespace(const char c);

struct tokeniser_t
{
    String _str = "";
    tokeniser_t(const String &str);
    String next();
    String nextLower();
};

```

Main Function:

```

#include "FlinBITWiFi.h"
#include <SparkFun_ADXL345.h>

// Accelerometer

ADXL345 adxl = ADXL345(2);

// Serial

String SerialInputString = "";
bool SerialInputComplete = false;

// WiFi

char AP_SSID[80];
char AP_Password[80] = "12345678";
char AP_IP_Text[80];
int AP_Channel = random(0, 13) + 1;

IPAddress AP_IP(192, 168, 1, 1);
IPAddress AP_Gateway = AP_IP;
IPAddress AP_Subnet(255, 255, 255, 0);

// DNS

DNSServer DNS;
const uint16_t DNSPort = 53;

// Web Server

const uint16_t ServerPort = 80;
ESP8266WebServer Server(ServerPort);

// Web Socket

const uint16_t SocketPort = 81;
WebSocketsServer Socket(SocketPort);

// SPIFFS

File LogFile;
const String LogDir = "/logs/";

// #define DEBUG

void setup()
{
  //
  // Set up Serial
  //

```

```

Serial.begin(9600);

#ifdef DEBUG_ESP_CORE
  Serial.setDebugOutput(true);
#endif

SerialInputString.reserve(200);

//
// Set up ADXL
//

adxl.powerOn(); // Power on the ADXL345
adxl.setRangeSetting(16); // Give the range settings
// Accepted values are 2g, 4g, 8g or 16g
// Higher Values = Wider Measurement Range
// Lower Values = Greater Sensitivity

adxl.setSpiBit(false); // Configure the device: 4 wire SPI mode = '0' or 3 wire SPI mode = 1
// Default: Set to 1
// SPI pins on the ATmega328: 11, 12 and 13 as reference in SPI Library
adxl.setActivityXYZ(1, 1, 1); // Set to activate movement detection in the axes
"adxl.setActivityXYZ(X, Y, Z);" (1 == ON, 0 == OFF)

//
// Set up SPIFFS
//
SPIFFS.begin();

//
// Get WiFi MAC Address and set SSID
//
uint8_t mac[6];
WiFi.macAddress(mac);
snprintf(AP_SSID, sizeof(AP_SSID), "SportMonitor_%02X%02X%02X", mac[3], mac[4], mac[5]);
ReadParameterFromSPIFFS("/SSID.txt", AP_SSID, sizeof(AP_SSID));
Serial.print("WiFi SSID: ");
Serial.println(AP_SSID);

ReadParameterFromSPIFFS("/password.txt", AP_Password, sizeof(AP_Password));

snprintf(AP_IP_Text, sizeof(AP_IP_Text), "%s", AP_IP.toString().c_str());

#ifdef DEBUG
  Serial.print("SSID: ");
  Serial.println(AP_SSID);
  Serial.print("Password: ");
  Serial.println(AP_Password);
  Serial.print("IP: ");
  Serial.println(AP_IP_Text);
#endif

```

```

//
// Set up WiFi
//
WiFi.mode(WIFI_AP);
WiFi.softAPConfig(AP_IP, AP_Gateway, AP_Subnet);
WiFi.softAP(AP_SSID, AP_Password, AP_Channel, false);

//
// Set up DNS
//
DNS.setErrorReplyCode(DNSReplyCode::NoError);
DNS.start(DNSPort, "*", AP_IP);

//
// Set up WebServer
//
Server.on("/hotspot-detect.html", &ServerHandleHotspotDetectHtml);
Server.on("/ncsi.txt", &ServerHandleNCSITxt);
Server.on("/connecttest.txt", &ServerHandleConnectTestTxt);
Server.on("/success.txt", &ServerHandleSuccessTxt);

Server.onNotFound(&ServerHandleRequest);
Server.begin();

//
// Set up WebSocket
//
Socket.begin();
Socket.onEvent([(uint8_t num, WStype_t type, uint8_t *payload, size_t length)
{
    switch (type)
    {
        //
        // Device connected to the web socket
        //
        case WStype_CONNECTED: {

            } break;

        //
        // Device disconnected from the web socket
        //
        case WStype_DISCONNECTED: {

            } break;

        //
        // Received text over web socket
        //
        case WStype_TEXT: {
            // payload should be null-terminated-string

```

```

if (payload[length - 1] == '\0' || payload[length] == '\0')
{
    const String str = (const char *)payload;

    bool wasLogger = false;
    if (str.length() > 1 && str[0] == '/' && str[1] != '/')
    {
        tokeniser_t commands(str);
        const String &command = commands.nextLower();
        auto boardcastLogging = []() {
            if (LogFile)
                Socket.broadcastTXT("/logger running");
            else
                Socket.broadcastTXT("/logger notrunning");
        };
        if (command == "/logstart")
        {
            wasLogger = true;
            bool overwrite = commands.nextLower() == "overwrite";
            const String &fname = commands.next();
            ServerStartLogging(fname, overwrite);
            boardcastLogging();
        }
        else if (command == "/logstop")
        {
            wasLogger = true;
            ServerStopLogging();
            boardcastLogging();
        }
        else if (command == "/islogging")
        {
            wasLogger = true;
            boardcastLogging();
        }
        else if (command == "/logclear")
        {
            Dir dir = SPIFFS.openDir(LogDir);

            while (dir.next())
            {
                SPIFFS.remove(dir.fileName());
                dir = SPIFFS.openDir(LogDir);
            }
        }
        else if (command == "/store")
        {
            const String &filename = commands.next();
            const String &text = commands.next();
            WriteParameterToSPIFFS(filename, text);
        }
    }
}

```

```

        if (!wasLogger)
        {
            Serial.print(str);
        }

#ifdef DEBUG
        Socket.broadcastTXT("/echo " + str);
#endif
        if (LogFile)
        {
            size_t sz = str.length();
            if (LogFile.write((const uint8_t *)str.c_str(), sz) != sz)
                Socket.broadcastTXT("/echo > Failed to save\n");
#ifdef DEBUG
            else
                Socket.broadcastTXT("/echo > Saved\n");
#endif
        }
    }
}
// else error
} break;

//
// Received binary blob over web socket
//
case WStype_BIN: {
    // payload is binary
} break;
};
}

void LogString(const String &str)
{
    if (LogFile)
    {
        size_t sz = str.length();
        if (LogFile.write((const uint8_t *)str.c_str(), sz) != sz)
            Socket.broadcastTXT("/echo > Failed to save\n");
#ifdef DEBUG
        else
            Socket.broadcastTXT("/echo > Saved");
#endif
    }
}

unsigned long lastMillis = 0;
unsigned long deltaMillis = 0;
unsigned long sampleCount = 0;

```

```

float maxZ = -100.0; //variable initialisation for maximum
float minZ = 100.0; //variable initialisation for minimum
float amplitudeZ = 0.0; //variable initialisation for amplitude
float maxY = -100.0; //variable initialisation for maximum
float minY = 100.0; //variable initialisation for minimum
float amplitudeY = 0.0; //variable initialisation for amplitude
float maxX = -100.0; //variable initialisation for maximum
float minX = 100.0; //variable initialisation for minimum
float amplitudeX = 0.0; //variable initialisation for amplitude

void loop()
{
  DNS.processNextRequest();
  Socket.loop();
  Server.handleClient();
  if (SerialEvent())
  {
    Socket.broadcastTXT("/echo " + SerialInputString);
    LogString(SerialInputString);

    if (SerialInputString.length() > 1 && SerialInputString[0] == '/' && SerialInputString[1] != '/')
    {
      tokeniser_t commands(SerialInputString);
      const String &command = commands.nextLower();
      if (command == "/store")
      {
        const String &filename = commands.next();
        const String &text = commands.next();
#ifdef DEBUG
        Serial.print("/store ");
        Serial.print(filename);
        Serial.print(" ");
        Serial.println(text);
#endif
        WriteParameterToSPIFFS(filename, text);
      }
    }
  }

  unsigned long current = millis();

  if (lastMillis > current)
  {
    // millis wrapped around
    deltaMillis += (((unsigned long) - 1) - lastMillis) + current;
  }
  else
  {
    deltaMillis += current - lastMillis;
  }
}

```

```

lastMillis = current;
++sampleCount;

// Collect the accelerometer data and set the values to x, y and z
int x, y, z;
float X, Y, Z;
adxl.readAccel(&x, &y, &z);

// convert from LSB/G to G
X = (float)x;
Y = (float)y;
Z = (float)z;

float accX = X / 32.0;    // Sensitivity at 16g at 10 bits to calculate G (taken from datasheet)
float accY = Y / 32.0;
float accZ = Z / 32.0;

//update minimum and maximum value if required

maxX = max(maxX, accX); //find the maximum
minX = min(minX, accX); //find the minimum

maxY = max(maxZ, accY); //find the maximum
minY = min(minZ, accY); //find the minimum

maxZ = max(maxZ, accZ); //find the maximum
minZ = min(minZ, accZ); //find the minimum

amplitudeX = 0.0; //Impact dose in x direction (not necessary, provided just in case
amplitudeY = 0.0; //Horizontal impact dose (landing)
amplitudeZ = 0.0; //Vertical impact dose (braking)

//After 1 second, perform the amplitude calculation for the max and minimum G force
if (deltaMillis > 1000)
{
    amplitudeX = absolute(maxX) + absolute(minX);
    amplitudeY = absolute(maxY) + absolute(minY);
    amplitudeZ = absolute(maxZ) + absolute(minZ);

    // Convert our values to a string
    char str[100];
    snprintf(str, sizeof(str), "%f, %f, %f, %lu\n", amplitudeX, amplitudeY, amplitudeZ, sampleCount);

    // Print and save our string
    Socket.broadcastTXT(str);
    Serial.print(str);
    LogString(str);

```



```

// Reset our variables
deltaMillis = 0;
sampleCount = 0;
amplitudeX = 0;
amplitudeY = 0;
amplitudeZ = 0;
maxZ = -100;
minZ = 100;
maxY = -100;
minY = 100;
maxX = -100;
minX = 100;

}

delay(1);
}

void ReadParameterFromSPIFFS(const String &filename, char buffer[], uint16_t maxbytes)
{
  //
  // If available, obtain parameter from SPIFFS
  //

  if (SPIFFS.exists(filename))
  {
#ifdef DEBUG
    Serial.println(filename + " exists. Reading.");
#endif
    File hParameterFile = SPIFFS.open(filename, "r");
    if (hParameterFile)
    {
      while (hParameterFile.available())
      {
        size_t l = hParameterFile.readBytesUntil('\n', buffer, maxbytes);
        buffer[l] = 0;
      }
      hParameterFile.close();
    }
    else
    {
#ifdef DEBUG
      Serial.println("Error reading file " + filename);
#endif
    }
  }
  else
  {
#ifdef DEBUG
    Serial.println(filename + " doesn't exists.");
#endif
  }
}

```

```

}
}

void WriteParameterToSPIFFS(const String &filename, const String &buffer)
{
    //
    // Write parameter to SPIFFS. Always overwrite.
    //

    File hParameterFile = SPIFFS.open(filename, "w");
    if (hParameterFile) {
        hParameterFile.println(buffer);
        hParameterFile.close();
    }
}

void ServerStartLogging(const String &fname, const bool overwrite)
{
    if (LogFile)
        return;

    String name = (LogDir + fname);

    if (name.endsWith("/"))
        name += "log.txt";
    else if (!name.endsWith(".txt"))
        name += ".txt";

    String message = "/echo Opened file ";
    message += name + "\n";
    Socket.broadcastTXT(message);

    LogFile = SPIFFS.open(name, ((overwrite || !SPIFFS.exists(name)) ? "w" : "a"));
}

void ServerStopLogging()
{
    if (!LogFile)
        return;

    LogFile.close();
}

void ServerHandleRequest()
{
    String uri = Server.uri();
    uri = uri.endsWith("/") ? uri + "index.html" : uri;

    if (!ServerSendFile(Server, uri))
    {
        ServerSendDirectory(Server, uri);
    }
}

```

```
}
}
```

```
void ServerHandleCaptive(const char *text)
{
    Server.sendHeader("Cache-Control", "no-cache, no-store, must-revalidate");
    Server.sendHeader("Pragma", "no-cache");
    Server.sendHeader("Expires", "-1");
    Server.send(200, "text/html", text);
}
```

```
void ServerHandleHotspotDetectHtml()
{
#ifdef DEBUG
    Serial.println("Handling hotspot-detect.html");
#endif

```

```
ServerHandleCaptive("<html><head><title>Success</title></head><body>Success</body></html>")
;
}
```

```
void ServerHandleNCSITxt()
{
#ifdef DEBUG
    Serial.println("Handling ncsi.txt");
#endif
    ServerHandleCaptive("Microsoft NCSI");
}
```

```
void ServerHandleConnectTestTxt()
{
#ifdef DEBUG
    Serial.println("Handling connecttest.txt");
#endif
    ServerHandleCaptive("Microsoft Connect Test");
}
```

```
void ServerHandleSuccessTxt()
{
#ifdef DEBUG
    Serial.println("Handling success.txt");
#endif
    ServerHandleCaptive("success\n");
}
```

```
bool ServerSendFile(ESP8266WebServer &server, const String &path)
{
    String dataType = F("text/plain");
    String lowerPath = path.substring(path.length() - 5, path.length());
    lowerPath.toLowerCase();
    if (lowerPath.endsWith(".src")) lowerPath = lowerPath.substring(0, path.lastIndexOf("."));
}
```

```

else if (lowerPath.endsWith(".gz"))    dataType = F("application/x-gzip");
else if (lowerPath.endsWith(".html"))  dataType = F("text/html");
else if (lowerPath.endsWith(".htm"))   dataType = F("text/html");
else if (lowerPath.endsWith(".png"))   dataType = F("image/png");
else if (lowerPath.endsWith(".js"))    dataType = F("application/javascript");
else if (lowerPath.endsWith(".css"))   dataType = F("text/css");
else if (lowerPath.endsWith(".gif"))   dataType = F("image/gif");
else if (lowerPath.endsWith(".jpg"))   dataType = F("image/jpeg");
else if (lowerPath.endsWith(".ico"))   dataType = F("image/x-icon");
else if (lowerPath.endsWith(".svg"))   dataType = F("image/svg+xml");
else if (lowerPath.endsWith(".mp3"))   dataType = F("audio/mpeg");
else if (lowerPath.endsWith(".wav"))   dataType = F("audio/wav");
else if (lowerPath.endsWith(".ogg"))   dataType = F("audio/ogg");
else if (lowerPath.endsWith(".xml"))   dataType = F("text/xml");
else if (lowerPath.endsWith(".pdf"))   dataType = F("application/x-pdf");
else if (lowerPath.endsWith(".zip"))   dataType = F("application/x-zip");

```

```
String pathWithGz = path + ".gz"; // String + char* does not return a String!
```

```
File file;
```

```

if (SPIFFS.exists(pathWithGz))
{
    file = SPIFFS.open(pathWithGz, "r");
}
else if (SPIFFS.exists(path))
{
    file = SPIFFS.open(path, "r");
}
else
{
#ifdef DEBUG
    Serial.print("Failed to find file ");
    Serial.print(pathWithGz);
    Serial.print(" or ");
    Serial.print(path);
    Serial.println("");
#endif
    return false;
}

#ifdef DEBUG
    Serial.print("Streaming file ");
    Serial.print(path);
    Serial.println("");
#endif

server.setContentLength(file.size());
size_t sent = server.streamFile(file, dataType);
file.close();
return true;

```

```

}

void ServerSendDirectory(ESP8266WebServer &server, const String &path)
{
    int lastIndex = path.lastIndexOf("/") + 1;
    if (lastIndex <= 0)
        lastIndex = 1;
    const String &substr = path.substring(0, lastIndex);

#ifdef DEBUG
    if (substr != LogDir)
    {
        String error = "Failed to read file '" + path + "'\n\n" + substr;
        server.send(404, "text/plain", error);
    }
    else
#endif
    {
        Dir dir = SPIFFS.openDir(substr);

        String doc =
            R"(<html><head><meta charset="utf-8"></head><body>)"
            R"(<a href="/"><h1 style="margin:0 0 0 0;">Home</h1></a><br/>)"
            R"(<h2 style="margin:0 0 0 0;">)" + substr + R"(</h2><br/>);"
        while (dir.next())
        {
            String &&fname = dir.fileName();
            if (fname.endsWith(".gz"))
                fname = fname.substring(0, fname.length() - 3);
            doc += String(R"(<a href=")" + fname + R"(")" + fname + "</a><br/>");
        }
        doc += "</body></html>";

        server.send(200, "text/html", doc);
    }
}

bool SerialEvent()
{
    if (SerialInputComplete)
    {
        SerialInputString = "";
        SerialInputComplete = false;
    }
    while (Serial.available())
    {
        char in = (char)Serial.read();
        SerialInputString += in;
        if (in == '\n')
        {
            SerialInputComplete = true;
        }
    }
}

```

```

    break;
}
}
return SerialInputComplete;
}

```

```

bool IsWhitespace(const char c)
{
    return c == ' ' || c == '\t' || c == '\r' || c == '\n';
}

```

```

tokeniser_t::tokeniser_t(const String &str) : _str(str) {}

```

```

String tokeniser_t::next()
{
    size_t i = 0;
    for (; i < _str.length() && IsWhitespace(_str[i]); ++i); // find next not-space (start of token)
    if (i >= _str.length())
    {
        _str = "";
        return "";
    }

    size_t j = i;
    for (; j < _str.length() && !IsWhitespace(_str[j]); ++j); // find next whitespace (end of token)

    String rtn = _str.substring(i, j);
    _str = _str.substring(j, _str.length());
    return rtn;
}

```

```

String tokeniser_t::nextLower()
{
    String str = next();
    str.toLowerCase();
    return str;
}

```

```

float absolute(float number) {
    if (number < 0) {
        number = -number;
    }
    return number;
}

```

Appendix K: Participant Consent Forms



CONSENT FORM FOR PARTICIPATION IN RESEARCH
(by experiment)
Netball Players

Design and Implementation of a Wearable Device to Measure Lower-Limb Mechanical Load during Competitive Netball Play

I
being over the age of 18 years hereby consent to participate as requested in the Letter of Introduction and Information Sheet for the research project on the design and implementation of a wearable device to measure lower-limb mechanical load during competitive netball play.

1. I have read the information provided.
2. Details of procedures and any risks have been explained to my satisfaction.
3. I agree to video recording of my participation.
4. I am aware that I should retain a copy of the Letter of Introduction, Information Sheet and Consent Form for future reference.
5. I understand that:
 - I may not directly benefit from taking part in this research.
 - I am free to withdraw from the project at any time and am free to decline to answer particular questions.
 - Only researchers and supervisors listed under this project will have access to collected data, where it will be identifiable as my own.
 - I will not be identified, and individual information will remain confidential, in all explained publications.
 - Whether I participate or not, or withdraw after participating, will have no effect on my progress within the Contax Netball Club.
 - I may ask that the recording/observation be stopped at any time, and that I may withdraw at any time from the session or the research without disadvantage.

Participant's signature.....Date.....

I certify that I have explained the study to the volunteer and consider that she/he understands what is involved and freely consents to participation.

Researcher's name.....

Researcher's signature.....Date.....

Appendix L: Individual Participant Analysis MATLAB Script

This section contains example MATLAB script for individual data analysis (participant 3):

main.m:

```
%MAIN

%Run and adapt file according to data sets

m = mass ();

step440 = extractFeature('460drop.xls', m, 1, 'N', 1); %red
step44001 = extractFeature('460drop01.xls', m, 1, 'N', 1);

shuffle = extractFeature('Shuffle.xls', m, 1, 'N', 1); %orange
shuffle01 = extractFeature('Shuffle01.xls', m, 1, 'N', 1);
shuffle02 = extractFeature('Shuffle02.xls', m, 1, 'N', 1);

walk = extractFeature('Walk.xls', m, 1, 'Y', 1); %yellow
walk01 = extractFeature('Walk01.xls', m, 1, 'Y', 1);
walk02 = extractFeature('Walk02.xls', m, 1, 'Y', 1);

jog = extractFeature('Jog.xls', m, 1, 'Y', 1); %green
jog01 = extractFeature('Jog01.xls', m, 1, 'Y', 1);
jog02 = extractFeature('Jog02.xls', m, 1, 'Y', 1);

run = extractFeature('Run.xls', m, 1, 'Y', 1); %cyan
run01 = extractFeature('Run01.xls', m, 1, 'Y', 1);
run02 = extractFeature('Run02.xls', m, 1, 'Y', 1);

sprint = extractFeature('Sprint.xls', m, 1, 'Y', 1); %blue
sprint01 = extractFeature('Sprint01.xls', m, 1, 'Y', 1);
sprint02 = extractFeature('Sprint02.xls', m, 1, 'Y', 1);

jump = extractFeature('Jump.xls', m, 2, 'N', 1); %purple
jump01 = extractFeature('Jump01.xls', m, 2, 'N', 1);

RO = extractFeature('RO.xls', m, 1, 'Y', 1); %magenta
RO01 = extractFeature('RO01.xls', m, 1, 'Y', 1);
RO02 = extractFeature('RO02.xls', m, 1, 'Y', 1);

F2 = extractFeature('2F.xls', m, 1, 'Y', 1); %black
F201 = extractFeature('2F01.xls', m, 1, 'Y', 1);
F202 = extractFeature('2F02.xls', m, 1, 'Y', 1);

Pivot = extractFeature('Pivot.xls', m, 1, 'Y', 1); %pink
Pivot01 = extractFeature('Pivot01.xls', m, 1, 'Y', 1);
Pivot02 = extractFeature('Pivot02.xls', m, 1, 'Y', 1);

cut = extractFeature('Cut.xls', m, 1, 'Y', 1); %grey
cut01 = extractFeature('Cut01.xls', m, 1, 'Y', 1);
cut02 = extractFeature('Cut02.xls', m, 1, 'Y', 1);

%Colour vector with RGB triplets for each data file
red = [204 0 0]; orange = [255 128 0]; yellow = [204 204 0]; green = [102
204 0]; cyan = [0 255 255]; blue = [0 0 255]; purple = [127 0 255]; magenta
= [255 0 127]; black = [0 0 0]; pink = [255 102 255]; grey = [160 160 160];
```



```
c = 1/255*[red; red;orange; orange; orange; yellow; yellow; yellow; green;
green; green; cyan; cyan; cyan; blue; blue; blue; purple; purple; magenta;
magenta; magenta; black; black; black; pink; pink; pink; grey; grey; grey];
```

```
step440v = vectors(step440, step44001);
shufflev = vectors(shuffle, shuffle01, shuffle02);
walkv = vectors(walk, walk01, walk02);
jogv = vectors(jog, jog01, jog02);
runv = vectors(run, run01,run02);
sprintv = vectors(sprint, sprint01, sprint02);
jumpv = vectors(jump,jump01);
ROv = vectors(RO, RO01, RO02);
F2v = vectors(F2, F201, F202);
pivotv = vectors(Pivot, Pivot01,Pivot02);
cutv = vectors(cut, cut01, cut02);
```

```
P3 = struct('step440', step440, 'step44001', step44001, 'shuffle', shuffle,
'shuffle01', shuffle01, 'shuffle02', shuffle02, 'walk', walk, 'walk01',
walk01, 'walk02', walk02, 'jog', jog, 'jog01', jog01, 'jog02', jog02,
'run', run, 'run01', run01, 'run02',run02,'sprint', sprint, 'sprint01',
sprint01, 'sprint02', sprint02, 'jump', jump, 'jump01', jump01, 'RO', RO,
'RO01', RO01, 'RO02', RO02, 'F2', F2, 'F201', F201, 'F202', F202,'Pivot',
Pivot, 'Pivot01', Pivot01, 'Pivot02', Pivot02, 'cut', cut, 'cut01', cut01,
'cut02', cut02, 'step440v', step440v, 'shufflev', shufflev, 'walkv', walkv,
'jogv', jogv, 'runv', runv, 'sprintv', sprintv, 'jumpv', jumpv, 'ROv', ROv,
'F2v', F2v, 'pivotv',pivotv, 'cutv', cutv);
```

```
%Use correlate to produce results, specify which files to include in
correlation graphs
```

```
correlate(c,step440, step44001, shuffle, shuffle01, shuffle02, walk,
walk01, walk02, jog, jog01, jog02, run, run01, run02, sprint, sprint01,
sprint02, jump, jump01, RO, RO01, RO02, F2, F201, F202, Pivot,
Pivot01,Pivot02, cut, cut01, cut02);
```

```
%Use tabulate to produce a table with all variables for all movements
```

```
tabulate(step440, step44001, shuffle, shuffle01, shuffle02, walk, walk01,
walk02, jog, jog01, jog02, run, run01, run02, sprint, sprint01, sprint02,
jump, jump01, RO, RO01, RO02, F2, F201, F202, Pivot, Pivot01,Pivot02, cut,
cut01, cut02);
```

mass.m:

```
function [m] = mass_tb()
%calculates mass of the participant using Tpose data on force plate 1 and 2

file = xlsread('Tpose.xls'); %Open Tpose
file([1,2,3,4,5],:)=[]; %ignore NAN
f1x = file(:,3); %FP1x
f1y = file(:,4); %FP1y
f1z = file(:,5); %FP1z
f2x = file(:,12); %FP2x
f2y = file(:,13); %FP2y
f2z = file(:,14); %FP2z

total1 = mean(sqrt(f1x.^2 + f1y.^2 + f1z.^2));
total2 = mean(sqrt(f2x.^2 + f2y.^2 + f2z.^2));
m = (total1+total2)/9.81; %Final mass

end
```

extractFeature.m:

```
function [out] = extractFeature(filename, BW, heelstrike_No,
toeoff_Present, first_FP, second_FP)
% extracts non-windowed features from data files
% filename: data file to load and analyse (str)
% BW: body weight of subject (kg)
% heelstrike_No: specifies which step to analyse (1 = 1st step, 2 = 2nd
step) for datasets starting on plate
% toeoff_Present: 'Y' if toe-off, 'N' if no toe-off (eg.440Step,Jump,2F)
% first_FP: force plate on which step occurs (1,2,3,4)
% second_FP: specified if a singular step covers 2 force plates (1,2,3,4)

%READ DATA (filename)
file = xlsread(filename); %Read a xls file
file([1,2,3,4],:)=[]; %delete 1st 5 rows of NAN

frame = file(:,1); %number of frames in the data
sub_frame = file(:,2); %number of sub frames in the data
time = (frame*0.004 + sub_frame*0.0005); %convert frame rate to seconds,
frame250Hz, subframe2000Hz

FSx1 =file(:,89); FSy1 = file(:,90); FSz1 = file(:,91); %Column data
containing x, y, z axis of Feather

%select force plate data (first_FP,secod_FP)
switch first_FP %choose first forceplate
    case 1; Fz1 = 5; Fy1 = 4; Fx1 = 3; %Plate 1 x,y,z force
    case 2; Fz1 = 14; Fy1 = 13; Fx1 = 12; %Plate 2 x,y,z force
    case 3; Fz1 = 23; Fy1 = 22; Fx1 = 21; %Plate 3 x,y,z force
    case 4; Fz1 = 32; Fy1 = 31; Fx1 = 30; %Plate 4 x,y,z force
end

if (nargin == 7)
    switch second_FP % second force plate
        case 1; Fz2 = 5; Fy2 = 4; Fx2 = 3;
        case 2; Fz2 = 14; Fy2 = 13; Fx2 = 12;
        case 3; Fz2 = 23; Fy2 = 22; Fx2 = 21;
        case 4; Fz2 = 32; Fy2 = 31; Fx2 = 30;
    end
end

switch nargin
    case 6 %if no crossover
        Fx_data = file(:,Fx1);
        Fy_data = file(:,Fy1);
        Fz_data = file(:,Fz1);

    case 7 %if crossover
        Fx_data = file(:,Fx1) + file(:,Fx2);
        Fy_data = file(:,Fy1) + file(:,Fy2);
        Fz_data = file(:,Fz1) + file(:,Fz2);
end

%Find heel-strike in row number (heelstrike_NO)
if (heelstrike_No == 1) %first occurrence of non-zero data is
step
    heel_strike = find(Fz_data,1); %heelstrike first non-zero
```

```

end
if (heelstrike_No == 2)          %second occurrence of non-zero data is step
    heel_strike = find(~Fz_data, 1, 'last') + 1; %heelstrike is position
after last zero for movements starting on force plate
end

%Find toe-off in row number (toeoff_present)
Fz_N = Fz_data/9.81/BW;        %convert from N to BW
if (toeoff_Present == 'Y')    %toe off is last non-zero data point
    toe_off = find(Fz_data,1,'last');
end
if (toeoff_Present == 'N')    %toeoff is when Fz_N reaches 0.3BW after max
VGRF (balance achieved, landing ended)
    [~,i] = min(Fz_N);
    temp = Fz_N([i:end],:);
    toe_off = find(temp>-0.5,1) + i;
end

%for acceleration peaks, seek peak within 0.5s of heelstrike
acc_upperlim = heel_strike + 500;
if (acc_upperlim > length(time))
    acc_upperlim = length(time);
end

%Display the upper limit of accelerometer
x = [filename, ', heel_strike = ', num2str(time(heel_strike, 1)), ',
acc_upperlim = ', num2str(time(acc_upperlim, 1))];
disp(x)

%Peak Force Calculation after heelstrike
Fx_N = Fx_data/9.81/BW;        %Normalise force to BW
peak_Fx = min(Fx_data);        %Take peak
peak_Fx_N = min(Fx_N);
Fx = struct('data', Fx_data, 'data_N', Fx_N, 'peak', peak_Fx, 'peak_N',
peak_Fx_N); %Struct with peak force data in x axis
Fy_N = Fy_data/9.81/BW;
peak_Fy = min(Fy_data);
peak_Fy_N = min(Fy_N);
Fy = struct('data', Fy_data, 'data_N', Fy_N, 'peak', peak_Fy, 'peak_N',
peak_Fy_N); %Struct with peak force data in Y axis
peak_Fz = min(Fz_data);
peak_Fz_N = min(Fz_N);
Fz = struct('data', Fz_data, 'data_N', Fz_N, 'peak', peak_Fz, 'peak_N',
peak_Fz_N); %Struct with peak force data in z axis

% Feather ACCELERATION
F_col= round(acc_upperlim/1000); %Reduce sampling to 1 Hz
F_x_amp = FSx1(F_col:F_col,1);
F_y_amp = FSy1(F_col:F_col,1);
F_z_amp = FSz1(F_col:F_col,1);

feather = struct('F_x_amp', F_x_amp, 'F_y_amp', F_y_amp, 'F_z_amp',
F_z_amp); %feather structure to save the amplitude at chosen time

out = struct('Fx',Fx,'Fy',Fy,'Fz',Fz, 'time', time, 'feather',
feather); %output structure

end

```

correlate.m:

```
function correlate(c, varargin)
% fn_plotVar(c, varargin) - processes unlimited number of data
structs, forms correlation graphs, exports correlation results to .xls
% c: matrix of RGB triplets, number of triplets must equal number of files
analysed
% varargin: data structs for files, can provide any number of files
% NOTE: change name of exported .xls here if processing different
dates/subjects

%-----VECTORS-----
totalFiles = nargin-1;

%Fz
Fz_Peak = []; for i = 1:totalFiles; Fz_Peak = [Fz_Peak,
varargin{i}.Fz.peak]; end
Fz_Peak_N = []; for i = 1:totalFiles; Fz_Peak_N = [Fz_Peak_N,
varargin{i}.Fz.peak_N]; end

%Fy
Fy_Peak = []; for i = 1:totalFiles; Fy_Peak = [Fy_Peak,
varargin{i}.Fy.peak]; end
Fy_Peak_N = []; for i = 1:totalFiles; Fy_Peak_N = [Fy_Peak_N,
varargin{i}.Fy.peak_N]; end

%Fx
Fx_Peak = []; for i = 1:totalFiles; Fx_Peak = [Fx_Peak,
varargin{i}.Fx.peak]; end
Fx_Peak_N = []; for i = 1:totalFiles; Fx_Peak_N = [Fx_Peak_N,
varargin{i}.Fx.peak_N]; end

%Feather
Feather_x_amp = []; for i = 1:totalFiles; Feather_x_amp = [Feather_x_amp,
varargin{i}.feather.F_x_amp]; end
Feather_y_amp = []; for i = 1:totalFiles; Feather_y_amp = [Feather_y_amp,
varargin{i}.feather.F_y_amp]; end
Feather_z_amp = []; for i = 1:totalFiles; Feather_z_amp = [Feather_z_amp,
varargin{i}.feather.F_z_amp]; end

%-----PLOT-----
t = plotFeatures(Fz_Peak_N, Feather_x_amp,c, 'Shank', 'Fz Peaks (BW)', 'Ax
Amp (g)'); %
t = [t; plotFeatures(Fx_Peak_N, Feather_y_amp,c, 'Shank', 'Fx Peaks (BW)',
'Az Amp (g)')];
t = [t; plotFeatures(Fy_Peak_N, Feather_z_amp,c, 'Shank', 'Fy Peaks (BW)',
'Ay Amp (g)')];

%-----EXPORT-----
writetable(t, '280919.xls');

end
```

plotFeatures.m:

```
function [out] = plotFeatures(x, y, c, t, xlabel, ylabel)
%plotFeat(x, y, c, t, xlabel, ylabel) - creates and saves plot of specified
data with line of linear fit, calculates rsq value
% x: x data
% y: y data
% c: colour vector
% t, xlabel, ylabel: str with title/label
% Auto-generated by MATLAB on 11-Jul-2018 13:58:27

%Create name of equal length strings for purposes of excel export
i='S'; %only shank

switch xlabel
    case 'Fz Peaks (N)'; j = 'Fz P N';
    case 'Fz Peaks (BW)'; j = 'Fz P B';

    case 'Fy Peaks (N)'; j = 'Fy P N';
    case 'Fy Peaks (BW)'; j = 'Fy P B';

    case 'Fx Peaks (N)'; j = 'Fx P N';
    case 'Fx Peaks (BW)'; j = 'Fx P B';

    case 'Ft Peaks (N)'; j = 'Ft P N';
    case 'Ft Peaks (BW)'; j = 'Ft P B';
end
switch ylabel
    case 'Ax Amp (g)'; k = 'AxAm';

    case 'Ay Amp (g)'; k = 'AyAm';

    case 'Az Amp (g)'; k = 'AzAm';

    case 'Fz Peaks (N)'; k = 'Fz P N';
    case 'Fz Peaks (BW)'; k = 'Fz P B';

    case 'Fy Peaks (N)'; k = 'Fy P N';
    case 'Fy Peaks (BW)'; k = 'Fy P B';

    case 'Fx Peaks (N)'; k = 'Fx P N';
    case 'Fx Peaks (BW)'; k = 'Fx P B';

end

name = convertCharsToStrings(strcat(i, ', ', j, ', ', k));

% Create figure
figure1 = figure('visible','off');
plotAxes = axes('Parent',figure1);
hold(plotAxes,'on');
scatterPlot = scatter(x,y,25,c,'DisplayName','data1',...
    'MarkerFaceColor','flat',...
    'MarkerEdgeColor','none');
grid on;

% Find x values for plotting the fit based on xlim
axesLimits = xlim(plotAxes);
xFit = linspace(axesLimits(1), axesLimits(2));
```

```

% Preallocate for "Show equations" coefficients
coeffs1 = cell(1,1);
% Find coefficients for polynomial (order = 1)
linearCoefficients = polyfit(x,y,1);
% Evaluate polynomial
yFit = polyval(linearCoefficients,xFit);

% Plot the fit
fitLine = plot(xFit,yFit,'DisplayName',' linear','Tag','linear',...
    'Parent',plotAxes,...
    'Color',[0.929 0.694 0.125]);

% Set new line in proper position
setLineOrder(plotAxes,fitLine,scatterPlot);
% Save type of fit for "Show equations"
fittypesArray1(1) = 2;
% Save coefficients for "Show Equation"
coeffs1{1} = linearCoefficients;
% "Show equations" was selected
showEquations(fittypesArray1,coeffs1,5,plotAxes);

% Create ylabel
ylabel({ylab},'HorizontalAlignment','center');
% Create xlabel
xlabel({xlab},'HorizontalAlignment','center');
% Create title
title({t});

%Calculate rsq
model = fitlm(x,y);
rsq = model.Rsquared.Ordinary;

% Create textbox
annotation(figure1,'textbox',...
    [0.166601145328826 0.81863091037403 0.120290322580645
    0.0275229357798166],...
    'String', strcat('Rsq = ',num2str(rsq)),...
    'FontName','Helvetica Neue',...
    'FitBoxToText','off',...
    'EdgeColor',[1 1 1]);

%Create single row table for output
m = linearCoefficients(1);
yInt = linearCoefficients(2);
out = table(name, m, yInt,rsq);

%Save figure
saveas(figure1, strcat(t,', ', xlab,', ', ylab, '.png'));

%-----MATLAB GENERATED CODE-----
%
function setLineOrder(axesh1, newLine1, associatedLine1)
%SETLINEORDER(AXESH1,NEWLIN1,ASSOCIATEDLINE1)
% Set line order
% AXESH1: axes
% NEWLIN1: new line
% ASSOCIATEDLINE1: associated line

```

```

% Get the axes children
hChildren = get(axesh1, 'Children');
% Remove the new line
hChildren(hChildren==newLine1) = [];
% Get the index to the associatedLine
lineIndex = find(hChildren==associatedLine1);
% Reorder lines so the new line appears with associated data
hNewChildren = [hChildren(1:lineIndex-
1);newLine1;hChildren(lineIndex:end)];
% Set the children:
set(axesh1, 'Children', hNewChildren);

%-----%
function showEquations(fittypes1, coeffs1, digits1, axesh1)
%SHOWEQUATIONS(FITTTYPES1,COEFFS1,DIGITS1,AXESH1)
% Show equations
% FITTTYPES1: types of fits
% COEFFS1: coefficients
% DIGITS1: number of significant digits
% AXESH1: axes

n = length(fittypes1);
txt = cell(length(n + 1) ,1);
txt{1,:} = ' ';
for i = 1:n
    txt{i + 1,:} =
getEquationString(fittypes1(i),coeffs1{i},digits1,axesh1);
end
text(.05,.95,txt, 'parent', axesh1, ...
    'verticalalignment', 'top', 'units', 'normalized');

%-----%
function [s1] = getEquationString(fittype1, coeffs1, digits1, axesh1)
%GETEQUATIONSTRING(FITTTYPE1,COEFFS1,DIGITS1,AXESH1)
% Get "Show Equation" text
% FITTTYPE1: type of fit
% COEFFS1: coefficients
% DIGITS1: number of significant digits
% AXESH1: axes

if isequal(fittype1, 0)
    s1 = 'Cubic spline interpolant';
elseif isequal(fittype1, 1)
    s1 = 'Shape-preserving interpolant';
else
    op = '+-';
    format1 = ['%s %0.', num2str(digits1), 'g*x^{%s} %s'];
    format2 = ['%s %0.', num2str(digits1), 'g'];
    xl = get(axesh1, 'xlim');
    fit = fittype1 - 1;
    s1 = sprintf('y =');
    th = text(xl* [.95;.05],1,s1, 'parent', axesh1, 'vis', 'off');
    if abs(coeffs1(1) < 0)
        s1 = [s1 ' -'];
    end
    for i = 1:fit
        s1 = length(s1);
        if ~isequal(coeffs1(i),0) % if exactly zero, skip it
            s1 = sprintf(format1,s1,abs(coeffs1(i)),num2str(fit+1-i),
op((coeffs1(i+1)<0)+1));

```

```

end
if (i==fit) && ~isequal(coeffs1(i),0)
    s1(end-5:end-2) = []; % change x^1 to x.
end
set(th, 'string', s1);
et = get(th, 'extent');
if et(1)+et(3) > xl(2)
    s1 = [s1(1:s1) sprintf('\n      ') s1(s1+1:end)];
end
end
if ~isequal(coeffs1(fit+1),0)
    s1 = length(s1);
    s1 = sprintf(format2,s1,abs(coeffs1(fit+1)));
    set(th, 'string', s1);
    et = get(th, 'extent');
    if et(1)+et(3) > xl(2)
        s1 = [s1(1:s1) sprintf('\n      ') s1(s1+1:end)];
    end
end
delete(th);
% Delete last "+"
if isequal(s1(end), '+')
    s1(end-1:end) = []; % There is always a space before the +.
end
if length(s1) == 3
    s1 = sprintf(format2,s1,0);
end
end
end

```

vector.m:

```

function out = vectors(varargin)
%fn_plotVar(c, varargin) - processes unlimited number of data structs, forms
correlation graphs, exports correlation results to .xls
% varargin: data structs for files, can provide any number of files
% NOTE: change name of exported .xls here if processing different
dates/subjects

%-----VECTORS-----

totalFiles = nargin;
%Fz
Fz_Peak = []; for i = 1:totalFiles; Fz_Peak = [Fz_Peak,
varargin{i}.Fz.peak]; end
Fz_Peak_N = []; for i = 1:totalFiles; Fz_Peak_N = [Fz_Peak_N,
varargin{i}.Fz.peak_N]; end

%Fy
Fy_Peak = []; for i = 1:totalFiles; Fy_Peak = [Fy_Peak,
varargin{i}.Fy.peak]; end
Fy_Peak_N = []; for i = 1:totalFiles; Fy_Peak_N = [Fy_Peak_N,
varargin{i}.Fy.peak_N]; end

%Fx
Fx_Peak = []; for i = 1:totalFiles; Fx_Peak = [Fx_Peak,
varargin{i}.Fx.peak]; end
Fx_Peak_N = []; for i = 1:totalFiles; Fx_Peak_N = [Fx_Peak_N,
varargin{i}.Fx.peak_N]; end

```



```

%Feather
Feather_x_amp = []; for i = 1:totalFiles; Feather_x_amp = [Feather_x_amp,
varargin{i}.feather.F_x_amp]; end
Feather_y_amp = []; for i = 1:totalFiles; Feather_y_amp = [Feather_y_amp,
varargin{i}.feather.F_y_amp]; end
Feather_z_amp = []; for i = 1:totalFiles; Feather_z_amp = [Feather_z_amp,
varargin{i}.feather.F_z_amp]; end

out = struct('Fx_Peak_N', Fx_Peak_N, 'Fy_Peak_N', Fy_Peak_N, 'Fz_Peak_N',
Fz_Peak_N, 'Feather_x_amp', Feather_x_amp, 'Feather_y_amp', Feather_y_amp,
'Feather_z_amp', Feather_z_amp);

end

```

tabulate.m:

```

function tabulate(varargin)

%-----VECTORS-----

totalFiles = nargin;

%Fz
Fz_Peak_N = []; for i = 1:totalFiles; Fz_Peak_N = [Fz_Peak_N,
varargin{i}.Fz.peak_N]; end

%Fy
Fy_Peak_N = []; for i = 1:totalFiles; Fy_Peak_N = [Fy_Peak_N,
varargin{i}.Fy.peak_N]; end

%Fx
Fx_Peak_N = []; for i = 1:totalFiles; Fx_Peak_N = [Fx_Peak_N,
varargin{i}.Fx.peak_N]; end

%Feather
Feather_x_amp = []; for i = 1:totalFiles; Feather_x_amp = [Feather_x_amp,
varargin{i}.feather.F_x_amp]; end
Feather_y_amp = []; for i = 1:totalFiles; Feather_y_amp = [Feather_y_amp,
varargin{i}.feather.F_y_amp]; end
Feather_z_amp = []; for i = 1:totalFiles; Feather_z_amp = [Feather_z_amp,
varargin{i}.feather.F_z_amp]; end

t = table(Fx_Peak_N.', Fy_Peak_N.', Fz_Peak_N.', Feather_x_amp.',
Feather_y_amp.', Feather_z_amp. ');
writetable(t, 'variables_tb.xls');

end

```

Appendix M: Combined Analysis MATLAB Script: Scatter

This section contains the MATLAB scripts for combined data analysis. Due to limitations of *scatter* function not accepting different markers for different participants, each data points were graphed individually into the same plot.

main.m:

```
%Structs must be saved for individual participants prior to the execution
of this code. Structs could be saved by right click->save as to this folder
%directory upon execution of individual analysis, or saved through code.

%Load relevant file and structs
file = xlsread('summary_data.xls'); %This was created manually with each
struct data

P1 = load('P1.mat');
P2 = load('P2.mat');
P3 = load('P3.mat');

%-----SUMMARY VECTORS-----

% For graphing all participant dataset on a scatter plot with different
% colours and shape. Scatter cannot take multiple different marker types,
% hence cannot pass an array like colour. Instead, each value pairs must be
passed and graphed individually

%Extract peak forces and acceleration amplitudes
Fx_Peak_N = file(:,1);
Fy_Peak_N = file(:,2);
Fz_Peak_N = file(:,3);

Feather_x_amp = file(:,4);
Feather_y_amp = file(:,5);
Feather_z_amp = file(:,6);

red = [204 0 0]; orange = [255 128 0]; yellow = [204 204 0]; green = [102
204 0]; cyan = [0 255 255]; blue = [0 0 255]; purple = [127 0 255]; magenta
= [255 0 127]; black = [0 0 0]; pink = [255 102 255]; grey = [160 160 160];

%Create a colour struct with each movement
c = 1/255*[red; red;red; red;red; red;red;
red;orange;orange;orange;orange;orange;orange;orange;yellow;yellow;yellow;y
ellow;yellow;yellow;yellow;yellow;yellow; green;
green;green;green;green;green;green;green; cyan;
cyan;cyan;cyan;cyan;cyan;cyan;cyan;cyan; blue;
blue;blue;blue;blue;blue;blue;blue; purple;
purple;purple;purple;purple;purple;purple;
magenta;magenta;magenta;magenta;magenta;magenta;magenta;magenta;magenta;
black; black;black;black;black;black;black;black;black;
pink;pink;pink;pink;pink;pink;pink; grey;
grey;grey;grey;grey;grey;grey;grey;grey; ];

%Plot data in individual graphs for x, y and z axis acceleration
amplitudes
t = plotFeatures(Fz_Peak_N, Feather_x_amp,c, 'VGRF and IS Shank
Acceleration', 'Fz Peaks (BW)', 'Ax Amp (g)');
```

```

t = [t; plotFeatures(Fx_Peak_N, Feather_y_amp,c, 'BF and ML Shank
Acceleration', 'Fx Peaks (BW)', 'Az Amp (g)')];
t = [t; plotFeatures(Fy_Peak_N, Feather_z_amp,c, 'Shank', 'Fy Peaks (BW)',
' Ay Amp (g)')];

%walk
walk1p1f=Fz_Peak_N(16,1); walk1p1a=Feather_x_amp(16,1);
walk2p1f=Fz_Peak_N(17,1);walk2p1a=Feather_x_amp(17,1);walk3p1f=Fz_Peak_N(18
,1);walk3p1a=Feather_x_amp(18,1);
walk1p2f=Fz_Peak_N(19,1); walk1p2a=Feather_x_amp(19,1);
walk2p2f=Fz_Peak_N(20,1);walk2p2a=Feather_x_amp(20,1);walk3p2f=Fz_Peak_N(21
,1);walk3p2a=Feather_x_amp(21,1);
walk1p3f=Fz_Peak_N(22,1); walk1p3a=Feather_x_amp(22,1);
walk2p3f=Fz_Peak_N(23,1);walk2p3a=Feather_x_amp(23,1);walk3p3f=Fz_Peak_N(24
,1);walk3p3a=Feather_x_amp(24,1);

%shuffle
shu1p1f=Fz_Peak_N(9,1); shu1p1a=Feather_x_amp(9,1);
shu2p1f=Fz_Peak_N(10,1);shu2p1a=Feather_x_amp(10,1);shu3p1f=Fz_Peak_N(11,1)
;shu3p1a=Feather_x_amp(11,1);
shu1p2f=Fz_Peak_N(12,1); shu1p2a=Feather_x_amp(12,1);
shu1p3f=Fz_Peak_N(13,1); shu1p3a=Feather_x_amp(13,1);
shu2p3f=Fz_Peak_N(14,1);shu2p3a=Feather_x_amp(14,1);shu3p3f=Fz_Peak_N(15,1)
;shu3p3a=Feather_x_amp(15,1);

%jog
jog1p1f=Fz_Peak_N(25,1); jog1p1a=Feather_x_amp(25,1);
jog2p1f=Fz_Peak_N(26,1);jog2p1a=Feather_x_amp(26,1);jog3p1f=Fz_Peak_N(27,1)
;jog3p1a=Feather_x_amp(27,1);
jog1p2f=Fz_Peak_N(28,1); jog1p2a=Feather_x_amp(28,1);
jog2p2f=Fz_Peak_N(29,1);jog2p2a=Feather_x_amp(29,1);
jog1p3f=Fz_Peak_N(30,1); jog1p3a=Feather_x_amp(30,1);
jog2p3f=Fz_Peak_N(31,1);jog2p3a=Feather_x_amp(31,1);jog3p3f=Fz_Peak_N(32,1)
;jog3p3a=Feather_x_amp(32,1);

%run
run1p1f=Fz_Peak_N(33,1); run1p1a=Feather_x_amp(33,1);
run2p1f=Fz_Peak_N(34,1);run2p1a=Feather_x_amp(34,1);run3p1f=Fz_Peak_N(35,1)
;run3p1a=Feather_x_amp(35,1);
run1p2f=Fz_Peak_N(36,1); run1p2a=Feather_x_amp(36,1);
run2p2f=Fz_Peak_N(37,1);run2p2a=Feather_x_amp(37,1);run3p2f=Fz_Peak_N(38,1)
;run3p2a=Feather_x_amp(38,1);
run1p3f=Fz_Peak_N(39,1); run1p3a=Feather_x_amp(39,1);
run2p3f=Fz_Peak_N(40,1);run2p3a=Feather_x_amp(40,1);run3p3f=Fz_Peak_N(41,1)
;run3p3a=Feather_x_amp(42,1);

%sprint
spr1p1f=Fz_Peak_N(42,1); spr1p1a=Feather_x_amp(42,1);
spr2p1f=Fz_Peak_N(43,1);spr2p1a=Feather_x_amp(43,1);spr3p1f=Fz_Peak_N(44,1)
;spr3p1a=Feather_x_amp(44,1);
spr1p2f=Fz_Peak_N(45,1); spr1p2a=Feather_x_amp(45,1);
spr2p2f=Fz_Peak_N(46,1);spr2p2a=Feather_x_amp(46,1);
spr1p3f=Fz_Peak_N(47,1); spr1p3a=Feather_x_amp(47,1);
spr2p3f=Fz_Peak_N(48,1);spr2p3a=Feather_x_amp(48,1);spr3p3f=Fz_Peak_N(49,1)
;spr3p3a=Feather_x_amp(49,1);

```

%jump

```

jmp1p1f=Fz_Peak_N(50,1); jmp1p1a=Feather_x_amp(50,1);
jmp2p1f=Fz_Peak_N(51,1); jmp2p1a=Feather_x_amp(51,1); jmp3p1f=Fz_Peak_N(52,1)
; jmp3p1a=Feather_x_amp(52,1);
jmp1p2f=Fz_Peak_N(53,1); jmp1p2a=Feather_x_amp(53,1);
jmp2p2f=Fz_Peak_N(54,1); jmp2p2a=Feather_x_amp(54,1);
jmp1p3f=Fz_Peak_N(55,1); jmp1p3a=Feather_x_amp(55,1);
jmp2p3f=Fz_Peak_N(56,1); jmp2p3a=Feather_x_amp(56,1);

```

%RO

```

ro1p1f=Fz_Peak_N(57,1); ro1p1a=Feather_x_amp(57,1);
ro2p1f=Fz_Peak_N(58,1); ro2p1a=Feather_x_amp(58,1); ro3p1f=Fz_Peak_N(59,1); ro
3p1a=Feather_x_amp(59,1);
ro1p2f=Fz_Peak_N(60,1); ro1p2a=Feather_x_amp(60,1);
ro2p2f=Fz_Peak_N(61,1); ro2p2a=Feather_x_amp(61,1); ro3p2f=Fz_Peak_N(62,1); ro
3p2a=Feather_x_amp(62,1);
ro1p3f=Fz_Peak_N(63,1); ro1p3a=Feather_x_amp(63,1);
ro2p3f=Fz_Peak_N(64,1); ro2p3a=Feather_x_amp(64,1); ro3p3f=Fz_Peak_N(65,1); ro
3p3a=Feather_x_amp(65,1);

```

%F2

```

f21p1f=Fz_Peak_N(66,1); f21p1a=Feather_x_amp(66,1);
f22p1f=Fz_Peak_N(67,1); f22p1a=Feather_x_amp(67,1); f23p1f=Fz_Peak_N(68,1); f2
3p1a=Feather_x_amp(68,1);
f21p2f=Fz_Peak_N(69,1); f21p2a=Feather_x_amp(69,1);
f22p2f=Fz_Peak_N(70,1); f22p2a=Feather_x_amp(70,1); f23p2f=Fz_Peak_N(71,1); f2
3p2a=Feather_x_amp(71,1);
f21p3f=Fz_Peak_N(72,1); f21p3a=Feather_x_amp(72,1);
f22p3f=Fz_Peak_N(73,1); f22p3a=Feather_x_amp(73,1); f23p3f=Fz_Peak_N(74,1); f2
3p3a=Feather_x_amp(74,1);

```

%Cut

```

cut1p1f=Fz_Peak_N(82,1); cut1p1a=Feather_x_amp(82,1);
cut2p1f=Fz_Peak_N(83,1); cut2p1a=Feather_x_amp(83,1); cut3p1f=Fz_Peak_N(84,1)
; cut3p1a=Feather_x_amp(84,1);
cut1p2f=Fz_Peak_N(85,1); cut1p2a=Feather_x_amp(85,1);
cut2p2f=Fz_Peak_N(86,1); cut2p2a=Feather_x_amp(86,1); cut3p2f=Fz_Peak_N(87,1)
; cut3p2a=Feather_x_amp(87,1);
cut1p3f=Fz_Peak_N(88,1); cut1p3a=Feather_x_amp(88,1);
cut2p3f=Fz_Peak_N(89,1); cut2p3a=Feather_x_amp(89,1); cut3p3f=Fz_Peak_N(90,1)
; cut3p3a=Feather_x_amp(90,1);

```

%step 440

```

step1p1f=Fz_Peak_N(1,1); step1p1a=Feather_x_amp(1,1);
step2p1f=Fz_Peak_N(2,1); step2p1a=Feather_x_amp(2,1); step3p1f=Fz_Peak_N(3,1)
; step3p1a=Feather_x_amp(3,1);
step1p2f=Fz_Peak_N(4,1); step1p2a=Feather_x_amp(4,1);
step2p2f=Fz_Peak_N(5,1); step2p2a=Feather_x_amp(5,1); step3p2f=Fz_Peak_N(6,1)
; step3p2a=Feather_x_amp(6,1);
step1p3f=Fz_Peak_N(7,1); step1p3a=Feather_x_amp(7,1);
step2p3f=Fz_Peak_N(8,1); step2p3a=Feather_x_amp(8,1);

```

%Pivot

```

pvt1p1f=Fz_Peak_N(75,1); pvt1p1a=Feather_x_amp(75,1);
pvt2p1f=Fz_Peak_N(76,1); pvt2p1a=Feather_x_amp(76,1);
pvt1p2f=Fz_Peak_N(77,1); pvt1p2a=Feather_x_amp(77,1);
pvt2p2f=Fz_Peak_N(78,1); pvt2p2a=Feather_x_amp(78,1);
pvt1p3f=Fz_Peak_N(79,1); pvt1p3a=Feather_x_amp(79,1);
pvt2p3f=Fz_Peak_N(80,1); pvt2p3a=Feather_x_amp(80,1); pvt3p3f=Fz_Peak_N(81,1)
; pvt3p3a=Feather_x_amp(81,1);

```

```

%Create a combined graph
createfigure( walk1p1f, walk1p1a, shulp1f,shulp1a, jog1p1f, jog1p1a,
run1p1f, run1p1a,spr1p1f, spr1p1a,jmp1p1f, jmp1p1a, rolp1f,
rolp1a,f21p1f,f21p1a, cut1p1f,cut1p1a,step1p1f, step1p1a,
pvt1p1f,pvt1p1a,...
    walk1p2f, walk1p2a, shulp2f,shulp2a, jog1p2f, jog1p2a, run1p2f,
run1p2a,spr1p2f, spr1p2a,jmp1p2f, jmp1p2a, rolp2f, rolp2a,f21p2f,f21p2a,
cut1p2f,cut1p2a,step1p2f, step1p2a, pvt1p2f,pvt1p2a,...
    walk1p3f, walk1p3a, shulp3f,shulp3a, jog1p3f, jog1p3a, run1p3f,
run1p3a,spr1p3f, spr1p3a,jmp1p3f, jmp1p3a, rolp3f, rolp3a,f21p3f,f21p3a,
cut1p3f,cut1p3a,step1p3f, step1p3a, pvt1p3f,pvt1p3a,...
    walk2p1f, walk2p1a, shu2p1f,shu2p1a, jog2p1f, jog2p1a, run2p1f,
run2p1a,spr2p1f, spr2p1a,jmp2p1f, jmp2p1a, ro2p1f, ro2p1a,f22p1f,f22p1a,
cut2p1f,cut2p1a,step2p1f, step2p1a, pvt2p1f,pvt2p1a,...
    walk2p2f, walk2p2a, jog2p2f, jog2p2a, run2p2f, run2p2a,spr2p2f,
spr2p2a,jmp2p2f, jmp2p2a, ro2p2f, ro2p2a,f22p2f,f22p2a,
cut2p2f,cut2p2a,step2p2f, step2p2a, pvt2p2f,pvt2p2a,...
    walk2p3f, walk2p3a, shu2p3f,shu2p3a, jog2p3f, jog2p3a, run2p3f,
run2p3a,spr2p3f, spr2p3a,jmp2p3f, jmp2p3a, ro2p3f, ro2p3a,f22p3f,f22p3a,
cut2p3f,cut2p3a,step2p3f, step2p3a, pvt2p3f,pvt2p3a,...
    walk3p1f, walk3p1a, shu3p1f,shu3p1a, jog3p1f, jog3p1a, run3p1f,
run3p1a,spr3p1f, spr3p1a,jmp3p1f, jmp3p1a, ro3p1f, ro3p1a,f23p1f,f23p1a,
cut3p1f,cut3p1a,step3p1f, step3p1a,...
    walk3p2f, walk3p2a, run3p2f, run3p2a, ro3p2f, ro3p2a,f23p2f,f23p2a,
cut3p2f,cut3p2a,step2p2f, step2p2a,...
    walk3p3f, walk3p3a, shu3p3f,shu3p3a, jog3p3f, jog3p3a, run3p3f,
run3p3a,spr3p3f, spr3p3a, ro3p3f, ro2p3a,f23p3f,f23p3a, cut3p3f,cut3p3a,
pvt3p3f,pvt3p3a,...
    Fz_Peak_N, Feather_x_amp);

```

createfigure.m:

```

function createfigure(R1, R2, R3,R4,R5, R6,R7, R8, R9,
R10,R11,R12,R13,R14,R15,
R16,R17,R18,R19,R20,R21,R22,R23,R24,R25,R26,R27,R28,R29,R30,R31,R32,R33,R34
,R35,R36,R37,R38,R39,R40,R41,R42,R43,R44,R45,R46,R47,R48,R49,R50,R51,R52,R5
3,R54,R55,R56,R57,R58,R59,R60,R61,R62,R63,R64,R65,R66,R67,R68,R69,R70,R71,R
72,R73,R74,R75,R76,R77,R78,R79,R80,R81,R82,R83,R84,R85,R86,R87,R88,R89,R90,
R91,R92,R93,R94,R95,R96,R97,R98,R99,R100,R101,R102,R103,R104,R105,R106,R107
,R108,R109,R110,R111,R112,R113,R114,R115,R116,R117,R118 ,R119,R120,R121
,R122,R123,
R124,R125,R126,R127,R128,R129,R130,R131,R132,R133,R134,R135,R136,R137,R138,
R139,R140,R141,R142,R143,R144,R145,R146,R147,R148,R149,R150,R151,R152,R153,
R154,R155,R156,R157,R158,R159 ,R160,R161,R162 ,R163,R164,R165
,R166,R167,R168,R169,R170,R171,R172,R173,R174,R175,R176,R177,R178,R179,R180
, Fz_Peak_N, Feather_x_amp);

```

```

%Create a combined scatter plot with different markers and colours for all
%individuals

```

```

% Create figure
figure1 = figure;

```

```

% Create axes
axes1 = axes('Parent',figure1);
hold(axes1,'on');

```

```

% Create scatter
scatter(R1,R2,'DisplayName','P1 walk',...
'MarkerFaceColor',[1 0.843137264251709 0],...
'MarkerEdgeColor',[1 0.843137264251709 0]);

```

```

% Create scatter
scatter(R3,R4,'DisplayName','P1_shuffle',...
    'MarkerFaceColor',[0.4666666668653488 0.674509823322296
0.18823529779911],...
    'MarkerEdgeColor',[0.4666666668653488 0.674509823322296
0.18823529779911]);

% Create scatter
scatter(R5,R6,'DisplayName','P1_jog','MarkerFaceColor',[0 1 1],...
    'MarkerEdgeColor',[0 1 1]);

% Create scatter
scatter(R7,R8,'DisplayName','P1_run','MarkerFaceColor',[0 0 1],...
    'MarkerEdgeColor',[0 0 1]);

% Create scatter
scatter(R9,R10,'DisplayName','P1_sprint',...
    'MarkerFaceColor',[0.494117647409439 0.184313729405403
0.556862771511078],...
    'MarkerEdgeColor',[0.494117647409439 0.184313729405403
0.556862771511078]);

% Create scatter
scatter(R11,R12,'DisplayName','P1_jump',...
    'MarkerFaceColor',[1 0.600000023841858 0.7843137383461],...
    'MarkerEdgeColor',[1 0.600000023841858 0.7843137383461]);

% Create scatter
scatter(R13,R14,'DisplayName','P1_RO','MarkerFaceColor',[1 0 1],...
    'MarkerEdgeColor',[1 0 1]);

% Create scatter
scatter(R15,R16,'DisplayName','P1_F2','MarkerFaceColor',[0 0 0],...
    'MarkerEdgeColor',[0 0 0]);

% Create scatter
scatter(R17,R18,'DisplayName','P1_cut',...
    'MarkerFaceColor',[0.501960813999176 0.501960813999176
0.501960813999176],...
    'MarkerEdgeColor',[0.501960813999176 0.501960813999176
0.501960813999176]);

% Create scatter
scatter(R19,R20,'DisplayName','P1_step440','MarkerFaceColor',[1 0 0],...
    'MarkerEdgeColor',[1 0 0]);

% Create scatter
scatter(R21,R22,'DisplayName','P1_Pivot',...
    'MarkerFaceColor',[0.87058824300766 0.490196079015732 0],...
    'MarkerEdgeColor',[0.87058824300766 0.490196079015732 0]);

%P2
% Create scatter
scatter(R23,R24,'DisplayName','P2_walk',...
    'MarkerFaceColor',[1 0.843137264251709 0],...
    'MarkerEdgeColor',[1 0.843137264251709 0],...
    'Marker','x');

% Create scatter

```

```

scatter(R25,R26,'DisplayName','P2 shuffle',...
    'MarkerFaceColor',[0.466666668653488 0.674509823322296
0.18823529779911],...
    'MarkerEdgeColor',[0.466666668653488 0.674509823322296
0.18823529779911],...
    'Marker','x');

% Create scatter
scatter(R27,R28,'DisplayName','P2 jog','MarkerFaceColor',[0 1 1],...
    'MarkerEdgeColor',[0 1 1],...
    'Marker','x');

% Create scatter
scatter(R29,R30,'DisplayName','P2 run','MarkerFaceColor',[0 0 1],...
    'MarkerEdgeColor',[0 0 1],...
    'Marker','x');

% Create scatter
scatter(R31,R32,'DisplayName','P2 sprint',...
    'MarkerFaceColor',[0.494117647409439 0.184313729405403
0.556862771511078],...
    'MarkerEdgeColor',[0.494117647409439 0.184313729405403
0.556862771511078],...
    'Marker','x');

% Create scatter
scatter(R33,R34,'DisplayName','P2 jump',...
    'MarkerFaceColor',[1 0.600000023841858 0.7843137383461],...
    'MarkerEdgeColor',[1 0.600000023841858 0.7843137383461],...
    'Marker','x');

% Create scatter
scatter(R35,R36,'DisplayName','P2 RO','MarkerFaceColor',[1 0 1],...
    'MarkerEdgeColor',[1 0 1],...
    'Marker','x');

% Create scatter
scatter(R37,R38,'DisplayName','P2 F2','MarkerFaceColor',[0 0 0],...
    'MarkerEdgeColor',[0 0 0],...
    'Marker','x');

% Create scatter
scatter(R39,R40,'DisplayName','P2 cut',...
    'MarkerFaceColor',[0.501960813999176 0.501960813999176
0.501960813999176],...
    'MarkerEdgeColor',[0.501960813999176 0.501960813999176
0.501960813999176],...
    'Marker','x');

% Create scatter
scatter(R41,R42,'DisplayName','P2 step440','MarkerFaceColor',[1 0 0],...
    'MarkerEdgeColor',[1 0 0],...
    'Marker','x');

% Create scatter
scatter(R43,R44,'DisplayName','P2 Pivot',...
    'MarkerFaceColor',[0.87058824300766 0.490196079015732 0],...
    'MarkerEdgeColor',[0.87058824300766 0.490196079015732 0],...
    'Marker','x');

```

```

%P3
% Create scatter
scatter(R45,R46,'DisplayName','P3 walk',...
        'MarkerFaceColor',[1 0.843137264251709 0],...
        'MarkerEdgeColor',[1 0.843137264251709 0],...
        'Marker','v');

% Create scatter
scatter(R47,R48,'DisplayName','P3 shuffle',...
        'MarkerFaceColor',[0.4666666668653488 0.674509823322296
0.18823529779911],...
        'MarkerEdgeColor',[0.4666666668653488 0.674509823322296
0.18823529779911],...
        'Marker','v');

% Create scatter
scatter(R49,R50,'DisplayName','P3 jog','MarkerFaceColor',[0 1 1],...
        'MarkerEdgeColor',[0 1 1],...
        'Marker','v');

% Create scatter
scatter(R51,R52,'DisplayName','P3 run','MarkerFaceColor',[0 0 1],...
        'MarkerEdgeColor',[0 0 1],...
        'Marker','v');

% Create scatter
scatter(R53,R54,'DisplayName','P3 sprint',...
        'MarkerFaceColor',[0.494117647409439 0.184313729405403
0.556862771511078],...
        'MarkerEdgeColor',[0.494117647409439 0.184313729405403
0.556862771511078],...
        'Marker','v');

% Create scatter
scatter(R55,R56,'DisplayName','P3 jump',...
        'MarkerFaceColor',[1 0.600000023841858 0.7843137383461],...
        'MarkerEdgeColor',[1 0.600000023841858 0.7843137383461],...
        'Marker','v');

% Create scatter
scatter(R57,R58,'DisplayName','P3 RO','MarkerFaceColor',[1 0 1],...
        'MarkerEdgeColor',[1 0 1],...
        'Marker','v');

% Create scatter
scatter(R59,R60,'DisplayName','P3 F2','MarkerFaceColor',[0 0 0],...
        'MarkerEdgeColor',[0 0 0],...
        'Marker','v');

% Create scatter
scatter(R61,R62,'DisplayName','P3 cut',...
        'MarkerFaceColor',[0.501960813999176 0.501960813999176
0.501960813999176],...
        'MarkerEdgeColor',[0.501960813999176 0.501960813999176
0.501960813999176],...
        'Marker','v');

% Create scatter
scatter(R63,R64,'DisplayName','P3 step440','MarkerFaceColor',[1 0 0],...

```



```

    'MarkerEdgeColor',[1 0 0],...
    'Marker','v');

% Create scatter
scatter(R65,R66,'DisplayName','P3 Pivot',...
    'MarkerFaceColor',[0.87058824300766 0.490196079015732 0],...
    'MarkerEdgeColor',[0.87058824300766 0.490196079015732 0],...
    'Marker','v');

%OTHER TRIAL DATA
% Create scatter
scatter(R67,R68,'DisplayName','P1 walk',...
    'MarkerFaceColor',[1 0.843137264251709 0],...
    'MarkerEdgeColor',[1 0.843137264251709 0]);

% Create scatter
scatter(R69,R70,'DisplayName','P1 shuffle',...
    'MarkerFaceColor',[0.4666666668653488 0.674509823322296
0.18823529779911],...
    'MarkerEdgeColor',[0.4666666668653488 0.674509823322296
0.18823529779911]);

% Create scatter
scatter(R71,R72,'DisplayName','P1 jog','MarkerFaceColor',[0 1 1],...
    'MarkerEdgeColor',[0 1 1]);

% Create scatter
scatter(R73,R74,'DisplayName','P1 run','MarkerFaceColor',[0 0 1],...
    'MarkerEdgeColor',[0 0 1]);

% Create scatter
scatter(R75,R76,'DisplayName','P1 sprint',...
    'MarkerFaceColor',[0.494117647409439 0.184313729405403
0.556862771511078],...
    'MarkerEdgeColor',[0.494117647409439 0.184313729405403
0.556862771511078]);

% Create scatter
scatter(R77,R78,'DisplayName','P1 jump',...
    'MarkerFaceColor',[1 0.600000023841858 0.7843137383461],...
    'MarkerEdgeColor',[1 0.600000023841858 0.7843137383461]);

% Create scatter
scatter(R79,R80,'DisplayName','P1 RO','MarkerFaceColor',[1 0 1],...
    'MarkerEdgeColor',[1 0 1]);

% Create scatter
scatter(R81,R82,'DisplayName','P1 F2','MarkerFaceColor',[0 0 0],...
    'MarkerEdgeColor',[0 0 0]);

% Create scatter
scatter(R83,R84,'DisplayName','P1 cut',...
    'MarkerFaceColor',[0.501960813999176 0.501960813999176
0.501960813999176],...
    'MarkerEdgeColor',[0.501960813999176 0.501960813999176
0.501960813999176]);

% Create scatter

```

```

scatter(R85,R86,'DisplayName','P1_step440','MarkerFaceColor',[1 0 0],...
    'MarkerEdgeColor',[1 0 0]);

% Create scatter
scatter(R87,R88,'DisplayName','P1 Pivot',...
    'MarkerFaceColor',[0.87058824300766 0.490196079015732 0],...
    'MarkerEdgeColor',[0.87058824300766 0.490196079015732 0]);

%P2
% Create scatter
scatter(R89,R90,'DisplayName','P2 walk',...
    'MarkerFaceColor',[1 0.843137264251709 0],...
    'MarkerEdgeColor',[1 0.843137264251709 0],...
    'Marker','x');

% Create scatter
scatter(R91,R92,'DisplayName','P2 jog','MarkerFaceColor',[0 1 1],...
    'MarkerEdgeColor',[0 1 1],...
    'Marker','x');

% Create scatter
scatter(R93,R94,'DisplayName','P2 run','MarkerFaceColor',[0 0 1],...
    'MarkerEdgeColor',[0 0 1],...
    'Marker','x');

% Create scatter
scatter(R95,R96,'DisplayName','P2 sprint',...
    'MarkerFaceColor',[0.494117647409439 0.184313729405403
0.556862771511078],...
    'MarkerEdgeColor',[0.494117647409439 0.184313729405403
0.556862771511078],...
    'Marker','x');

% Create scatter
scatter(R97,R98,'DisplayName','P2 jump',...
    'MarkerFaceColor',[1 0.600000023841858 0.7843137383461],...
    'MarkerEdgeColor',[1 0.600000023841858 0.7843137383461],...
    'Marker','x');

% Create scatter
scatter(R99,R100,'DisplayName','P2 RO','MarkerFaceColor',[1 0 1],...
    'MarkerEdgeColor',[1 0 1],...
    'Marker','x');

% Create scatter
scatter(R101,R102,'DisplayName','P2 F2','MarkerFaceColor',[0 0 0],...
    'MarkerEdgeColor',[0 0 0],...
    'Marker','x');

% Create scatter
scatter(R103,R104,'DisplayName','P2 cut',...
    'MarkerFaceColor',[0.501960813999176 0.501960813999176
0.501960813999176],...
    'MarkerEdgeColor',[0.501960813999176 0.501960813999176
0.501960813999176],...
    'Marker','x');

% Create scatter
scatter(R105,R106,'DisplayName','P2_step440','MarkerFaceColor',[1 0 0],...

```

```

    'MarkerEdgeColor',[1 0 0],...
    'Marker','x');

% Create scatter
scatter(R107,R108,'DisplayName','P2 Pivot',...
    'MarkerFaceColor',[0.87058824300766 0.490196079015732 0],...
    'MarkerEdgeColor',[0.87058824300766 0.490196079015732 0],...
    'Marker','x');

%P3
% Create scatter
scatter(R109,R110,'DisplayName','P3 walk',...
    'MarkerFaceColor',[1 0.843137264251709 0],...
    'MarkerEdgeColor',[1 0.843137264251709 0],...
    'Marker','v');

% Create scatter
scatter(R111,R112,'DisplayName','P3 shuffle',...
    'MarkerFaceColor',[0.4666666668653488 0.674509823322296
0.18823529779911],...
    'MarkerEdgeColor',[0.4666666668653488 0.674509823322296
0.18823529779911],...
    'Marker','v');

% Create scatter
scatter(R113,R114,'DisplayName','P3 jog','MarkerFaceColor',[0 1 1],...
    'MarkerEdgeColor',[0 1 1],...
    'Marker','v');

% Create scatter
scatter(R115,R116,'DisplayName','P3 run','MarkerFaceColor',[0 0 1],...
    'MarkerEdgeColor',[0 0 1],...
    'Marker','v');

% Create scatter
scatter(R117,R118,'DisplayName','P3 sprint',...
    'MarkerFaceColor',[0.494117647409439 0.184313729405403
0.556862771511078],...
    'MarkerEdgeColor',[0.494117647409439 0.184313729405403
0.556862771511078],...
    'Marker','v');

% Create scatter
scatter(R119,R120,'DisplayName','P3 jump',...
    'MarkerFaceColor',[1 0.600000023841858 0.7843137383461],...
    'MarkerEdgeColor',[1 0.600000023841858 0.7843137383461],...
    'Marker','v');

% Create scatter
scatter(R121,R122,'DisplayName','P3 RO','MarkerFaceColor',[1 0 1],...
    'MarkerEdgeColor',[1 0 1],...
    'Marker','v');

% Create scatter
scatter(R123,R124,'DisplayName','P3 F2','MarkerFaceColor',[0 0 0],...
    'MarkerEdgeColor',[0 0 0],...
    'Marker','v');

% Create scatter

```

```

scatter(R125,R126,'DisplayName','P3 cut',...
    'MarkerFaceColor',[0.501960813999176 0.501960813999176
0.501960813999176],...
    'MarkerEdgeColor',[0.501960813999176 0.501960813999176
0.501960813999176],...
    'Marker','v');

% Create scatter
scatter(R127,R128,'DisplayName','P3 step440','MarkerFaceColor',[1 0 0],...
    'MarkerEdgeColor',[1 0 0],...
    'Marker','v');

% Create scatter
scatter(R129,R130,'DisplayName','P3 Pivot',...
    'MarkerFaceColor',[0.87058824300766 0.490196079015732 0],...
    'MarkerEdgeColor',[0.87058824300766 0.490196079015732 0],...
    'Marker','v');

%FINAL TRIAL DATA
scatter(R131,R132,'DisplayName','P1 walk',...
    'MarkerFaceColor',[1 0.843137264251709 0],...
    'MarkerEdgeColor',[1 0.843137264251709 0]);

% Create scatter
scatter(R133,R134,'DisplayName','P1 shuffle',...
    'MarkerFaceColor',[0.4666666668653488 0.674509823322296
0.18823529779911],...
    'MarkerEdgeColor',[0.4666666668653488 0.674509823322296
0.18823529779911]);

% Create scatter
scatter(R135,R136,'DisplayName','P1 jog','MarkerFaceColor',[0 1 1],...
    'MarkerEdgeColor',[0 1 1]);

% Create scatter
scatter(R137,R138,'DisplayName','P1 run','MarkerFaceColor',[0 0 1],...
    'MarkerEdgeColor',[0 0 1]);

% Create scatter
scatter(R139,R140,'DisplayName','P1 sprint',...
    'MarkerFaceColor',[0.494117647409439 0.184313729405403
0.556862771511078],...
    'MarkerEdgeColor',[0.494117647409439 0.184313729405403
0.556862771511078]);

% Create scatter
scatter(R141,R142,'DisplayName','P1 jump',...
    'MarkerFaceColor',[1 0.600000023841858 0.7843137383461],...
    'MarkerEdgeColor',[1 0.600000023841858 0.7843137383461]);

% Create scatter
scatter(R143,R144,'DisplayName','P1 RO','MarkerFaceColor',[1 0 1],...
    'MarkerEdgeColor',[1 0 1]);

% Create scatter
scatter(R145,R146,'DisplayName','P1 F2','MarkerFaceColor',[0 0 0],...
    'MarkerEdgeColor',[0 0 0]);

```

```

% Create scatter
scatter(R147,R148,'DisplayName','P1 cut',...
    'MarkerFaceColor',[0.501960813999176 0.501960813999176
0.501960813999176],...
    'MarkerEdgeColor',[0.501960813999176 0.501960813999176
0.501960813999176]);

% Create scatter
scatter(R149,R150,'DisplayName','P1 step440','MarkerFaceColor',[1 0 0],...
    'MarkerEdgeColor',[1 0 0]);

%P2
% Create scatter
scatter(R151,R152,'DisplayName','P2 walk',...
    'MarkerFaceColor',[1 0.843137264251709 0],...
    'MarkerEdgeColor',[1 0.843137264251709 0],...
    'Marker','x');

% Create scatter
scatter(R153,R154,'DisplayName','P2 run','MarkerFaceColor',[0 0 1],...
    'MarkerEdgeColor',[0 0 1],...
    'Marker','x');

% Create scatter
scatter(R155,R156,'DisplayName','P2 RO','MarkerFaceColor',[1 0 1],...
    'MarkerEdgeColor',[1 0 1],...
    'Marker','x');

% Create scatter
scatter(R157,R158,'DisplayName','P2 F2','MarkerFaceColor',[0 0 0],...
    'MarkerEdgeColor',[0 0 0],...
    'Marker','x');

% Create scatter
scatter(R159,R160,'DisplayName','P2 cut',...
    'MarkerFaceColor',[0.501960813999176 0.501960813999176
0.501960813999176],...
    'MarkerEdgeColor',[0.501960813999176 0.501960813999176
0.501960813999176],...
    'Marker','x');

% Create scatter
scatter(R161,R162,'DisplayName','P2 step440','MarkerFaceColor',[1 0 0],...
    'MarkerEdgeColor',[1 0 0],...
    'Marker','x');

%P3
% Create scatter
scatter(R163,R164,'DisplayName','P3 walk',...
    'MarkerFaceColor',[1 0.843137264251709 0],...
    'MarkerEdgeColor',[1 0.843137264251709 0],...
    'Marker','v');

% Create scatter
scatter(R165,R166,'DisplayName','P3 shuffle',...
    'MarkerFaceColor',[0.4666666668653488 0.674509823322296
0.18823529779911],...

```

```

    'MarkerEdgeColor',[0.4666666668653488 0.674509823322296
0.18823529779911],...
    'Marker','v');

% Create scatter
scatter(R167,R168,'DisplayName','P3 jog','MarkerFaceColor',[0 1 1],...
    'MarkerEdgeColor',[0 1 1],...
    'Marker','v');

% Create scatter
scatter(R169,R170,'DisplayName','P3 run','MarkerFaceColor',[0 0 1],...
    'MarkerEdgeColor',[0 0 1],...
    'Marker','v');

% Create scatter
scatter(R171,R172,'DisplayName','P3 sprint',...
    'MarkerFaceColor',[0.494117647409439 0.184313729405403
0.556862771511078],...
    'MarkerEdgeColor',[0.494117647409439 0.184313729405403
0.556862771511078],...
    'Marker','v');

% Create scatter
scatter(R173,R174,'DisplayName','P3 RO','MarkerFaceColor',[1 0 1],...
    'MarkerEdgeColor',[1 0 1],...
    'Marker','v');

% Create scatter
scatter(R175,R176,'DisplayName','P3 F2','MarkerFaceColor',[0 0 0],...
    'MarkerEdgeColor',[0 0 0],...
    'Marker','v');

% Create scatter
scatter(R177,R178,'DisplayName','P3 cut',...
    'MarkerFaceColor',[0.501960813999176 0.501960813999176
0.501960813999176],...
    'MarkerEdgeColor',[0.501960813999176 0.501960813999176
0.501960813999176],...
    'Marker','v');

% Create scatter
scatter(R179,R180,'DisplayName','P3 Pivot',...
    'MarkerFaceColor',[0.87058824300766 0.490196079015732 0],...
    'MarkerEdgeColor',[0.87058824300766 0.490196079015732 0],...
    'Marker','v');

% Create scatter
scatter1 = scatter(Fz_Peak_N,Feather_x_amp,...
    'DisplayName','Feather_x_amp vs Fz_Peak_N',...
    'MarkerEdgeColor','none');

% Get xdata from plot
xdata1 = get(scatter1, 'xdata');
% Get ydata from plot
ydata1 = get(scatter1, 'ydata');
% Make sure data are column vectors
xdata1 = xdata1(:);
ydata1 = ydata1(:);

```

```

% Remove NaN values and warn
nanMask1 = isnan(xdata1(:)) | isnan(ydata1(:));
if any(nanMask1)
    warning('GeneratedCode:IgnoringNaNs', ...
        'Data points with NaN coordinates will be ignored.');
```

```

    xdata1(nanMask1) = [];
    ydata1(nanMask1) = [];
end

% Find x values for plotting the fit based on xlim
axesLimits1 = xlim(axes1);
xplot1 = linspace(axesLimits1(1), axesLimits1(2));

% Preallocate for "Show equations" coefficients
coeffs1 = cell(1,1);

% Find coefficients for polynomial (order = 1)
fitResults1 = polyfit(xdata1,ydata1,1);
% Evaluate polynomial
yplot1 = polyval(fitResults1,xplot1);

% Save type of fit for "Show equations"
fittypesArray1(1) = 2;

% Save coefficients for "Show Equation"
coeffs1{1} = fitResults1;

% Plot the fit
fitLine1 = plot(xplot1,yplot1,'DisplayName','    linear','Tag','linear',...
    'Parent',axes1);

% Set new line in proper position
setLineOrder(axes1,fitLine1,scatter1);
%Calculate rsq
model = fitlm(xplot1,yplot1);

rsq = model.Rsquared.Ordinary;

% "Show equations" was selected
showEquations(fittypesArray1,coeffs1,5,axes1);

% Create ylabel
ylabel('A(IS) Amplitude (g)');
```

```

% Create xlabel
xlabel({'Fz Peaks Force (BW)'});

% Uncomment the following line to preserve the X-limits of the axes
%xlim(axes1,[0 1.2]);
% Uncomment the following line to preserve the Y-limits of the axes
% ylim(axes1,[0 7]);
% Set the remaining axes properties
set(axes1,'OuterPosition',[0 0 0.788589492078352 1]);
% Create legend
legend1 = legend(axes1,'show');
set(legend1,'Location','northeastoutside','FontSize',8);

```

```

%-----%
function setLineOrder(axesh1, newLine1, associatedLine1)
%SETLINEORDER (AXESH1,NEWLINE1,ASSOCIATEDLINE1)
% Set line order
% AXESH1: axes
% NEWLINE1: new line
% ASSOCIATEDLINE1: associated line

% Get the axes children
hChildren = get(axesh1, 'Children');
% Remove the new line
hChildren(hChildren==newLine1) = [];
% Get the index to the associated line
lineIndex = find(hChildren==associatedLine1);
% Reorder lines so the new line appears with associated data
hNewChildren = [hChildren(1:lineIndex-
1);newLine1;hChildren(lineIndex:end)];
% Set the children:
set(axesh1, 'Children', hNewChildren);

%-----%
function showEquations(fittypes1, coeffs1, digits1, axesh1)
%SHOWEQUATIONS (FITTTYPES1,COEFFS1,DIGITS1,AXESH1)
% Show equations
% FITTTYPES1: types of fits
% COEFFS1: coefficients
% DIGITS1: number of significant digits
% AXESH1: axes

n = length(fittypes1);
txt = cell(length(n + 1) ,1);
txt{1,:} = ' ';
for i = 1:n
    txt{i + 1,:} =
getEquationString(fittypes1(i), coeffs1{i}, digits1, axesh1);
end
text(.05, .95, txt, 'parent', axesh1, ...
    'verticalalignment', 'top', 'units', 'normalized');

%-----%
function [s1] = getEquationString(fittype1, coeffs1, digits1, axesh1)
%GETEQUATIONSTRING (FITTTYPE1,COEFFS1,DIGITS1,AXESH1)
% Get "Show Equation" text
% FITTTYPE1: type of fit
% COEFFS1: coefficients
% DIGITS1: number of significant digits
% AXESH1: axes

if isequal(fittype1, 0)
    s1 = 'Cubic spline interpolant';
elseif isequal(fittype1, 1)
    s1 = 'Shape-preserving interpolant';
else
    op = '+-';
    format1 = ['%s %0.', num2str(digits1), 'g*x^{%s} %s'];
    format2 = ['%s %0.', num2str(digits1), 'g'];
    xl = get(axesh1, 'xlim');
    fit = fittype1 - 1;
    s1 = sprintf('y =');
    th = text(xl* [.95;.05], 1, s1, 'parent', axesh1, 'vis', 'off');

```



```

if abs(coeffs1(1) < 0)
    s1 = [s1 ' -'];
end
for i = 1:fit
    s1 = length(s1);
    if ~isequal(coeffs1(i),0) % if exactly zero, skip it
        s1 = sprintf(format1,s1,abs(coeffs1(i)),num2str(fit+1-i),
op((coeffs1(i+1)<0)+1));
    end
    if (i==fit) && ~isequal(coeffs1(i),0)
        s1(end-5:end-2) = []; % change x^1 to x.
    end
    set(th,'string',s1);
    et = get(th,'extent');
    if et(1)+et(3) > xl(2)
        s1 = [s1(1:s1) sprintf('\n      ') s1(s1+1:end)];
    end
end
if ~isequal(coeffs1(fit+1),0)
    s1 = length(s1);
    s1 = sprintf(format2,s1,abs(coeffs1(fit+1)));
    set(th,'string',s1);
    et = get(th,'extent');
    if et(1)+et(3) > xl(2)
        s1 = [s1(1:s1) sprintf('\n      ') s1(s1+1:end)];
    end
end
delete(th);
% Delete last "+"
if isequal(s1(end),'+')
    s1(end-1:end) = []; % There is always a space before the +.
end
if length(s1) == 3
    s1 = sprintf(format2,s1,0);
end
end
end

```

Appendix N: Combined Analysis MATLAB Script: Bar

This section contains the MATLAB script for combined analysis of all participants and provide peak average VGRF (BW) and A_{IS} amplitude measure for each participant for all netball simulated movements.

barp.m:

```
load('P1.mat');
load('P2.mat');
load('P3.mat');

%P1
p1Fxp = [mean(P1.walkv.Fx_Peak_N), mean(P1.jogv.Fx_Peak_N),
mean(P1.runv.Fx_Peak_N), mean(P1.sprintv.Fx_Peak_N),
mean(P1.jumpv.Fx_Peak_N), mean(P1.cutv.Fx_Peak_N), mean(P1.ROv.Fx_Peak_N),
mean(P1.pivotv.Fx_Peak_N), mean(P1.shufflev.Fx_Peak_N),
mean(P1.F2v.Fx_Peak_N), mean(P1.step440v.Fx_Peak_N)];
p1Fyp = [mean(P1.walkv.Fy_Peak_N), mean(P1.jogv.Fy_Peak_N),
mean(P1.runv.Fy_Peak_N), mean(P1.sprintv.Fy_Peak_N),
mean(P1.jumpv.Fy_Peak_N), mean(P1.cutv.Fy_Peak_N), mean(P1.ROv.Fy_Peak_N),
mean(P1.pivotv.Fy_Peak_N), mean(P1.shufflev.Fy_Peak_N),
mean(P1.F2v.Fy_Peak_N), mean(P1.step440v.Fy_Peak_N)];
p1Fzp = [mean(P1.walkv.Fz_Peak_N), mean(P1.jogv.Fz_Peak_N),
mean(P1.runv.Fz_Peak_N), mean(P1.sprintv.Fz_Peak_N),
mean(P1.jumpv.Fz_Peak_N), mean(P1.cutv.Fz_Peak_N), mean(P1.ROv.Fz_Peak_N),
mean(P1.pivotv.Fz_Peak_N), mean(P1.shufflev.Fz_Peak_N),
mean(P1.F2v.Fz_Peak_N), mean(P1.step440v.Fz_Peak_N)];

% Below changed to be normalised to BW
p1AxaS = [mean(P1.walkv.Feather_x_amp), mean(P1.jogv.Feather_x_amp),
mean(P1.runv.Feather_x_amp), mean(P1.sprintv.Feather_x_amp),
mean(P1.jumpv.Feather_x_amp), mean(P1.cutv.Feather_x_amp),
mean(P1.ROv.Feather_x_amp), mean(P1.pivotv.Feather_x_amp),
mean(P1.shufflev.Feather_x_amp), mean(P1.F2v.Feather_x_amp),
mean(P1.step440v.Feather_x_amp)];

%P2
p2Fxp = [mean(P2.walkv.Fx_Peak_N), mean(P2.jogv.Fx_Peak_N),
mean(P2.runv.Fx_Peak_N), mean(P2.sprintv.Fx_Peak_N),
mean(P2.jumpv.Fx_Peak_N), mean(P2.cutv.Fx_Peak_N), mean(P2.ROv.Fx_Peak_N),
mean(P2.pivotv.Fx_Peak_N), mean(P2.shufflev.Fx_Peak_N),
mean(P2.F2v.Fx_Peak_N), mean(P2.step440v.Fx_Peak_N)];
p2Fyp = [mean(P2.walkv.Fy_Peak_N), mean(P2.jogv.Fy_Peak_N),
mean(P2.runv.Fy_Peak_N), mean(P2.sprintv.Fy_Peak_N),
mean(P2.jumpv.Fy_Peak_N), mean(P2.cutv.Fy_Peak_N), mean(P2.ROv.Fy_Peak_N),
mean(P2.pivotv.Fy_Peak_N), mean(P2.shufflev.Fy_Peak_N),
mean(P2.F2v.Fy_Peak_N), mean(P2.step440v.Fy_Peak_N)];
p2Fzp = [mean(P2.walkv.Fz_Peak_N), mean(P2.jogv.Fz_Peak_N),
mean(P2.runv.Fz_Peak_N), mean(P2.sprintv.Fz_Peak_N),
mean(P2.jumpv.Fz_Peak_N), mean(P2.cutv.Fz_Peak_N), mean(P2.ROv.Fz_Peak_N),
mean(P2.pivotv.Fz_Peak_N), mean(P2.shufflev.Fz_Peak_N),
mean(P2.F2v.Fz_Peak_N), mean(P2.step440v.Fz_Peak_N)];

% Below changed to be normalised to BW
p2AxaS = [mean(P2.walkv.Feather_x_amp), mean(P2.jogv.Feather_x_amp),
mean(P2.runv.Feather_x_amp), mean(P2.sprintv.Feather_x_amp),
```

```

mean(P2.jumpv.Feather_x_amp), mean(P2.cutv.Feather_x_amp),
mean(P2.ROv.Feather_x_amp), mean(P2.pivotv.Feather_x_amp),
mean(P2.shufflev.Feather_x_amp), mean(P2.F2v.Feather_x_amp),
mean(P2.step440v.Feather_x_amp)];

%P3
p3Fxp = [mean(P3.walkv.Fx_Peak_N), mean(P3.jogv.Fx_Peak_N),
mean(P3.runv.Fx_Peak_N), mean(P3.sprintv.Fx_Peak_N),
mean(P3.jumpv.Fx_Peak_N), mean(P3.cutv.Fx_Peak_N), mean(P3.ROv.Fx_Peak_N),
mean(P3.pivotv.Fx_Peak_N), mean(P3.shufflev.Fx_Peak_N),
mean(P3.F2v.Fx_Peak_N), mean(P3.step440v.Fx_Peak_N)];
p3Fyp = [mean(P3.walkv.Fy_Peak_N), mean(P3.jogv.Fy_Peak_N),
mean(P3.runv.Fy_Peak_N), mean(P3.sprintv.Fy_Peak_N),
mean(P3.jumpv.Fy_Peak_N), mean(P3.cutv.Fy_Peak_N), mean(P3.ROv.Fy_Peak_N),
mean(P3.pivotv.Fy_Peak_N), mean(P3.shufflev.Fy_Peak_N),
mean(P3.F2v.Fy_Peak_N), mean(P3.step440v.Fy_Peak_N)];
p3Fzp = [mean(P3.walkv.Fz_Peak_N), mean(P3.jogv.Fz_Peak_N),
mean(P3.runv.Fz_Peak_N), mean(P3.sprintv.Fz_Peak_N),
mean(P3.jumpv.Fz_Peak_N), mean(P3.cutv.Fz_Peak_N), mean(P3.ROv.Fz_Peak_N),
mean(P3.pivotv.Fz_Peak_N), mean(P3.shufflev.Fz_Peak_N),
mean(P3.F2v.Fz_Peak_N), mean(P3.step440v.Fz_Peak_N)];

% Below changed to be normalised to BW
p3AxaS = [mean(P3.walkv.Feather_x_amp), mean(P3.jogv.Feather_x_amp),
mean(P3.runv.Feather_x_amp), mean(P3.sprintv.Feather_x_amp),
mean(P3.jumpv.Feather_x_amp), mean(P3.cutv.Feather_x_amp),
mean(P3.ROv.Feather_x_amp), mean(P3.pivotv.Feather_x_amp),
mean(P3.shufflev.Feather_x_amp), mean(P3.F2v.Feather_x_amp),
mean(P3.step440v.Feather_x_amp)];

%%
c = categorical({'walk', 'jog', 'run', 'sprint', 'jump', 'cut', 'RO',
'Pivot', 'shuffle', '2F', 'step440'});

Fxp = [p1Fxp;p2Fxp;p3Fxp];
Fyp = [p1Fyp;p2Fyp;p3Fyp];
Fzp = [p1Fzp;p2Fzp;p3Fzp];
Fte = [p1AxaS;p2AxaS;p3AxaS];

createBarPlot(c, Fzp.', 'Fz Peaks (BW)');
createBarPlot(c,

```

createBarPlot.m:

```

function createBarPlot(c1, ymatrix1, ylab)
%CREATEFIGURE1(c1, ymatrix1)
% C1: bar xvector
% YMATRIX1: bar matrix data

% Auto-generated by MATLAB on 08-Sep-2018 23:59:03

% Create figure
figure1 = figure('Name','Figure');
figure('visible','off');

% Create axes
axes1 = axes('Parent',figure1);
hold(axes1,'on');

% Create multiple lines using matrix input to bar
bar1 = bar(c1,ymatrix1,'Parent',axes1);
set(bar1(3),'DisplayName','P3');
set(bar1(2),'DisplayName','P2');
set(bar1(1),'DisplayName','P1');

% Create ylabel
ylabel({ylab},'HorizontalAlignment','center');

% Create xlabel
xlabel('Movement');
ylabel({'Movement'},'HorizontalAlignment','center');

box(axes1,'on');
% Create legend
legend1 = legend(axes1,'show');
set(legend1,'Location','eastoutside');

saveas(figure1, strcat(ylab, '.png'));

end

```

Appendix O: Impact Zones: 4 Participants

Figure 53 reflects the impact zone of netball simulated movements from correlated A_{IS} amplitude from Delsys Trigno and peak VGRF obtained from force plates from the 2018 study (Corbo, 2018):

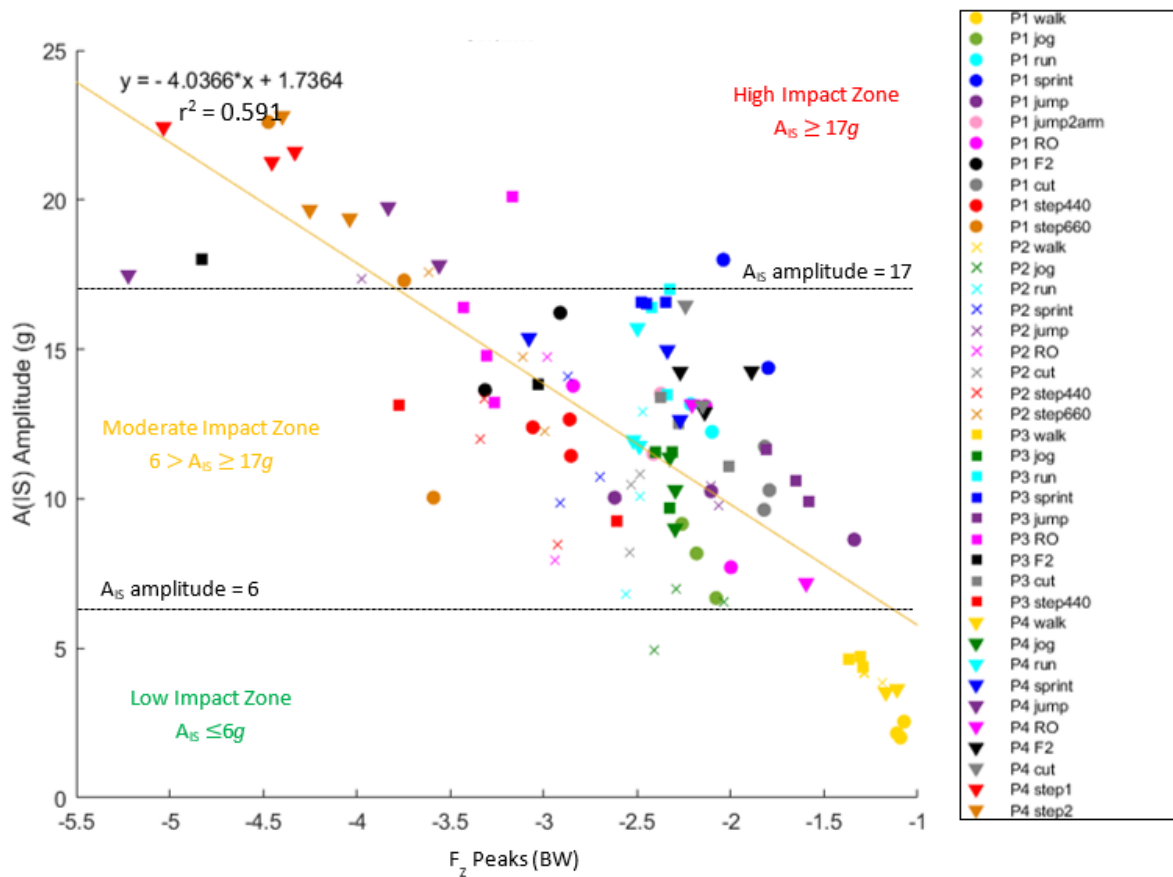


Figure 57: A_{IS} amplitude (g) vs F_z peaks (BW) correlation with impact zones